THE UNIVERSITY of EDINBURGH

Edinburgh Research Explorer

Neotethyan Ankara Melange, central Turkey: Formation by accretion of seamounts and supra-subduction zone ophiolites in an oceanic fore-arc setting

Citation for published version:
Robertson, AHF, Parlak, O, Taslı, K, Dumitrica, P & Ustaömer, T 2023, 'Neotethyan Ankara Melange, central Turkey: Formation by accretion of seamounts and supra-subduction zone ophiolites in an oceanic fore-arc setting', *Journal of Asian Earth Sciences: X* , vol. 10, 100151. https://doi.org/10.1016/j.jaesx.2023.100151

Digital Object Identifier (DOI):
10.1016/j.jaesx.2023.100151

Link:
Link to publication record in Edinburgh Research Explorer

Document Version:
Publisher's PDF, also known as Version of record

Published In:
Journal of Asian Earth Sciences: X

Publisher Rights Statement:
© 2023 The Author(s). Published by Elsevier Ltd. This is an open access article under the CC BY-NC-ND license

General rights
Copyright for the publications made accessible via the Edinburgh Research Explorer is retained by the author(s) and / or other copyright owners and it is a condition of accessing these publications that users recognise and abide by the legal requirements associated with these rights.

Take down policy
The University of Edinburgh has made every reasonable effort to ensure that Edinburgh Research Explorer content complies with UK legislation. If you believe that the public display of this file breaches copyright please contact openaccess@ed.ac.uk providing details, and we will remove access to the work immediately and investigate your claim.

Download date: 05. Jul. 2023

Journal of Asian Earth Sciences: X 10 (2023) 100151

Contents lists available at ScienceDirect

Journal of Asian Earth Sciences: X

journal homepage: www.sciencedirect.com/journal/journal-of-asian-earth-sciences-x

Neotethyan Ankara Melange, central Turkey: Formation by accretion of seamounts and supra-subduction zone ophiolites in an oceanic fore-arc setting

Alastair H.F. Robertson [a,*], Osman Parlak [b], Kemal Taslı [c], Paulian Dumitrica [d], Timur Ustaömer [e]

[a] School of GeoSciences, University of Edinburgh, Grant Institute, James Hutton Road, Edinburgh EH9 3FE, UK
[b] Çukurova Üniversitesi, Jeoloji Mühendisliği Bölümü, 01330 Balcalı, Adana, Turkey
[c] Mersin Üniversitesi, Jeoloji Mühendisliği Bölümü, Mersin, Turkey
[d] Institute of Earth Sciences, Université De Lausanne, Geopolis, Lausanne, Switzerland
[e] İstanbul Üniversitesi-Cerrahpaşa, Jeoloji Mühendisliği Bölümü, Büyükçekmece, İstanbul, Turkey

ARTICLE INFO

Keywords:
Ankara Melange
Ophiolites
Neotethys
Seamounts
Subduction
Accretion

ABSTRACT

The Neotethyan Ankara Melange is a global reference for oceanic accretionary processes preserved in a collisional orogen. Here we show, based on eight representative outcrops around Ankara, that the melange encompasses stratigraphically coherent volcanic-sedimentary successions of mainly Late Jurassic-Early Cretaceous age. Our results indicate that the melange has a relatively organised tectonostratigraphy, in contrast to previous interpretations that emphasised its chaotic nature. Coherent volcanic-sedimentary successions of Late Jurassic-Early Cretaceous age are interpreted as flank facies of a large oceanic seamount (probably plume related) and its capping carbonate platform (atoll), including reef-and back-reef facies. Remnants of other seamounts are dated as Late Triassic-Early Jurassic and Late Cretaceous. Variably dismembered supra-subduction zone ophiolites of latest Early Jurassic-Middle Jurassic age, including boninites, formed in an oceanic fore-arc setting, similar to that of the Cenozoic Izu-Bonin fore arc, NW Pacific. The melange in the Ankara region partly accreted during the Early Cretaceous (pre-Albian) in response to collision of the inferred large seamount with the oceanic (ophiolitic) fore arc. During the collision which involved subduction-erosion slices of proximal–distal seamount flank lithologies accreted sequentially, whereas the seamount core subducted. Also during the collision, the distal outer edge of the ophiolitic fore arc, mainly mantle harzburgite, detached from the over-riding lithosphere and was incorporated into the melange. Structural evidence emphasises the importance of tectonic processes (rather than olistostromes) in the melange accretion. The accretionary prism in the outcrops studied was covered by arc-related sediments and volcanics during the Late Cretaceous and deformed by collision-related processes during latest Cretaceous-Paleogene.

1. Introduction

The Neotethyan Ankara Melange is one of the type melanges in the world and therefore all aspect of its geology merit careful documentation and interpretation. In Turkey, the term Neotethyan melange refers to melange that formed within an ocean basin that existed during Triassic to early Cenozoic time, which is preserved as remnants within the İzmir-Ankara-Erzincan suture zone, also known as the Northern Neotethyan suture zone (Figs. 1, 2). We distinguish the Neotethyan Ankara Melange from the older Palaeotethyan Ankara Melange (also known as the Karakaya Complex), which formed in a pre-existing ocean basin (Palaeotethys) generally farther to the north during Late Palaeozoic-Late Triassic time (e.g., Pickett and Robertson, 1996; Okay and Göncüoğlu, 2004; Ustaömer et al., 2016).

In recent years, the Neotethyan Ankara Melange and its equivalents in both eastern and western Turkey have received a considerable amount of attention, mainly concerning the geochemistry and age of the ophiolitic rocks and the associated metamorphic rocks, and also the biostratigraphy and age of shallow-to deep-sea sedimentary rocks within the melange (e.g., Rojay et al., 2001, 2004; Tekin et al., 2002; Göncüoğlu et al., 2015; Sarıfakıoğlu et al., 2017; Bortolotti et al., 2018; Okay et al., 2019, 2022). Structural information including cross-sections

* Corresponding author.
E-mail address: Alastair.Robertson@ed.ac.uk (A.H.F. Robertson).

https://doi.org/10.1016/j.jaesx.2023.100151
Received 30 January 2023; Received in revised form 28 March 2023; Accepted 24 April 2023
Available online 17 June 2023
2590-0560/© 2023 The Author(s). Published by Elsevier Ltd. This is an open access article under the CC BY-NC-ND license (http://creativecommons.org/licenses/by-nc-nd/4.0/).

and microstructural analysis is available for some areas (Rojay, 2013). However, less emphasis has been placed on the facies and petrography of the associated sedimentary rocks and the structure of the melange as a whole. Here, we present and discuss new field-based information from the type area of the Neotethyan Ankara Melange in the vicinity of Ankara (Figs. 3, 4). We combine this with existing information to develop a new tectonic model involving oceanic collision of a large seamount and its capping carbonate platform (atoll) with supra-subduction zone (SSZ) oceanic lithosphere that formed in a fore-arc setting similar to that of the west Pacific Ocean during mid-Cenozoic time.

An important but still controversial issue is whether the melange formed by mainly sedimentary mass-transport processes (Boccaletti et al., 1966; Norman, 1972, 1973, 1984; Batman, 1978, 1981; Ünalan, 1981; Koçyiğit, 1991; Yılmazer, 1994; Duru and Aksay, 2002), or by mainly tectonic processes (Bailey and McCallien, 1950, 1953; Şengör and Yılmaz, 1981; Rojay, 2013; Çakır and Üner, 2016; Sarıfakıoğlu et al., 2017; Okay et al., 2022).

For the history of research on the Neotethyan Ankara Melange the reader is referred to Şengör (2003). Here, we emphasise the role of tectonic processes and argue that the Neotethyan Ankara Melange represents an accretionary prism that was formed by subduction-related processes in an intra-oceanic setting away from direct continental margin influence. The Neotethyan Ankara Melange should not be interpreted as a mass-transport unit that was dominantly formed by mass-flow processes as for traditional olistostromes (e.g., Festa et al., 2015). Tectonically controlled accretion does allow for a range of processes to be involved including deeper level structural processes (e.g., high pressure/low-temperature metamorphism) and also high-level sedimentary processes such as the accumulation of debris-flow deposits in trench and perched fore-arc basin settings (e.g., Koçyiğit, 1988, 1991).

Melanges are by their nature chaotic. The voluminous volcanic and sedimentary rocks in the Ankara Melange have indeed previously been mapped and interpreted mainly as pervasively mixed blocks in a sheared sedimentary and/or serpentinite matrix. However, where associations of similar rock types have been mapped in melanges elsewhere some degree of litho-tectonic organisation has commonly become apparent, as in SE Turkey (Hall, 1976), southeast central Turkey (Polat and Casey, 1995; Robertson et al., 2022), western Turkey (Collins and Robertson, 1997); Greece (Jones and Robertson, 1991), California (e.g., Wakabayashi, 2012), Japan (Mori et al., 2011; Sakai et al., 2021) and elsewhere around the Pacific rim (see Dilek and Ogawa, 2021). In the case of the Ankara Melange, the outcrop includes variably dismembered SSZ ophiolites that in some areas retain a high degree of lithological and structural coherence (Dilek and Thy, 2006; Dangerfield et al., 2011; Sarıfakıoğlu et al., 2014, 2017; Çelik et al., 2013; Okay et al., 2022). Here, we show that there is considerable tectono-stratigraphic coherence within the melange in some areas. When mapped and logged, many units that have hitherto been considered to have a block-in-matrix fabric were instead found to represent relatively intact successions of volcanic and sedimentary rocks (here termed volcanic-sedimentary). The recognition of this relative tectono-stratigraphic coherence allows pre-emplacement tectonic settings and the processes involved to be recognised with greater confidence.

In some areas, the outcrop of the Ankara Melange includes slices and blocks of Upper Cretaceous arc-related volcanic rocks and volcaniclastic sedimentary rocks which relate to the later stages of subduction, prior to continental collision during latest Cretaceous-Paleogene time (pre-Middle Eocene). These younger events and also the wider, regional context of the Ankara melange are the subject of a companion paper (Robertson et al., 2023; see Fig. 2 for outcrops in the wider region).

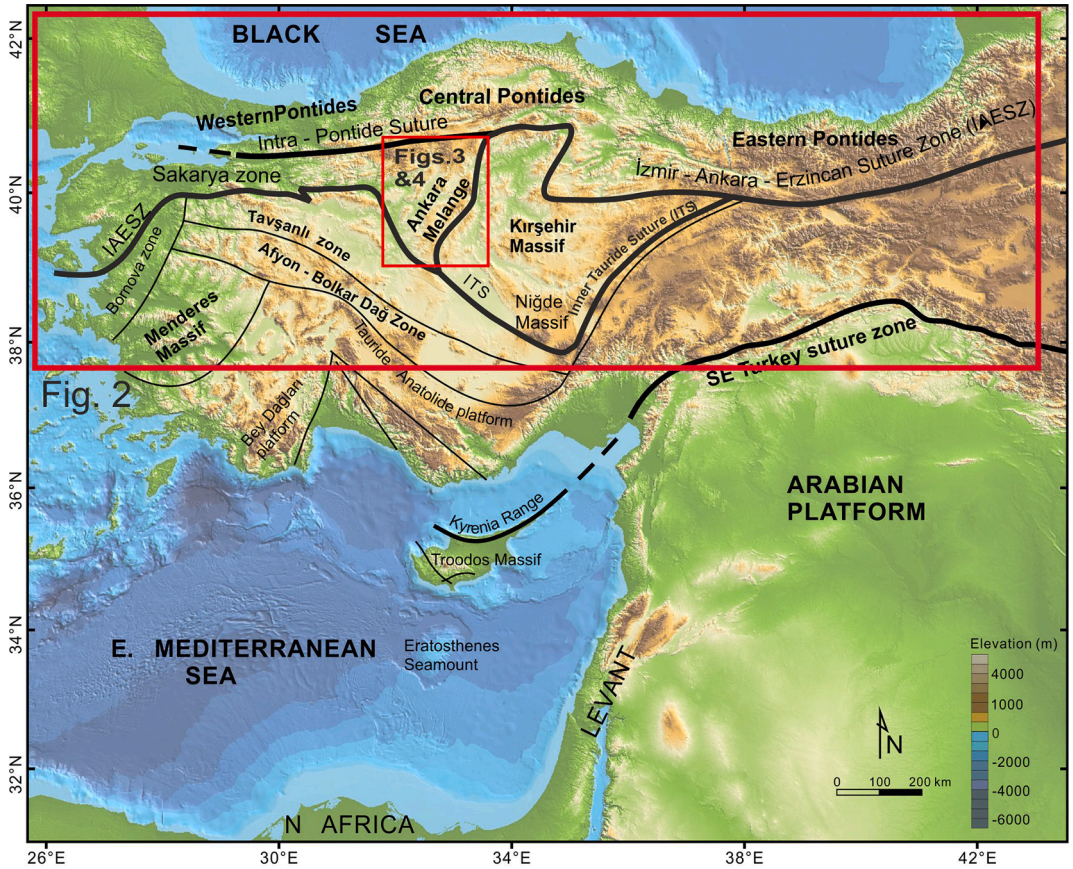

Fig. 1. Tectonic zones of Turkey, also showing the Mesozoic melanges and ophiolitic rocks, here termed the Neotethyan Ankara melange, as exposed in the vicinity of Ankara. Modified from Chen and Robertson (2020).

Here, we focus on pre-Late Cretaceous accretion while acknowledging that accretion probably continued until latest Cretaceous-Paleogene continental collision ended subduction.

Our specific objectives here are: (1) to summarise and compare eight different exposures in the vicinity of Ankara to help understand the tectonic settings and processes involved in the formation of the Neotethyan Ankara Melange; (2) to present new sedimentological, micropalaeontological, petrographical and structural evidence that sheds light on the formation of the Neotethyan Ankara Melange; (3) to interpret the processes of formation of the Neotethyan Ankara Melange, with emphasis on the accretion of a large Upper Jurassic-Lower Cretaceous oceanic seamount (tens of km in scale?), of which remnants are preserved in the Ankara region. Other smaller seamounts of different ages are also represented within the areas studied.

2. Melange nomenclature

Numerous definitions of melange exist to which the reader is referred (e.g., Raymond, 1984, 2018; Festa et al., 2010, 2012). Here, we follow Cowan's (1978) statement that 'melange should be purely descriptive, non-genetic, and inclusive of block-in-matrix rocks of olistostromal origin as well as those of tectonic origin.'

Several different names have been used for the Neotethyan Ankara Melange including Ophiolitic block melange (Norman, 1973a, 1984), North Anatolian Ophiolitic Mélange (Rojay et al., 2001, 2004), Ankara Ophiolitic Mélange (Rojay, 2013) and Ankara melange (Sarıfakıoğlu et al., 2014, 2017).

Many authors describe the Neotethyan Ankara Melange as 'ophiolitic melange' (Gansser, 1974; Çapan and Buket, 1975; Tankut, 1984, 1990; Tankut et al., 1998; Koçyiğit, 1988; Koçyiğit, 1991; Erdoğan et al., 1996; Rojay et al., 2004; Rojay, 2013; Nairn et al., 2012; Çelik et al., 2011, 2013; Okay et al., 2022). This term implies that the melange is mainly made up of dismembered ophiolitic rocks set in a pervasively sheared matrix, which is commonly ophiolitic serpentinite. However, on the 1:250,000 geological map of Turkey (MTA, 2011) about one third of the melange is mapped as ophiolite, one third as clastic and carbonate rocks, and one third as ophiolitic melange (see Fig. 3).

Our study indicates that the Neotethyan Ankara Melange encompasses: (1) variably dismembered ophiolites (including coherent units); (2) blocks and lenses of ophiolitic rocks, typically set in a matrix of sheared ophiolitic serpentinite (true ophiolitic melange); and (3) volcanic-sedimentary successions (including coherent stratigraphical units). Since many of the lithologies present are not ophiolitic, the term 'ophiolite-related melange' is preferred here, rather than 'ophiolitic melange' (Robertson et al., 2009). A future revised geological map of the Neotethyan Ankara Melange (outside the present scope) could usefully distinguish the above three lithological categories.

3. Methods and materials

Each of main outcrops of the Ankara Melange has some specific features, such that no one local area is representative of the Neotethyan Ankara Melange as a whole. We have studied representative exposures, extending from south of Ankara, generally northeastwards (Figs. 3, 4). For each area, we have made local cross-sections, particularly to determine the relationships between semi-intact ophiolites, ophiolitic melange, volcanic-sedimentary successions and post-accretionary (arc and fore-arc related) units. The post-accretionary units were incorporated into the melange as a result of late-stage collision-related processes, as summarised elsewhere (Robertson et al., 2023). In areas where relatively intact volcanic-sedimentary successions were encountered we measured logs to highlight the sedimentary and volcanic processes involved. The sedimentary lithologies present were studied in thin sections using an optical microscope to help determine paleoenvironments and provenance. Calcareous and siliceous facies were sampled, especially those interbedded with volcanic rocks to indicate their age and microfacies, supplementing existing micropalaeontological data (Akyürek et al., 1984; Hakyemez et al., 1986; Rojay et al., 2004; Bortolotti et al., 2013; Sarıfakıoğlu et al., 2017; Okay et al., 2019, 2022). We collected structural data (mainly for bedding and faults), mainly

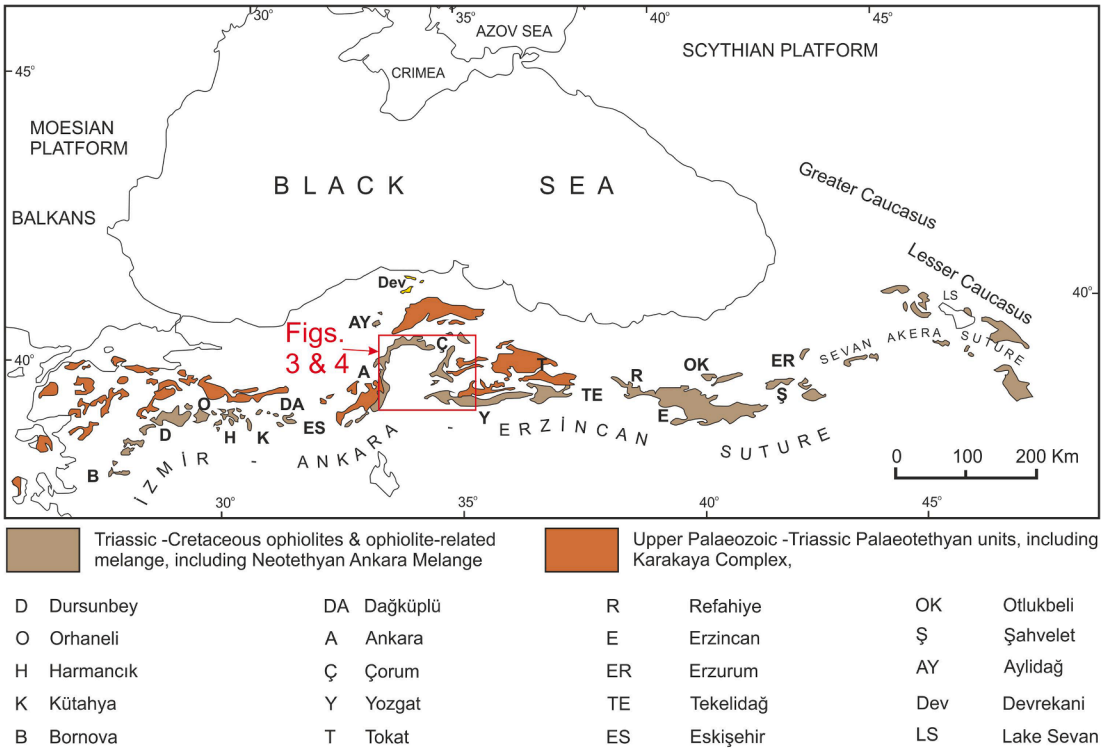

Fig. 2. Outline geological map showing the Palaeotethyan melange (Karakaya Complex) and the Neotethyan melange farther south. The overall study area is also indicated. Modified from Ustaömer et al. (2016).

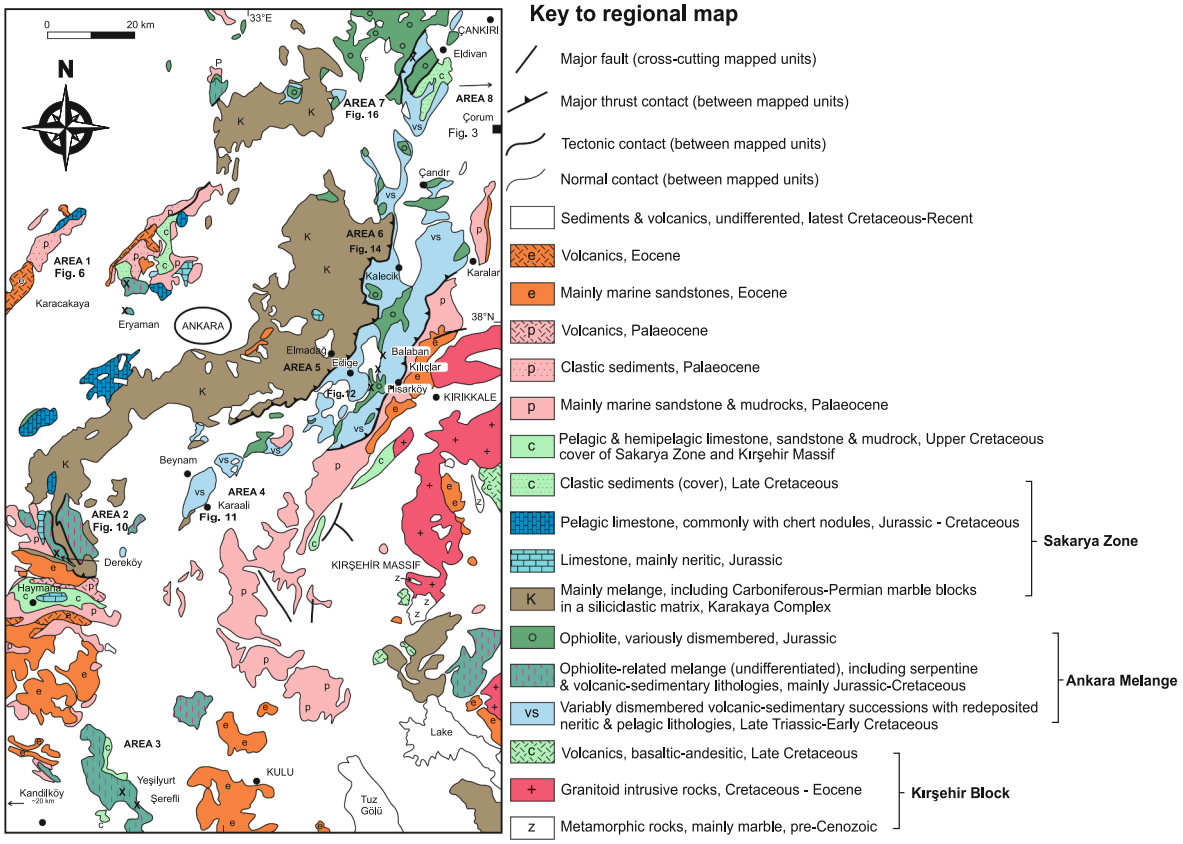

Fig. 3. Outline geological map of the main study area around Ankara, based on the 1:250,000 geological map of Turkey (MTA, 2011). The main locations studied are indicated. Following MTA (2011), outcrops of Neotethyan Ankara Melange are shown as: 1. Lavas and sedimentary rocks (vs); 2. Ophiolitic rocks (o) and ophiolitic melange (green with red vertical lines). However, these units are typically intergradational. Eight areas were studied: 1. NW: Karacakaya-Eryaman; 2. SW: Dereköy (NE of Haymana); 3. Far SW: W of Kulu; 4. S: Beynam-Karaali; 5. SE: Kılıçlar-Hisarköy (SE of Elmadağ); 6. NW: Kalecik-Çandır; 7. Far NW: Eldivan; 8. Çorum-northern margin of the Çankırı Basin (see Fig. 4 for locations). Key: similar symbols are used on the local maps and sections. (For interpretation of the references to colour in this figure legend, the reader is referred to the web version of this article.)

associated with the volcanic-sedimentary units and then combined these measurements with information from satellite images to help interpret the structure of the Ankara Melange (e.g., lineaments, folds, block distribution), supplementing published structural evidence (Rojay, 2013; Dangerfield et al., 2011; Okay et al., 2022).

4. Evidence from key outcrops

Below, we present new field-based data and combine this with existing information, based on our study of eight main outcrops, all of which show distinctive features. For each of these areas concerned we highlight critical aspects which are then integrated and interpreted in the Discussion.

The Ankara Melange outcrops discussed here are located along the western and northern segments of a regional northward-directed oroclinal bend, with the Neogene Çankırı Basin as its interior (Figs. 2, 3). The outcrops of the Neotethyan Ankara Melange are summarised below, generally in an anticlockwise direction following Rojay et al. (2000, 2004), starting from northwest of Ankara; i.e. Area 1, Karacakaya (NW of Ankara); Area 2, Dereköy (NE of Haymana); Area 3, W of Kulu (SW); Area 4, Beynam-Karaali (S of Ankara); Area 5, Edige-Kılıçlar (SE of Ankara); Area 6, Kalecik-Çandır; Area 7, Eldivan (SW of Çankırı); and finally Area 8, farther east (İskilip, Yapraklı, Laloğlu, Boğazkale and south of Çekerek (Fig. 4).

4.1. Area 1: NW (Karacakaya-Eryaman)

The melange is well exposed northwest of Ankara as a continuous, c. 25 sq. km outcrop in the vicinity of Karacakaya. Scattered outcrops farther south, near Eryaman, within the western outskirts of Ankara (Figs. 4, 5a, 6) have recently been assigned to the Alacaatlı Olistostromes, separate from the Neotethyan Ankara Melange (Okay et al., 2019; see below). In the north, the outcrop is unconformably overlain by Upper Cretaceous-Palaeocene cover sediments (Koçyiğit, 1991; MTA, 2011; Okay et al., 2019). Previous research (Rojay et al., 2004) indicates that the melange in this area is made up of thrust intercalations of pillow lava, pillow breccia, radiolarite and limestone blocks, commonly with a clastic matrix, together with ophiolitic lithologies, mainly ultramafic rocks (Fig. 6a). The lavas are mainly alkaline clinopyroxene-phyric basalts of within-plate type (WPB), but there are also mid-ocean ridge (MORB) and back-arc (BAB) type basalts in this area (Rojay et al., 2004). Associated limestones include coral, rudist bivalves and calcareous algae. Fossils from associated bioclastic limestones yielded Barremian-Aptian ages (Rojay et al., 2004). The outcrops in the northwest of Area 1 are thrust southeastwards over the Karakaya Complex (Fig. 3), which in turn is thrust generally southeastwards over the more easterly Neotethyan Ankara Melange outcrop (MTA, 2011; Rojay, 2013). A representative outcrop was studied in detail near Karacakaya (Fig. 6a, b). Satellite images (Fig. 7a) of this area reveal disrupted, lenticular bodies of radiolarite and serpentinite and scattered blocks of carbonate rocks. Curved trends indicate folding, apparently after initial accretion of the melange (see Structure, below). The outcrop is strongly imbricated, with repeated elongate, lenticular, thrust units of volcanic-sedimentary and serpentinite-dominated lithologies (Fig. 6b). Basaltic debris-flow deposits, volcanic breccia, pillow lava, massive lava and radiolarite are interbedded, together with scattered blocks of neritic

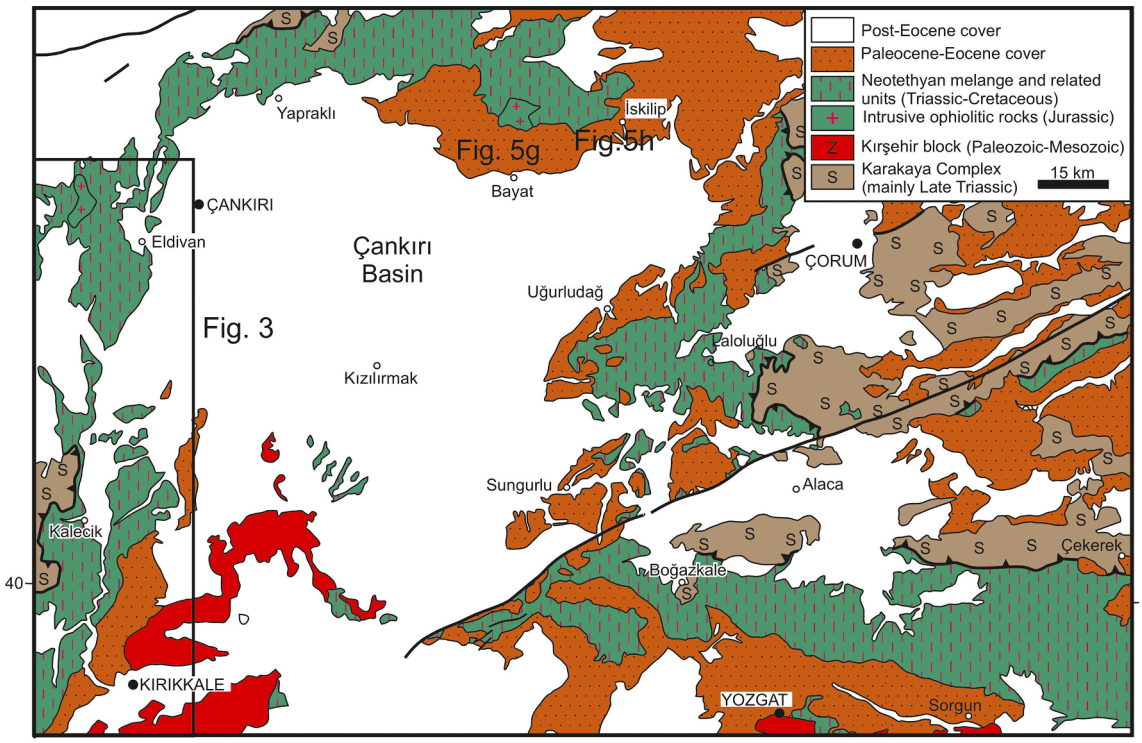

Fig. 4. Tectonic map of the wider region of the Neotethyan Ankara Melange. Sections studied near Yapraklı, İskilip and south of Çorum are indicated. See Fig. 3 for the main sections studied in the west of the area. Simplified from MTA (2011).

limestone (Fig. 8a, b; log 1). In places, lenticular units of highly brecciated pink pelagic limestone and radiolarite (up to 25 m thick) form inclusions within sheared serpentinite (Fig. 6a, b). Blocks of white neritic limestone, up to 4 m across (e.g., 0.4 km SSW Karacakaya; Fig. 9a), are dominated by very coarse breccia-conglomerate. Larger blocks are commonly surrounded by smaller subrounded blocks (<0.5 m in size), set in a sheared red matrix of siliceous/argillaceous shale. These limestone blocks commonly include small angular basaltic lithoclasts together with abundant bivalves (including rudists), gastropods, coral and coralline algae (Fig. 9b, c; Supplementary Fig. 1c). Benthic foraminifera in the limestones sampled are dated as Early Cretaceous (late Barremian-early Aptian) (Supplementary Table 1) (samples AM/105, 106, 109). Radiolarites between local basaltic units are dated as late Oxfordian-early Kimmeridgian (sample AM/107) and Cenomanian (sample AM/108). Interestingly, the latter sample includes a mixture of late Oxfordian-early Kimmeridgian Radiolaria and common Tithonian Radiolaria (Supplementary Table 2). This suggests that Tithonian Radiolaria were reworked during the Cenomanian while still unlithified, probably as a result of seafloor current activity.

Poorly exposed melange further south, near Eryaman (Fig. 6c), illustrates tight imbrication of ophiolitic serpentinite and gabbros, pillow lavas and radiolarites. The serpentinite is highly sheared, with inclusions of basaltic rocks, amphibolite (assumed remnant of metamorphic sole) and radiolarites. Previously, radiolarites have been dated from short successions within several blocks in this area and the results were combined to produce a composite succession (Bragin and Tekin, 1996). Unusually, these radiolarites indicate ages extending from late Norian to late Albian-Aptian, with Middle Jurassic apparently being the only major missing time interval (Bragin and Tekin, 1996). Elsewhere, the dated radiolarites were sampled from locally intact sections that indicate much shorter radiolarian time ranges (e.g., Supplementary Table 2; see below). However, as noted above the Eryaman outcrop has recently been remapped as part of the Alacaatlı Olistostromes, separate from the Neotethyan Ankara melange outcrop farther east (Okay et al., 2019) and might therefore represent accumulation in a different tectonic setting. For example, these radiolarites could have accumulated along the deep-sea margin of the Sakarya continent, which would explain the longevity of radiolarian accumulation there (Robertson et al., 2023).

The main points from Area 1 are: (1) MORB, IAT and BAB-type lavas are all present in close spatial proximity although as separate blocks; (2) Upper Jurassic radiolarites and Lower Cretaceous shallow-water limestones are present, and also Cenomanian radiolarites; (3) The outcrop is highly fragmented and folded, possibly in response to post-accretionary (collision-related) deformation; (4) Radiolarites at Eryaman are unusually long-ranging (Late Triassic-early Late Cretaceous) but might represent a different tectonic setting.

4.2. *Area 2: SW (Dereköy)*

Southwest of Ankara, the Ankara Melange is widely exposed near Dereköy, c. 13 km NE of Haymana (Fig. 3), where it forms two subparallel NNW-SSE trending strips, separated by an imbricate slice of the Palaeotethyan Ankara Melange (Karakaya Complex). In places, the Neotethyan melange is thrust over Maastrichtian-Paleogene fore-arc sedimentary rocks (Haymana Formation) (Ünalan et al., 1976; Okay and Altıner, 2016). The lower part of the thrust slice shown in Fig. 5b is dominantly ophiolitic, overlain by a wedge-shaped slice of 'pillow basalts and diabases, followed by radiolarite, and finally by blocky carbonate rocks' (Rojay, 2013). Intrapillow biomicritic limestone previously yielded a maximum Callovian-Hauterivian age, possibly Callovian to pre-late Tithonian in the absence of co-existing calpionellids (Rojay et al., 2001). Barremian ages were also reported from calcareous fossils within bioclastic limestones (Rojay et al., 2004). N-MORB was also reported from this area (Rojay et al., 2001, 2004).

Satellite images (Fig. 7b) reveal intercalated lava (brown) and radiolarite (red), interspersed with carbonate blocks (pale grey), mainly 10 s m across. The limestone blocks are generally distributed c. NNW-SSE, parallel to the tectonic trend of the melange. Bedding in the blocks is generally sub-parallel to this trend, but in places is curved suggesting that folding has taken place, probably associated with tectonic accretion

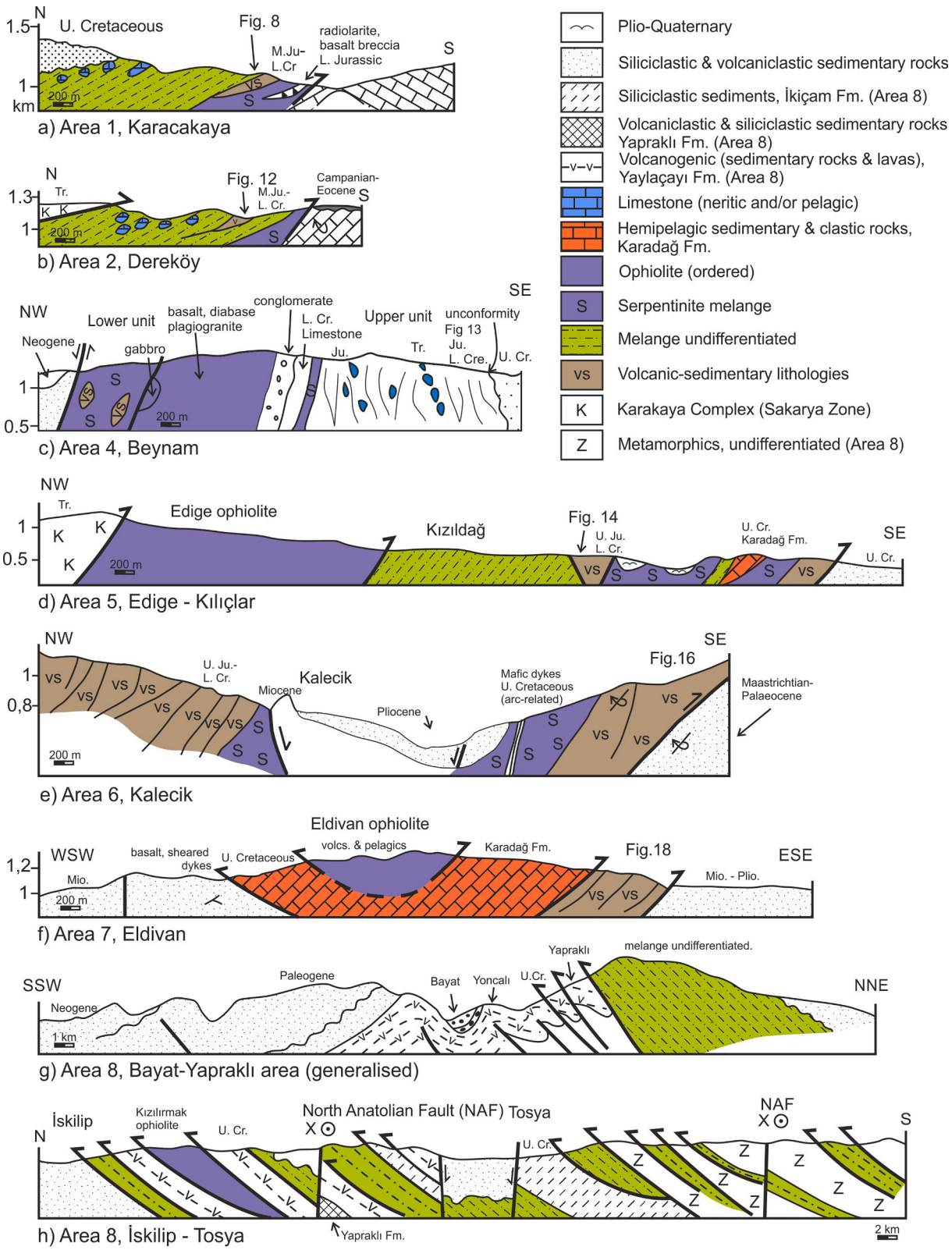

Fig. 5. Generalised cross-sections of the main study areas. a, Area 1, Karacakaya; simplified from Rojay (2013); b, Area 2, Dereköy; simplified from Rojay (2013); c, Area 4, Beynam-Karaali; simplified from Akyürek et al. (1997); d, Area 5, Edige-Kılıçlar; simplified from Sarıfakıoğlu et al. (2011); e, Area 6, Kalecik-Çandır; simplified from Sarıfakıoğlu et al. (2011) and Rojay (2013); f, Area 7, Eldivan; simplified from Sarıfakıoğlu et al. (2011); g, Area 8, Bayat-Yapraklı; simplified from Kaymakçı et al. (2009); h, Area 8, İsklip-Tosya, simplified from Rice et al. (2006).

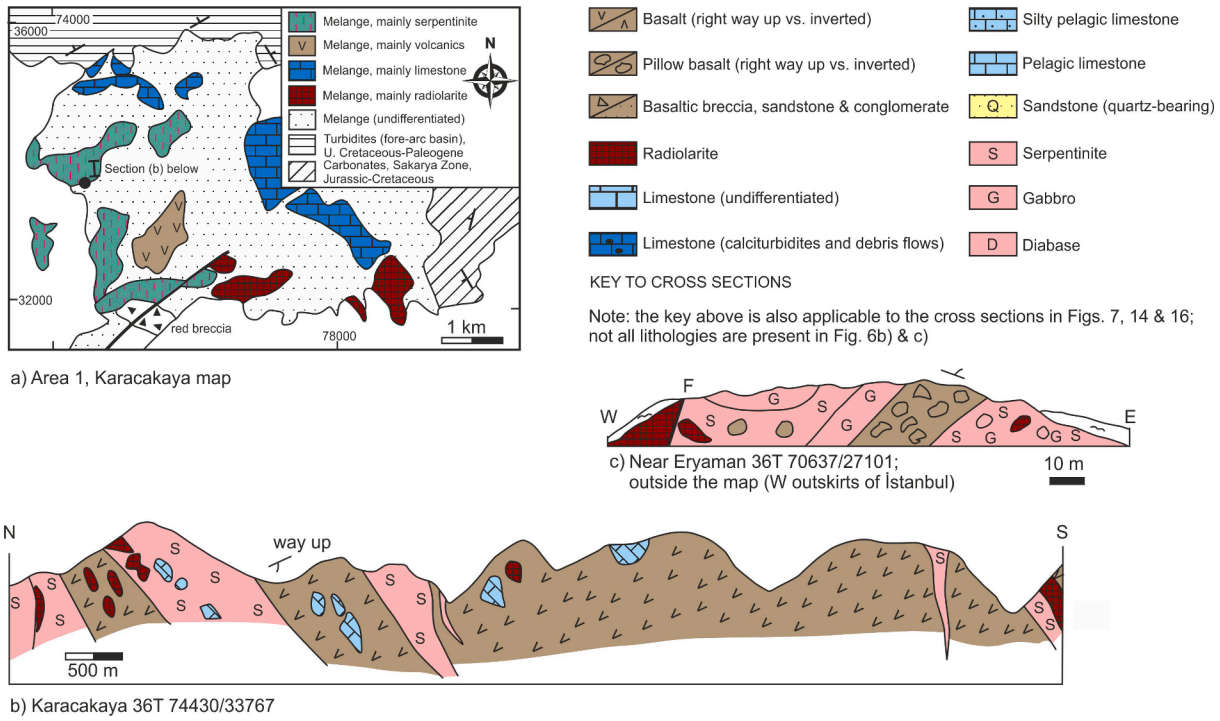

Fig. 6. Tectono-stratigraphy of the Ankara Melange in the northern part of Area 1, NW of Ankara (see Fig. 3). a, Outline geological map (simplified from Rojay, 2013); b, Local cross-section near Karacakaya (see a, for location); c, local cross-section along a main road section, near Eryaman, western outskirts of Ankara (not shown in a).

(Fig. 7b). The bedding is truncated at variable angles indicating tectonic dissection (see Structure, below). Two lithological assemblages characterise well-exposed melange west of Dereköy (Fig. 10a): (1) basaltic volcanogenic rocks, associated with limestones and radiolarites; (2) serpentinised harzburgite with lenticular radiolarite inclusions (Fig. 10b). Serpentinite is intersheared with volcanic-sedimentary lithologies (c. 2 km W of Dereköy) (Fig. 10c). Locally intact volcanogenic successions (Fig. 8a, b, log 2; Fig. 9d-f) are dominated by basalt and redeposited limestone largely in the form of talus (Fig. 9g). Detached blocks of neritic limestone rich in large bivalves occur throughout this volcanic-sedimentary outcrop (Fig. 9h,i). Calciturbidites and debris-flow deposits (samples AM/87, 89, 90, 91) contain benthic foraminifera of late Barremian-early Aptian age (Supplementary Table 1; Supplementary Fig. 1d). Radiolarites (samples AM/93 and AM/95) yielded radiolarians of Tithonian age (Supplementary Table 2).

The main points from the Dereköy area are: (1) A volcanic-sedimentary succession of Late Jurassic-Early Cretaceous age is interbedded with blocks and talus of neritic limestone including reef facies; (2) Shallow-water limestone blocks show evidence of folding and tectonic fragmentation, probably associated with melange accretion; (3) Radiolarites (and rarely also pelagic limestones) are locally intersheared with serpentinised ultramafic rocks, in contrast to the shallow-water facies of the volcanic-sedimentary succession.

4.3. Area 3: South (W of Kulu)

The Ankara Melange continues towards the south-southeast, broadly on tectonic strike, where it is extensively but poorly exposed in a low-relief area several tens of km west of Kulu (Uğuz et al., 1999) (Fig. 3). The melange in this area is mapped as ophiolitic, with scattered blocks of Upper Triassic and Jurassic-Cretaceous neritic limestones (MTA 100:000 Geological Map Ankara-J29). Much of the outcrop is, however, not ophiolitic. Basalt, radiolarite and minor sheared serpentinite are exposed, mainly in road cuttings and small quarries. For example, a large, lenticular neritic limestone block (c. 15 m across), near Yeşilyurt (GPS 36S 73920/21953), is accompanied by a trail of smaller limestone (<4 m) blocks that are orientated parallel to the c. 015° tectonic trend in this area. Spot samples of radiolarite were dated as late Norian (sample AM/99) and Bajocian (sample AM/95) (Supplementary Table 2).

There are also scattered blocks of marble, in which the metamorphic foliation dips in different directions within individual blocks. Three samples of these limestone blocks (samples AM/96, 97, 98) yielded Late Permian large foraminifera (Supplementary Table 1; Fig. 19A-L). These marble blocks are interpreted as fragments of the low-grade-metamorphosed Palaeotethyan Ankara melange (Karakaya Complex), as exposed within the Sakarya Zone. The blocks of marble are believed to have been tectonically incorporated into the Neotethyan Ankara melange related to latest Cretaceous-Paleogene late-stage subduction and/or continental collision (see Robertson et al., 2023). In places (e.g., near Şerefli; Fig. 3), the marble blocks are intersliced with volcaniclastic sandstone, volcaniclastic breccia and calciturbidites (locally inverted). Farther east, near Kozanlı (GPS: 36S 83446/19120), scattered generally elongate blocks of well-stratified carbonate rocks exhibit linear fault-bounded edges, as seen on satellite images. A large, gently dipping, block of well-bedded oolitic and bioclastic limestone (up to thick-bedded) contains benthic foraminifera of late Barremian-early Aptian age (samples AM/100, 101) (Supplementary Table 1). Similar facies occur within limestone blocks within isolated exposures of the Ankara Melange farther west (near Kandilköy). These Lower Cretaceous neritic limestones are interpreted as accreted fragments of a much larger carbonate platform (see Discussion).

The main points from Area 3 are: (1) Uppermost Triassic and Middle Jurassic radiolarites are present and also Upper Triassic and Lower Cretaceous carbonate rocks; (2) The Cretaceous limestones include shelf, as well as calciturbidites and debris-flow deposits; (3) Blocks of Upper Permian marble occur within the Neotethyan Ankara Melange in this area. Similar Upper Permian marble blocks have also been reported from Area 2 (Dereköy) (upper thrust sheet) (Akyürek et al., 1997). Numerous blocks of Permo-Triassic and Jurassic-Cretaceous carbonate rocks have also been mapped within the Neotethyan Ankara Melange

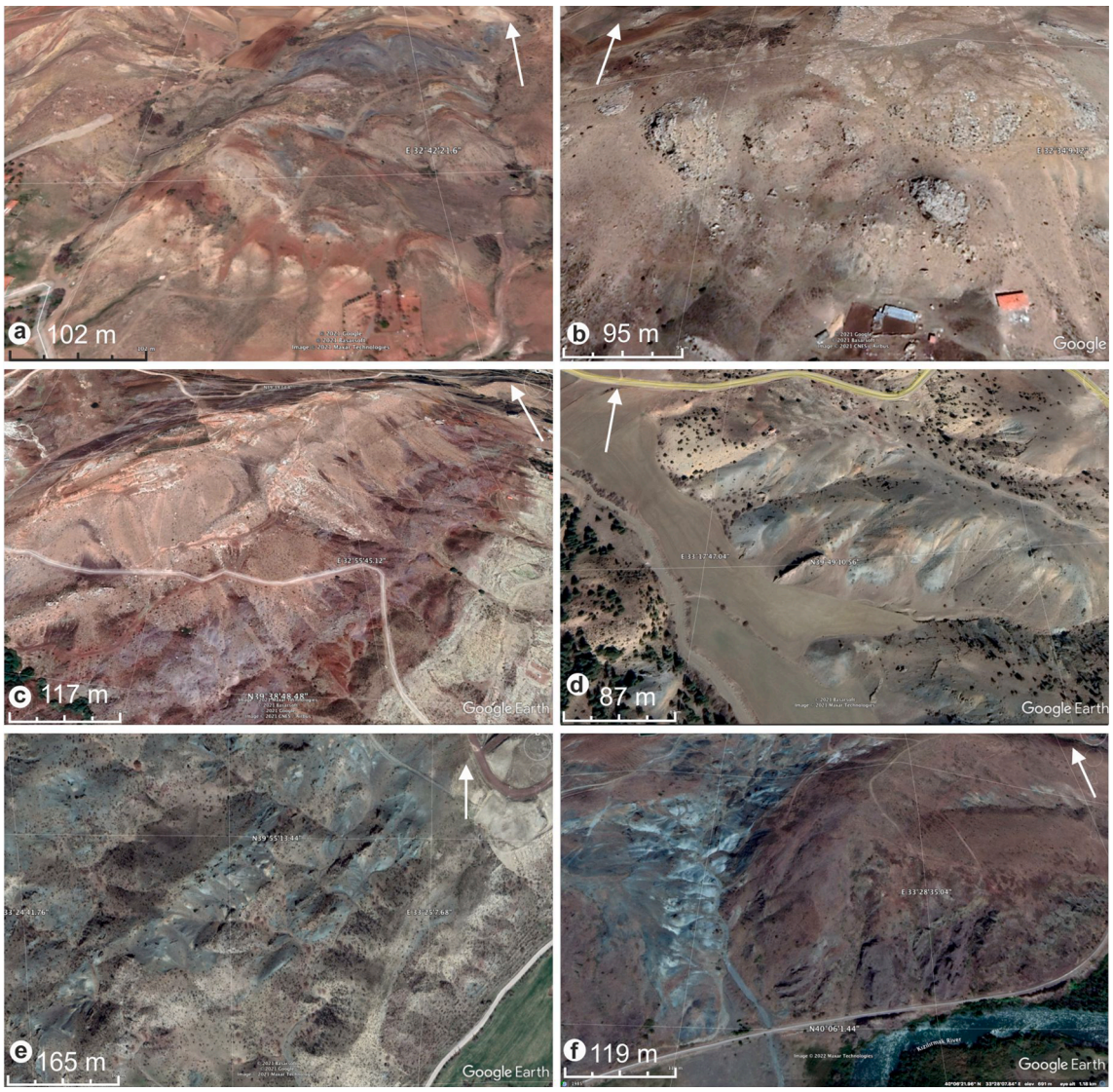

Fig. 7. Satellite images of key structural features. a, Imbrication of volcanic-sedimentary units (pink-brown–red) in the south and serpentinite-rich units (grey) in the north). The fabric shows isoclinal folding; near Karacakaya, Area 1; tilted view; b, Blocks of white neritic limestone; NW of Dereköy, Area 2; vertical view; c, Steeply dipping to inverted volcanic-sedimentary melange (upper unit) in the southeast, unconformably overlain by steeply dipping uppermost Cretaceous-Paleogene turbidites (Haymana Fm.). The ridge behind includes Lower Cretaceous limestones and ophiolitic rocks (Beynam ophiolite); NE of Karaali, Area 4; d, NE-SW trending serpentinite-dominated melange; SW of Hisarköy, Area 5; oblique view; e, Elongate bands of serpentinite (grey) and volcanic-sedimentary lithologies (purple-brown). Note the repetitive interlayering; SE of Kızılırmak River; vertical view; f, Upper Jurassic-Lower Cretaceous volcanic-sedimentary successions (reddish brown, N of Kızılırmak River); wedge-shaped serpentinite (grey) to the west; East of Kalecik (Area 6); oblique view. (For interpretation of the references to colour in this figure legend, the reader is referred to the web version of this article.)

along the northern and northeastern margins of the Çankırı Basin; e.g., Boğazkale area (Area 8) (Fig. 4) (Akçay et al., 2007; Sarıfakıoğlu et al., 2011, 2017). Upper Permian marble blocks are commonplace within the adjacent Palaeotethyan Ankara Melange (Karakaya Complex) (Norman, 1973a, 1984; Akyürek et al., 1984, 1997), suggesting this as the source of the Upper Permian marble blocks in the Neotethyan Ankara Melange.

4.4. Area 4: Beynam-Karaali

Several steeply dipping litho-tectonic units are exposed in the area between Karaali in the southeast and Beynam in the northwest (Figs. 4, 5c), particularly along the crest and both flanks of a prominent NE-SW trending ridge (Akyürek et al., 1984, 1997; Okay et al., 2022) (Fig. 7c). Sarıfakıoğlu et al. (2011, 2017) envisaged the outcrop as mainly ophiolitic melange with an over-riding ophiolite (Beynam ophiolite), folded into the core of a NE-SW trending large-scale syncline. In contrast, Okay et al. (2022) remapped the same ophiolite as being sandwiched between accretionary melanges of different age and composition (Fig. 5c).

In the southeast, adjacent to the Haymana Formation (pale coloured in Fig. 7c), an exposure of volcanic-sedimentary melange (here informally termed the upper unit (=Holos accretionary unit of Okay et al., 2022) includes alkaline basalts interbedded with pelagic limestone with *Halobia* sp. of Late Triassic age. Late Jurassic-Early Cretaceous (Kimmeridgian-Hauterivian) radiolarites were previously reported (Sarıfakıoğlu et al., 2011, 2017). The upper unit includes numerous blocks of neritic limestone with corals, calcareous algae, bivalves, belemnites, gastropods and also benthic foraminifer of late Norian-Rhaetian age. Rare blocks of pink micritic limestone (interpreted as slope facies) include thin-shelled bivalves and ammonites, also of Late Triassic age. Radiolarian cherts, interbedded with pelagic limestones and basalt were recently precisely dated as Middle-Late Jurassic (mainly Bathonian-

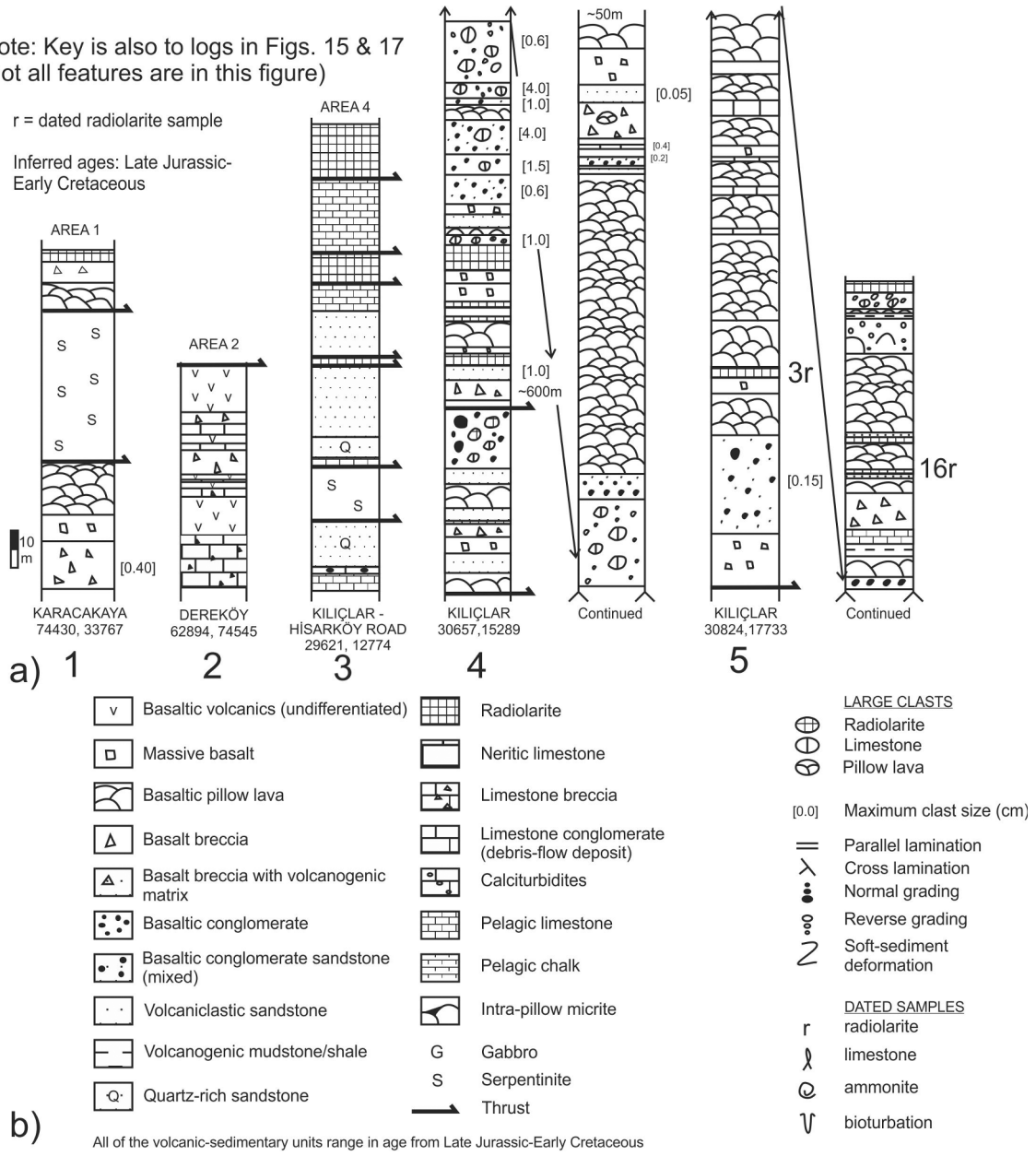

Fig. 8. A, measured sedimentary logs of volcanic-sedimentary successions in areas 1 (Karacakaya-Eryaman), 2 (Derekoy) and 4 (Edige-Kilıçlar); b, key to the logs in Fig. 8a, 15 and 17 and 19; see Fig. 3 for locations.

Oxfordian) (Okay et al., 2022).

The volcanic-sedimentary melange (upper unit) is in tectonic contact to the northwest with a thin, elongate strip of ophiolitic peridotite (locally with listwaenite blocks), followed by a thin slice of carbonate rocks that includes radiolarian-rich marls with Aptian-Albian radiolarians (Sarıfakıoğlu et al., 2011, 2017). Beneath, an important contact with ophiolite-related lithologies was mapped as tectonic by Sarıfakıoğlu et al. (2011, 2017), but as stratigraphic by Okay et al. (2022) (Fig. 11a). These lithologies include debris-flow conglomerates containing limestone and basalt clasts, with basaltic flows between. Pelagic limestones contain Calpionellids of Early Cretaceous (Berriasian) age (Okay et al., 2022).

The underlying relatively intact Beynam ophiolite (Otlubel accretionary unit of Okay et al., 2022) is exposed to the northwest (Fig. 11a). According to Sarıfakıoğlu et al. (2011, 2017), the ophiolite includes gabbro-dolerite with minor plagiogranite intrusions, sheeted dykes and basaltic lavas. According to Okay et al. (2022), the ophiolite comprises basalt, diabase and plagiogranite, with a lenticular slice of gabbro at the base. Zircons from two plagiogranites samples were dated by the U-Pb method as 161.2 ± 3.2 Ma (Mid-Late Jurassic, i.e., Callovian-Oxfordian, when errors are considered) (Okay et al., 2022). The basalts have IAT to boninitic chemical compositions (Okay et al., 2022).

Farther northwest the ophiolite is in high-angle tectonic contact with ophiolite-related melange ('lower unit'=Kuyumcudağ accretionary unit of Okay et al. (2022) (Fig. 11a), mainly sheared serpentinite. Subordinate sheared intercalations of volcanic-sedimentary lithologies include alkaline basalts, radiolarites dated as Middle Jurassic (Bajocian) and also pelagic limestones (Sarıfakıoğlu et al., 2011, 2017).

During this work, the volcanic-sedimentary melange in the southeast (upper unit) and the mainly ophiolitic melange in the northwest (lower unit) were examined in excellent local outcrops (Fig. 11a). In the southeast, near Karaali, the outcrop includes a relatively intact succession of inverted pillow lavas. Feldspar-phyric lava is interbedded with limestones that show evidence of redeposition by gravity flow processes

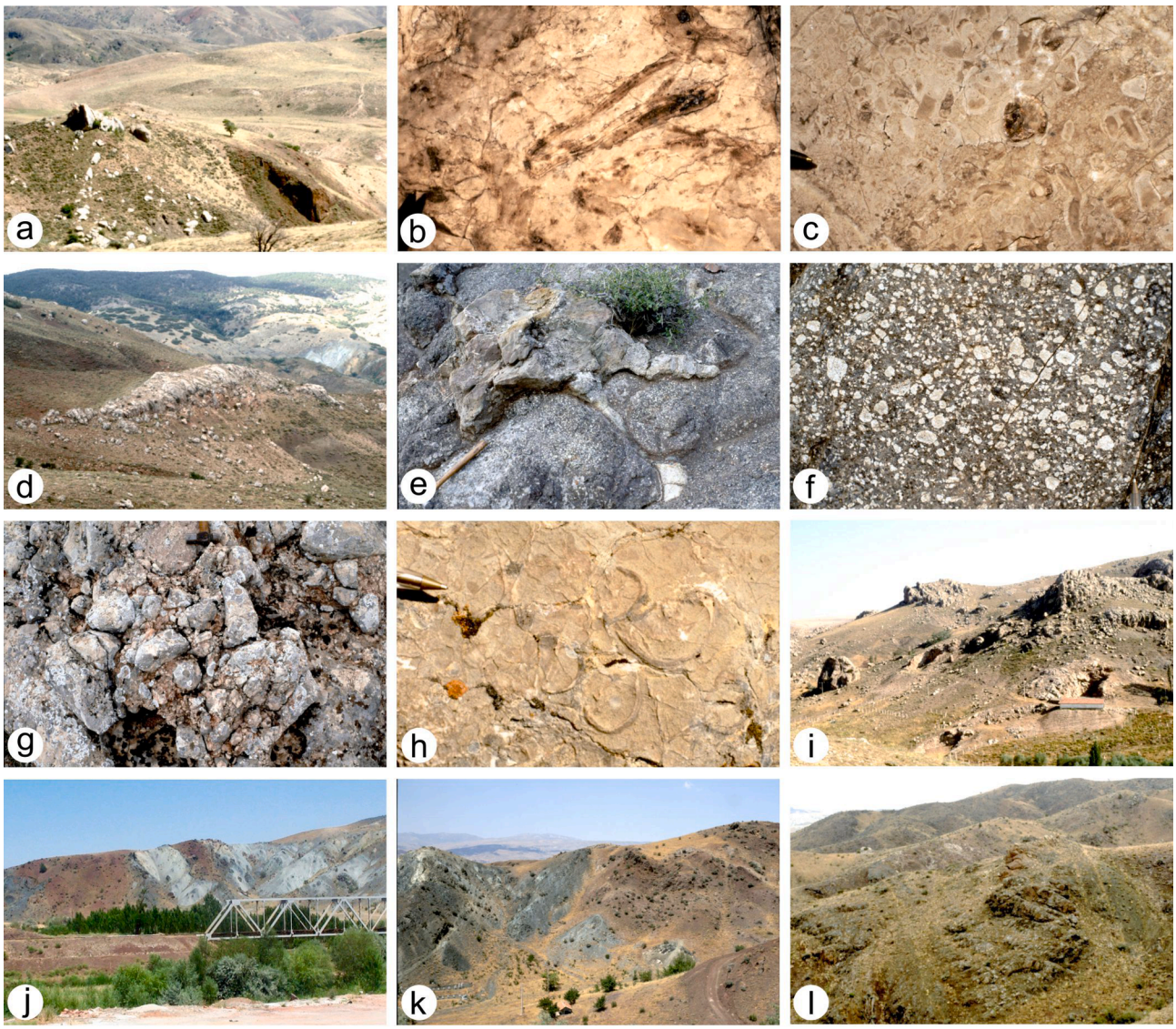

Fig. 9. Field photographs of Areas 1–2 and 5. a-c, Melange in Area 1, Karacakaya. a, Imbricated basaltic igneous rocks (vegetation covered), neritic limestone (white) and radiolarite (reddish-brown, to right), 0.4 km SW of Karacakaya; field of view in middle distance c. 250 m; view to N; b, Block of neritic limestone, dominated by rudist bivalves (some in life position); field of view 25 cm; c, As b, but with abundant coralline algae and some gastropods. b-c from near Karacakaya (GPS: 36 T 74430/33767); pen for scale in left; d-i, Melange in Area 2, Dereköy; d, Volcanogenic rocks with a lenticular slice of neritic limestone; sheared serpentinite (pale grey) behind, c. 1 km NW of Dereköy (GPS: 36S 63791/74110); field of view in middle distance c. 200 m; view to NE; e, Feldspar-porphyritic basalt, with abundant inter-pillow pelagic carbonate; pencil for scale in left; field of view in middle distance c. 200 m; view to NE; e, Feldspar-porphyritic basalt, with abundant inter-pillow pelagic carbonate; pencil for scale in lower left; f, Feldspar-phyric basalt (ankaramites), location as d; pen for scale in lower right; g, Limestone debris-flow deposits with sub-rounded to sub-angular clasts of neritic limestone in a poorly sorted granular matrix, locality as d; field of view c. 30 cm; h, Rudist bivalves in a large block of neritic limestone, showing reworked, mostly concave-downwards valves, locality as d; pen for scale in upper left; i, Volcanogenic unit with abundant blocks of neritic limestone (locality near d, GPS: 36S 61422/75294); house and track for scale; view to N; j. Melange in Area 5: SE of Elmadağ. View (to SE) of ophiolitic melange (mainly serpentinite; grey) on the right, intersliced with lava and sediments (reddish brown), near Kızılırmak (river), taken from the Ankara-Kırıkkale highway at GPS: 36S 36710/19452); railway bridge for scale; view to south; k, Intercalated slice of sheared ophiolitic melange (lower, left) and volcanic-sedimentary unit (upper right); same area as j; house and track for scale; view to SE; l, Alkaline volcanic rocks interbedded with volcanic debris-flow deposits, near Kılıçlar (Floyd 1993) (Fig. 8, log 4), GPS: 36S 30657/15289; field of view in middle distance c. 150 m; view to SE.

(turbidites and/or mass-flow deposits) together with scattered large limestone blocks (Fig. 11 a-c). The limestone blocks can be traced laterally for up to several hundred metres, following the NE-SW tectonic trend in this area. The bedding in the limestones is sub-parallel to the margins of the blocks. Local successions within individual limestone blocks include pink micritic limestone, passing depositionally upwards into limestone debris-flow deposits that include coral, coralline algae and scattered volcanic debris. Two samples from interbedded clasts in one block contain Lower Jurassic benthic foraminifera (Supplementary Table 1; sample AM/81, 82; Fig. 20a-c).

In the northwest (near Beynam), the melange (lower unit) is dominantly serpentinised ultramafic rocks, with inclusions of gabbro (layered and pegmatitic) and lenticular slices of basalt, radiolarite and brecciated pelagic limestone (locally recrystallised) (Fig. 11e). The serpentinite in this outcrop is cut by numerous narrow (several m-wide) shear zones. In the northeast (near Esen Yayla, outside the area mapped by Okay et al., 2022), the bedding in the volcanogenic succession is truncated at a high angle by sheared serpentinite (Fig. 11d) and brittle fragmentation is developed along the contacts between the adjacent units.

The main points from Area 4 (Beynam-Karaali) are: (1) Volcanic-

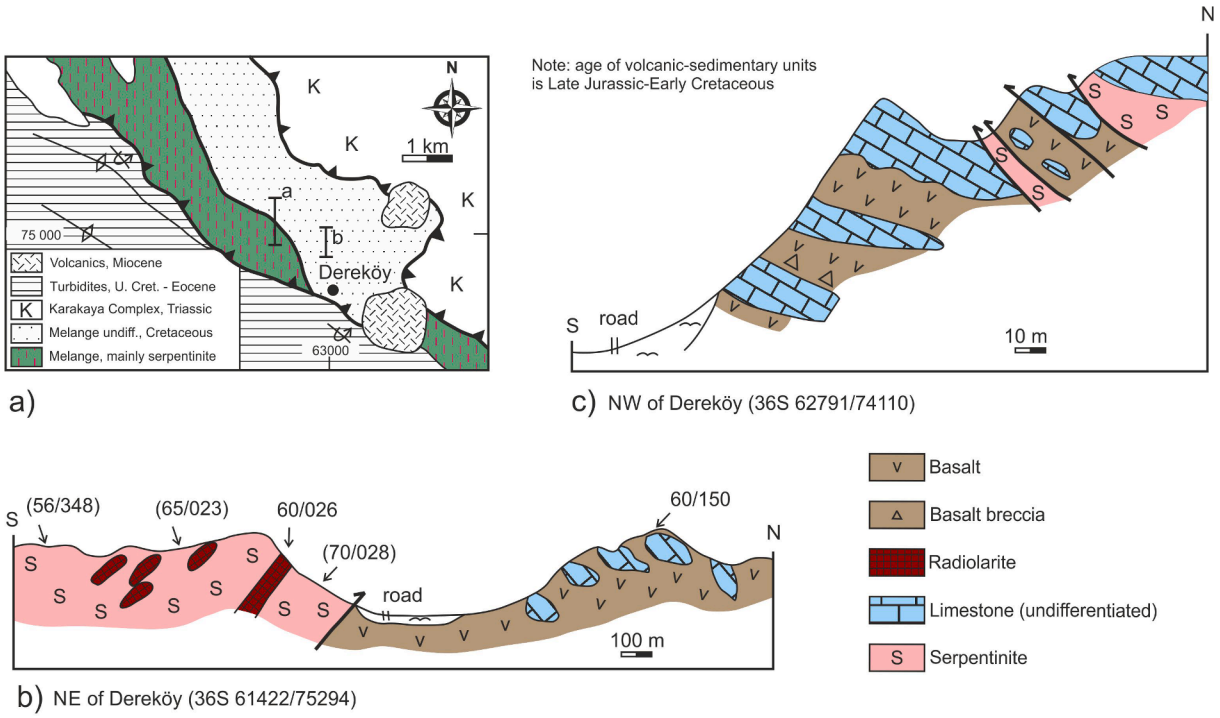

Fig. 10. Ankara Melange in Area 2, Dereköy, SW of Ankara (see Fig. 3 for location). a, Local geological map (based on Rojay, 2013) showing the location of the local sections; b-c, local cross-sections near Dereköy (c. 30 km E of Haymana). See Fig. 3 for key to map and Fig. 8b for key to sections.

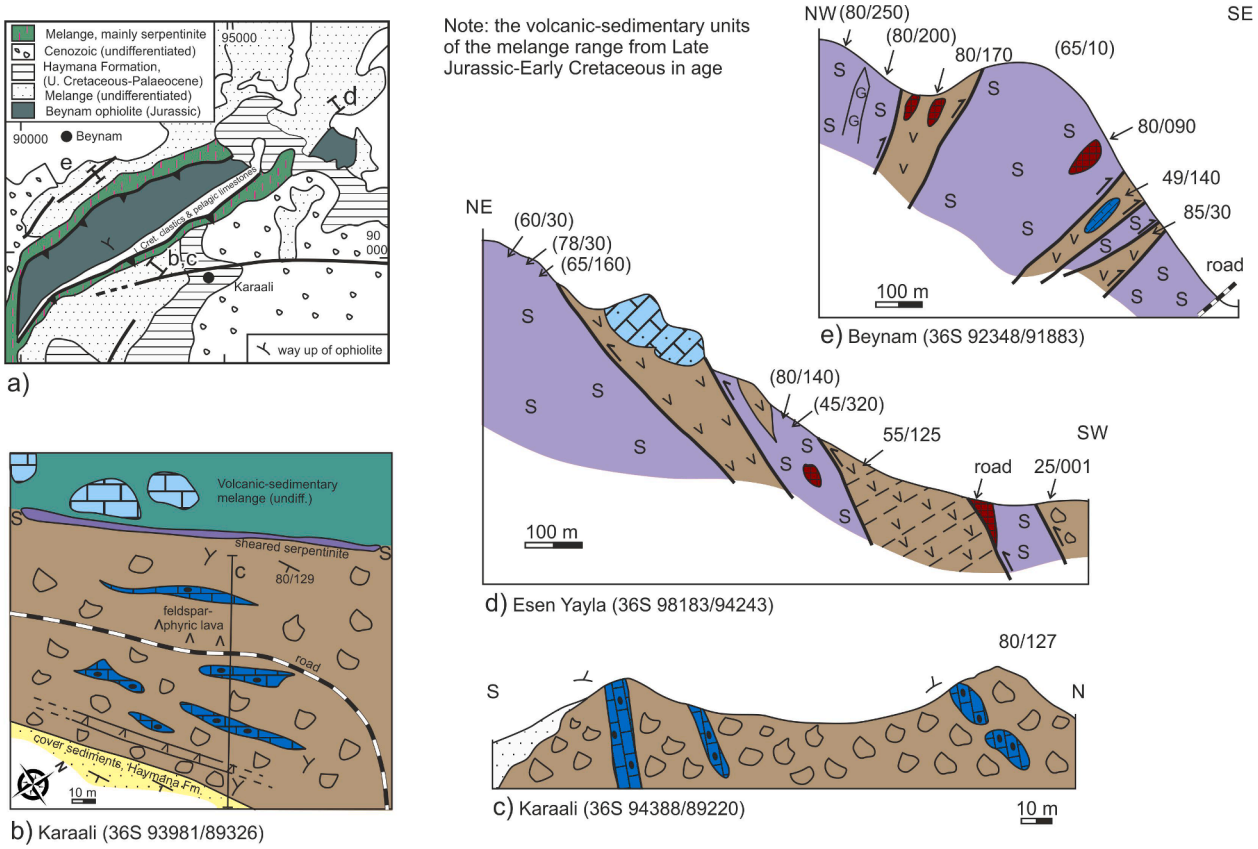

Fig. 11. Ankara Melange in Area 4, Beynam-Karaali, S of Ankara (see Fig. 3 for location). a, Outline geological map (based on Akyürek et al., 1997; Sarıfakıoğlu et al., 2011), showing the locations of local sections; b, local sketch map, near Karaali; c, local cross-section, also near Karaali; d, local cross-section to the northwest, near Esen Yayla; e, local cross-section to the northeast, near Beynam. See Fig. 3 for key to sections. Note: dips and strikes of shear planes are in brackets, and without brackets for bedding.

sedimentary units of maximum Late Triassic-Early Jurassic age and maximum Late Jurassic-Early Cretaceous age are exposed in the area; (2) The older; i.e. Upper Triassic-Lower Jurassic interval (upper unit) is associated with reef blocks, slope facies and lithified hemipelagic *Halobia*-bearing peripelagic ooze (drift deposits); (3) The younger unit (mainly Bathonian-Kimmeridgian) is interbedded with proximally derived redeposited neritic carbonate, radiolarites, pelagic limestones, basalt and basaltic volcanic debris, similar to Area 3 (Dereköy; see above). The two dated intervals might represent a single accreted Upper Triassic-Lower Cretaceous succession of shallow to deep water limestones and radiolarian sediments. More probably they represent two different successions of different age ranges that accreted separately and were later tectonically juxtaposed; (4) The relatively intact Upper Jurassic (Oxfordian-aged) boninitic ophiolite is interpreted as accreted SSZ-fore-arc oceanic lithosphere (Okay et al., 2022); (5) The overlying debris-flow conglomerates, basaltic flows and Early Cretaceous (Berriasian) pelagic limestones can be interpreted as part of the *in situ* cover of the ophiolite, further constraining its age; (6) The largely ophiolitic melange in the northwest (lower unit) includes Middle Jurassic radiolarites (Okay et al., 2022) which could be associated with the ophiolite; (7) This melange (lower unit) locally shows evidence of re-imbrication during or after initial accretion; (8) The thrust stack was rotated to sub-vertical (to locally inverted) after accumulation of the unconformably overlying latest Cretaceous-Paleogene sedimentary cover (Haymana Formation), which is also steeply dipping, presumably related to late-stage subduction and/or continental collision; (9) Accordingly, the melange should become structurally deeper generally towards the northwest (Okay et al., 2022); (10) The structural order is likely to record the accretion of seamount and fore-arc ophiolite units in a subduction trench setting; (11) The setting of the ophiolite in the mid-level of the tectono-stratigraphy, in contrast to several other areas (e.g., Edige and Beynam ophiolites) points to re-imbrication during or after initial accretion (see Structure below).

4.5. Area 5: Edige-Kılıçlar

This outcrop forms a substantial NNW-SSE trending belt (c. 14 km long × up to 6 km across) both to the north and the south of an imaginary line between Edige and Kılıçlar (Figs. 3, 12). Three main units are exposed related to the Neotethyan Ankara Melange: (1) variably dismembered volcanic-sedimentary successions; (2) ophiolitic melange; (3) semi-intact Edige ophiolite. The southeastern part of the area exposes lenses of volcanic-sedimentary lithologies and ultramafic ophiolitic melange, on an up to several kilometre scale (Fig. 9j), whereas the northwest of the area is dominated by the Edige ophiolite (Sarıfakıoğlu et al., 2011, 2017; Dönmez et al., 2009). In the northwest, the melange is overthrust by the Palaeotethyan Ankara Melange (Karakaya Complex) (Norman, 1973a, 1984), with a NW-dipping (c. 30°) contact (Fig. 5d; Supplementary Fig. 1a,b).

The volcanic-sedimentary unit is very well exposed as a NNE-SSW trending tectonic lens near Kılıçlar (Fig. 3). A section that was studied by Floyd (1993) consists, in decreasing order of abundance, of alternations of alkaline pillow lavas with inter-pillow carbonate sediment (Fig. 13c), matrix-supported conglomerates, volcaniclastic sandstones (with pelagic limestone clasts) (Fig. 9l), radiolarite, lava breccia and massive lava (Fig. 8a, b; log 4). The lavas are commonly highly vesicular and some are felspar-phyric. Another intact volcanic-sedimentary succession, c. 2 km to the ENE, includes interbedded pelagic limestones and

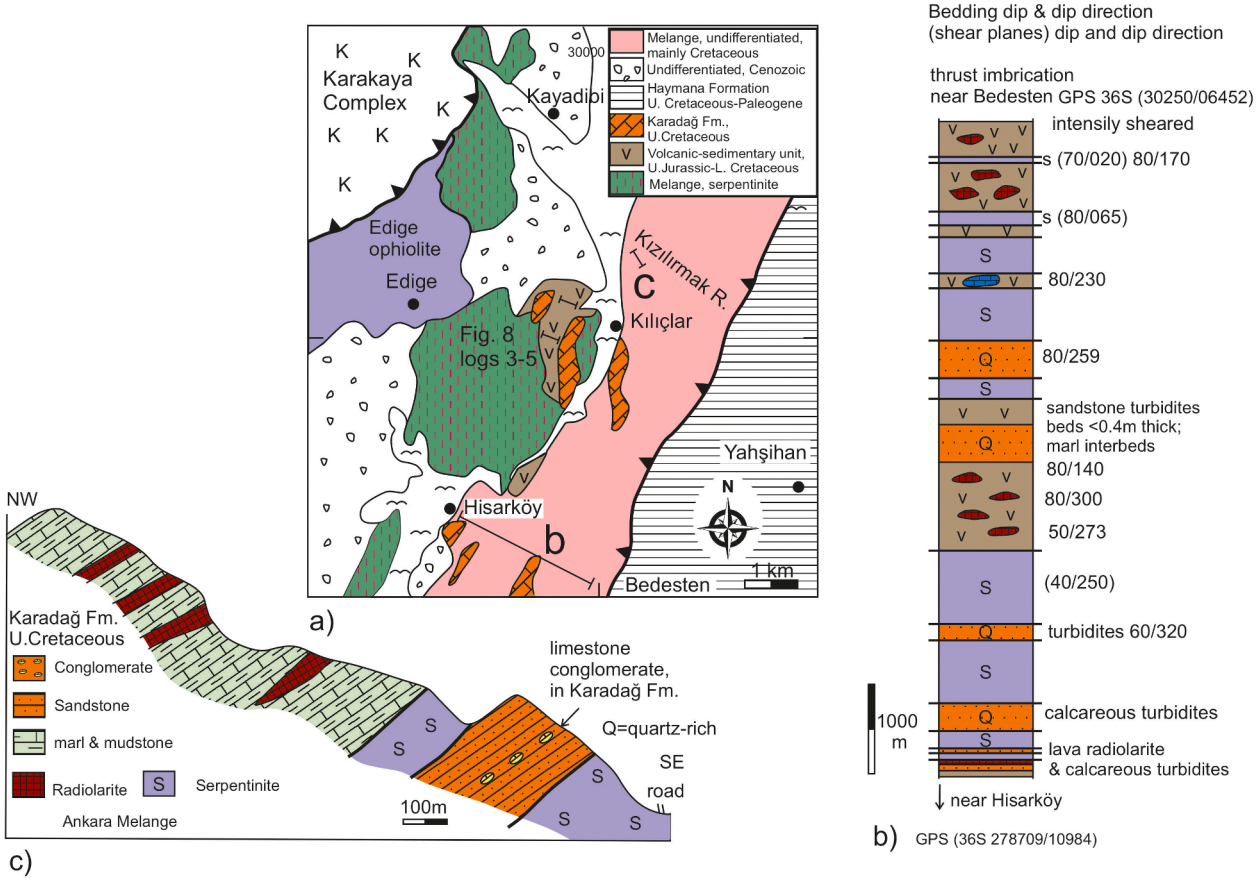

Fig. 12. Ankara Melange in Area 5, Edige-Kılıçlar, SE of Ankara (see Fig. 3 for location). a, Outline geological map (based on Sarıfakıoğlu et al., 2011) showing a local section (simplified from Rojay et al., 2004); b, Road log between Hisarköy and Bedesten; c, Local cross-section farther north. Dips and strikes are shown with brackets for shear planes but without brackets for bedding. See also Fig. 8, logs 3–5.

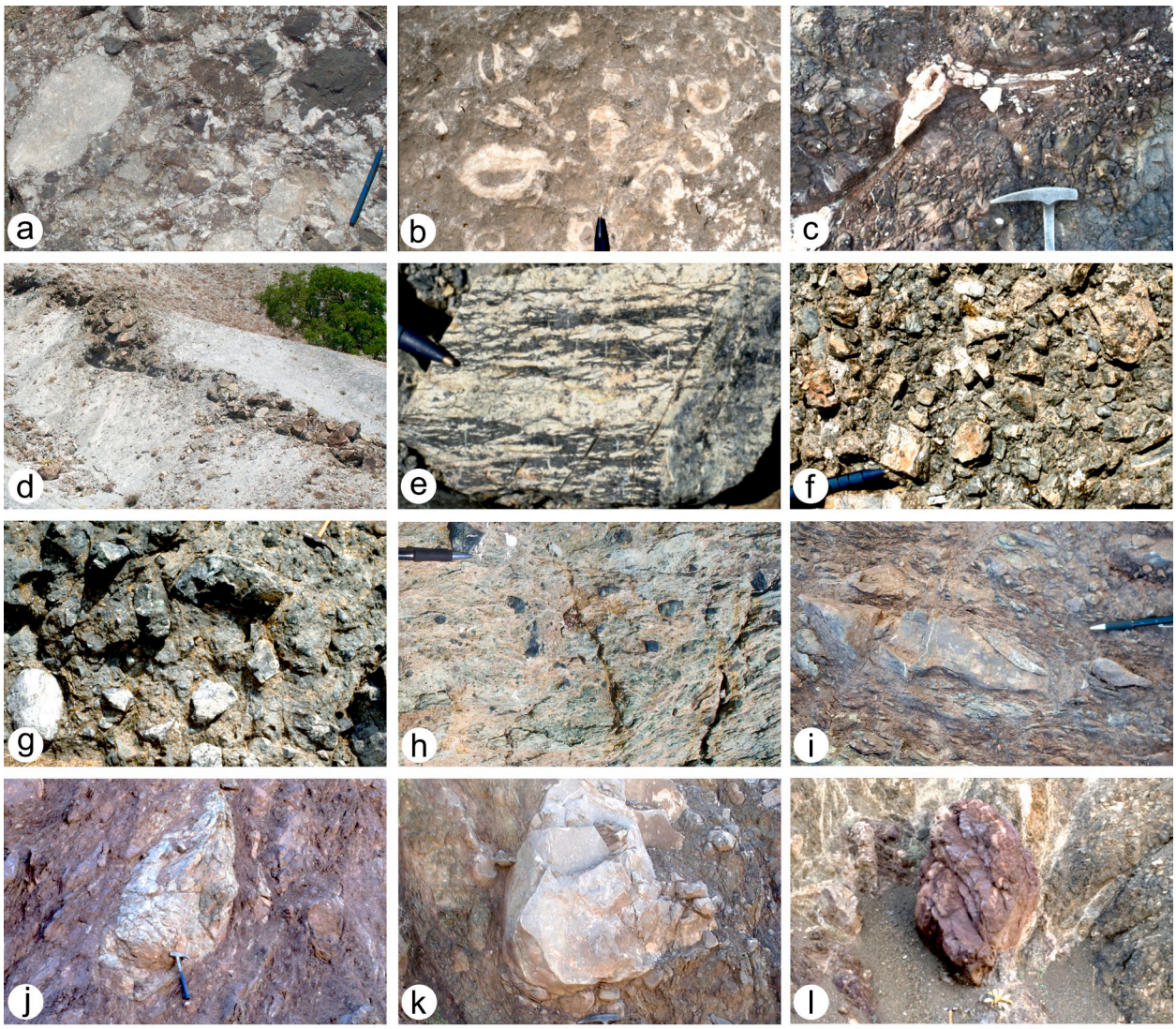

Fig. 13. Field photographs of outcrops in Area 5, Edige-Kılıçlar. a, Debris-flow conglomerate with clasts of neritic limestone (pale) and basalt (dark) in a matrix of smaller clasts of similar material; near Kılıçlar, near GPS: 36S 30657/15289; pen for scale; b. Massive rudist-rich limestone within a block of neritic limestone; location near a; pen for scale; c, Pillow lava with interpillow pelagic sediment; Kılıçlar area; GPS: 36S 30916/17735; hammer for scale; d, Massive ophiolitic gabbro, cut by isolated diabase dykes, Karaburun Tepe, GPS: 36S 255393/19132; main dyke is c. 2.5 m thick; e, Mylonitic serpentinite from near the tectonic contact between serpentinite and gabbro; pen for scale; e-h near Kılıçlar GPS near d; f, Serpentinite breccia; the angular and lack of clast sorting suggests a tectonic (physical origin), near GPS 36S 31534, 17307; pen for scale; g, Serpentinite breccia-conglomerate. The variable clast rounding and granular serpentinite matrix suggests a debris-flow deposit, GPS near d; hammer for scale (top right); h, Matrix-supported serpentinite breccia-conglomerate. The well-rounded clasts and abundant granular matrix again suggest a debris-flow origin, followed by shearing; GPS near d; pen for scale; i, Tectonically boudinaged massive lava in a matrix of strongly sheared basalt, radiolarite and mudstone. Highway cutting near Balaban bridge over the Kızılırmak, GPS: 36 T 33117/19800; hammer for scale (top right); j, Strongly sheared, mainly massive basalt set in a sheared volcaniclastic and shale matrix; location near l; hammer for scale; k, Rounded block of neritic limestone in a sheared volcaniclastic matrix; the block margins are slickensided; GPS as i; limestone block is c. 1.5 m long; l, Sheared block of radiolarite within sheared volcanogenic material; Bedesten-Hisarköy road section, near GPS: 36S 23870/10984; chert block is c. 1 m long.

radiolarites (Fig. 8a, b; log 5). Radiolarite from near the base of this succession was dated as probably Early Cretaceous (sample AM/3), from the higher part of the succession as Albian (sample AM/15), and from the highest levels of the succession (sample AM/16) as late Barremian-early Aptian (see Supplementary Table 2). A sample from this area was previously dated as Berriasian-late Hauterivian (Sarıfakıoğlu et al., 2011, 2017). In addition, a sample intercalated with OIB pillow lava from along the Elmadağ-Kırıkkale highway has been dated as late Valanginian-late Hauterivian (Bortolotti et al., 2013, 2018). The likely overall age range of the volcanic-sedimentary succession in Area 5 is thus late Valanginian-Albian.

The relatively intact Edige ophiolite is dominated by serpentinised harzburgite with dunite interlayers (including chromite), subordinate gabbro and localised basaltic extrusives. Crosscutting diabase dykes (Fig. 13d) have variable N-MORB, E-MORB and also IAT-type compositions (Tankut et al., 1998). Basic rocks are locally cut by boninitic and rhyolitic dykes, suggesting a range of primitive to evolved SSZ products. Associated radiolarites have been dated as Bajocian-early Callovian (Sarıfakıoğlu et al., 2011, 2017), suggesting a Mid-Late Jurassic age for the ophiolite, assuming that the radiolarites were originally interbedded with or overlay the extrusive rocks. Rare associated amphibolites (undated) are interpreted as fragments of the original metamorphic sole of the Edige ophiolite.

The melange in Area 5 (Edige-Kılıçlar) is characterised by sheared ophiolitic rocks and more intact volcanic-sedimentary units. Repetitions of these two lithological associations are remarkably regular in some

areas, as seen on satellite images (Fig. 7d, e). The serpentinite in the melange ranges from variably sheared to mylonitic (Fig. 13e), to brecciated (Fig. 13f). Rare occurrences of variably sheared, matrix-supported conglomerates composed of serpentinite could have a sedimentary origin, with a tectonic overprint (Fig. 13g, h). The volcanic rocks within the melange in this area are typically of OIB composition, although IAT is also reported (Rojay et al., 2004). The melange rarely includes blocks and talus of variably recrystallised shallow-water limestones (Fig. 13a, b). The contact zones (up to c. 10 m thick) between the volcanic-sedimentary and the serpentinite-dominated melange exhibit highly sheared phacoidal fabrics, as well exposed along the Ankara-Kırıkkale highway (e.g., near Balaban bridge; Fig. 13i-l) (see Structure, below).

Intercalated slices and blocks of clayey limestone (i.e. hemipelagic limestone), and both siliciclastic and volcaniclastic turbidites have been mapped as the Upper Cretaceous Karadağ Formation (Dönmez et al., 2009). In places, the outcrop encompasses clayey limestone, calcareous mudrock, calcareous sandstone turbidites and minor conglomerates (debris-flow deposits), in the form of numerous lenticular NNE-SSW trending tectonic lenses and blocks (typically up to 10 s of m across and 100 s m long). There are also numerous smaller lenticular bodies, mainly composed of clayey limestone, radiolarite, mudstone, thin to medium-bedded calciturbidites and sandstone turbidites (Kocatepe Member), which are also referred to the Karadağ Formation (Dönmez et al., 2009). The Karadağ Formation represents the highly deformed Upper Cretaceous sedimentary cover of the Ankara Melange, of post-accretionary origin in this area (Akyürek et al., 1984). The formation is interpreted as an Upper Cretaceous fore-arc basin succession that became tectonically intersliced with the Neotethyan Ankara Melange during latest Cretaceous-Paleogene final closure of the İzmir-Ankara ocean (Northern Neotethys) (see Robertson et al., 2023). In Area 5, the Neotethyan Ankara Melange is overlain by contrasting latest Cretaceous-Paleogene deep-water clastic sedimentary rocks (Haymana Formation) (Fig. 18l), which are outside the scope of this paper.

The main features of Area 5 are: (1) Variably dismembered Lower Cretaceous (Valanginian-Albian) volcanic-sedimentary successions; (2) Dismembered SSZ-type Edige ophiolite, possibly of Middle-Late Jurassic age assuming that the dated radiolarites originated with the ophiolite; (3) Upper Cretaceous mixed siliceous, calcareous and clastic deep-sea sedimentary rocks (Karadağ Formation) that were incorporated into the Ankara Melange, probably related to late-stage subduction and/or continental collision.

4.6. *Area 6: Kalecik-Çandır*

Farther north, the tectonic trend changes from NE-SW to more N-S. The Ankara Melange in this area is extensively exposed from near Kalecik to Çandır (Dönmez and Akçay, 2010) (Fig. 3).

Imbricated volcanic-sedimentary successions are very well exposed both to the west and the east of Kalecik, separated by a Neogene syncline (Fig. 5e), and they also crop out farther north near Çandır (Fig. 14a). Exposures to the west of Kalecik include vesicular alkaline basalt (Rojay et al., 2004), blocks of shallow-water limestone and also radiolarite (e.g., near Gölköy) that are dated as Bajocian (sample AM/50) (Supplementary Table 2). Relatively intact volcanic-sedimentary successions to the east of Kalecik are exposed on both sides of the Kızılırmak River (Fig. 7f). Elsewhere in the Kalecik-Çandır area (Area 6), the melange is characterised by anastomosing sheared serpentinite that encloses variably disrupted volcanic-sedimentary lithologies. In the southeast of the area, the melange is characterised by two main, lenticular thrust sheets and numerous smaller lenticular outcrops of mixed clastic-hemipelagic sediments that are mapped as the Upper Cretaceous Karadağ

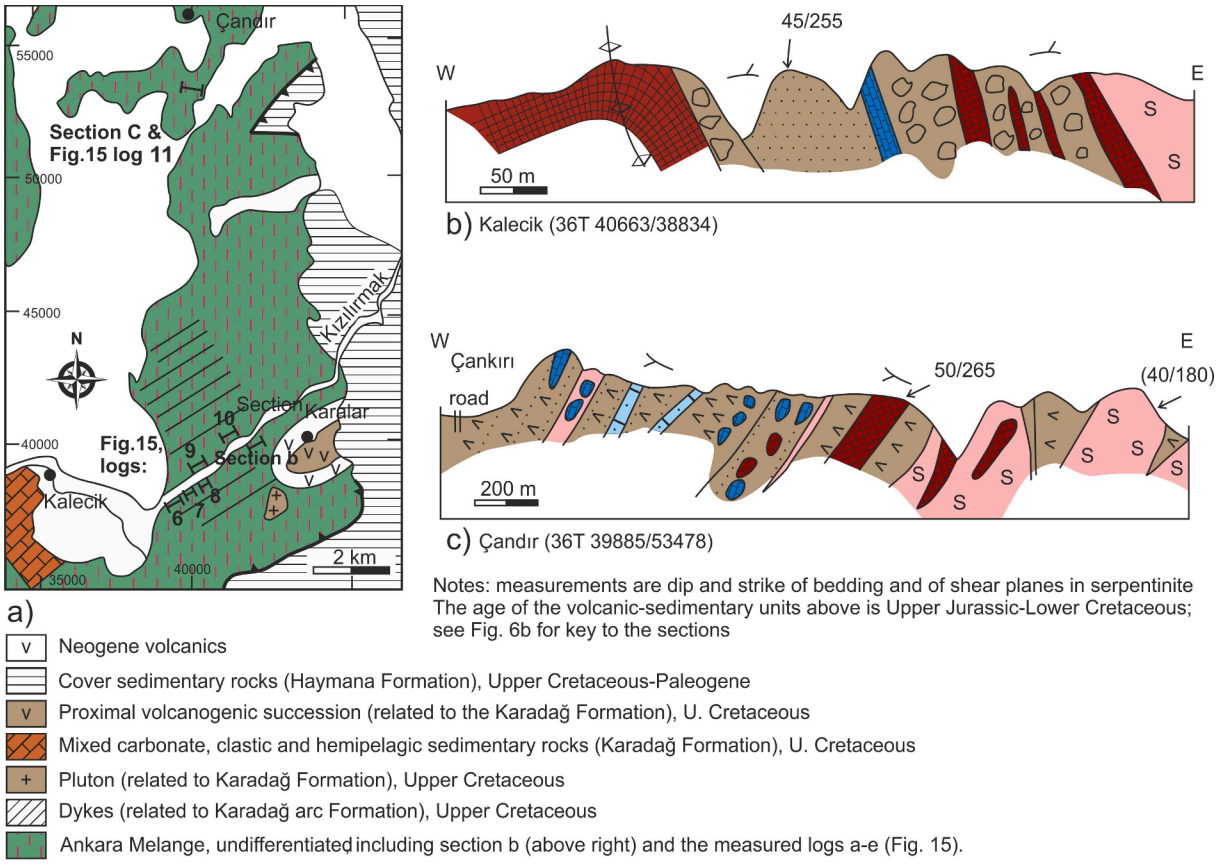

Fig. 14. Ankara Melange in Area 6: Kalecik-Çandır, NE of Ankara (see Fig. 3 for location). a, Outline geological map (based on Sarıfakıoğlu et al. (2011) and Rojay (2013); see Fig. 3 for key; b, local cross-section near Kalecik; c, local section near Çandır; see also Fig. 15, log 11.

Formation, as in Area 5 (Dönmez et al., 2009). Ophiolitic units, mainly gabbro and diabase, as exposed in the southeast of the area, are contiguous with the ophiolitic outcrops in Area 5 (Dönmez and Akçay, 2010).

Steeply dipping to inverted volcanic-sedimentary successions, mostly lavas and redeposited volcaniclastic sandstones, with radiolarian chert intercalations, were logged during this study on both sides of the Kızılırmak River (Fig. 15; logs 6–10). The relative abundances of pillow lava, massive lava, lava breccia and radiolarite vary between the logged successions. The redeposited units range from normal-graded volcaniclastic sandstones (turbidites) to matrix-supported volcaniclastic conglomerates, with shallow-water limestone clasts and redeposited interbeds (Supplementary Fig. 1h). N-MORB has been reported locally in this area (Rojay et al., 2004).

A radiolarite sample from near the base of one measured succession (Fig. 15; log 6) (sample AM/51) was dated as Berriasian, and two other samples from slightly higher in the succession were dated as probably Albian (sample AM/52) and probably Valanginian (sample AM/53). Radiolarite (sample AM/57) in another section slightly farther northeast (Fig. 15; log 10) was dated as Early Cretaceous. Radiolaria from a thin imbricated slice of radiolarite farther northeast (sample AM/60) was dated as probably Valanginian-Hauterivian (Supplementary Table 2). Radiolaria (sample AM/125) from a correlative section on the north bank of the Kızılırmak was dated as Bajocian (Fig. 7e and 15, log 9). Previously, eight samples of radiolarite from a c. 77 m-thick section of radiolarian chert south of Kalecik were dated as Oxfordian-early Hauterivian at the base to Berriasian-Early Aptian at the top (Sarıfakıoğlu et al., 2011, 2017).

An additional representative volcanic-sedimentary succession was logged farther north, in Area 6 south of Çandır (Fig. 14a, c). This is made up of pillow lava, lava breccia, normal-graded volcaniclastic sandstone, redeposited bioclastic limestone (Supplementary Fig. 1i) and matrix-supported conglomerate (Fig. 15, log 11). Clasts include basalt (Supplementary Fig. 1j-l) and neritic limestone with rudist bivalves. Lenticular volcaniclastic beds have erosional bases, overlain by rubbly lava debris, and grade upwards into calcarenite with neritic bioclastic material and small basaltic clasts (<2 cm). Redeposited limestones (samples AM/69, 70, 71) include benthic foraminifera of late Barremian-early Aptian age (Supplementary Table 1).

Area 6 (Kalecik-Çandır) has the following key features: (1) Long intact volcanic-sedimentary successions ranging from Berriasian to Albian, east of Kalecik; (2) Middle Jurassic (Bajocian) radiolarite, west of Kalecik; (3) Upper Cretaceous magmatic and volcaniclastic sedimentary rocks of the arc-related Kavak Formation are exposed in this area, although outside the scope of this paper (see Fig. 18i,j & Supplementary Fig. 1l) (see Robertson et al., 2023).

4.7. Area 7: Eldivan

Area 7, to the west of Eldivan (Fig. 3), includes a large outcrop of melange in the north (NW of Eldivan) (Fig. 5f) and also the relatively intact Eldivan ophiolite which is located at a high structural level in the tectono-stratigraphy (Akyürek et al., 1984). Lavas, pelagic limestones and mudrocks southwest of Eldivan (Fig. 16a) have been mapped as part

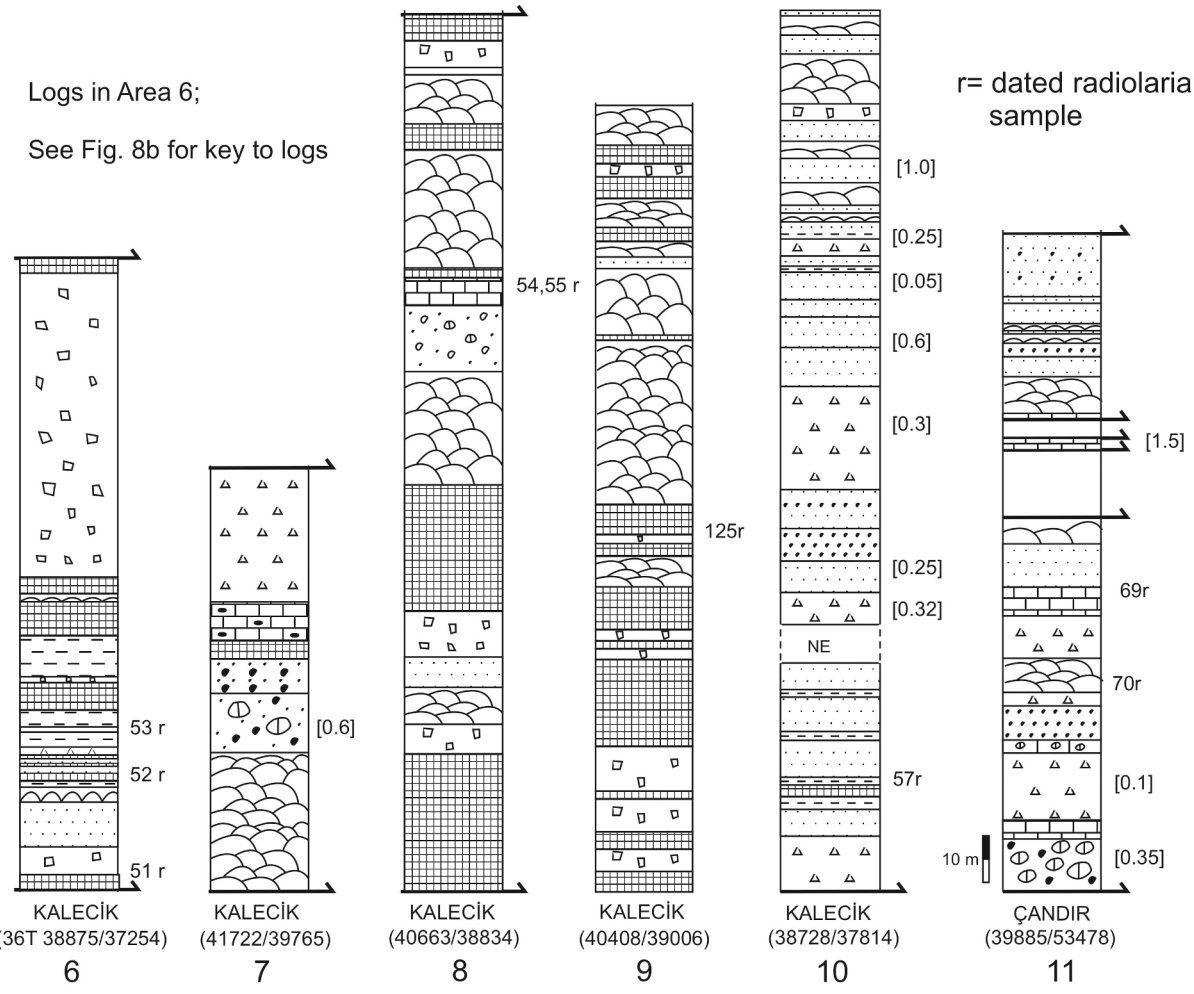

Fig. 15. Measured sedimentary logs of volcanic-sedimentary successions in Area 6 (Kalecik-Çandır); see Fig. 3 for location and Fig. 8b for key to logs.

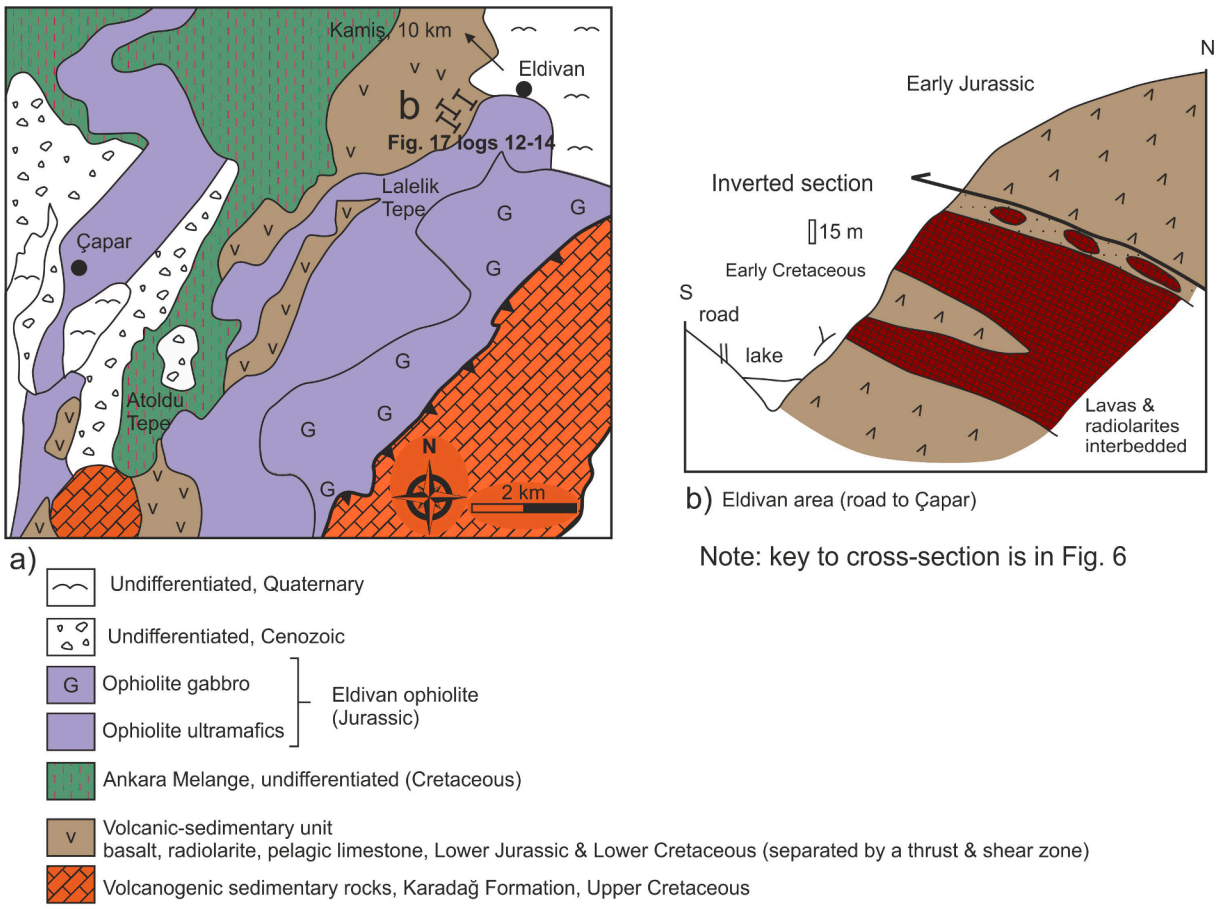

Fig. 16. Ankara Melange in Area 7, Eldivan, far N of Ankara (see Fig. 3 for location). a, Outline geological map (based on Sarıfakıoğlu et al. (2011), showing the location of local section (simplified from Rojay et al., 2004); b, Local cross-section SE of Eldivan; See also Fig. 17, logs 12–14.

of the Eldivan (MTA 100,000 map Çankırı-G30) by Sarıfakıoğlu et al. (2011, 2017) and by Dangerfield et al. (2011). These lavas include E-MORB (Rojay et al., 2004; Çelik et al., 2013). However, these lavas are chemically dissimilar to the SSZ-type ophiolitic lavas reported from this area (Dangerfield et al., 2011), and are instead correlated with one of the associated non-ophiolitic volcanic-sedimentary successions based on field and biostatigraphical evidence.

During this study, three sections were measured southwest of Eldivan (Fig. 16a) (Fig. 17, logs 12–14). These sections are stratigraphically inverted, mainly based on the younging directions of pillow lavas, in contrast to many of the sections measured elsewhere. Also, the local successions are unusually thick and laterally continuous (<100 s m) (Fig. 18a) compared to most other areas.

Radiolaria from two of the above sections were dated as Early Jurassic and also as Early Cretaceous. Specifically, a radiolarite (sample AM/111) from one section (Fig. 17, log 12) was dated as probably late Hettangian-Sinemurian (Fig. 17, log 12). Radiolarite from an adjacent section (log 13) yielded a Hauterivian age. Of two radiolarites from an adjacent section (log 14), the lower one (sample AM/115) gave a probable Aptian age, whereas the upper one (sample AM/117) was dated as Hettangian-Sinemurian (see also Supplementary Table 2).

The dated Early Jurassic pillow basalts are unusually rich in pink, ferruginous intra-pillow pelagic carbonate (Fig. 18b, c, e), together with subordinate amounts of pillow breccia, matrix-supported volcaniclastic sandstones, hyaloclastite with pillow lava fragments (Fig. 18d) and also rare massive lava flows.

The evidence from near Eldivan indicates that two different-aged successions of pillow lavas and interbedded deep-sea sediments (Early Jurassic and Early Cretaceous) are tectonically imbricated and preserved within the lower limb of a large recumbent fold. The northward dipping imbrication is consistent with southward emplacement. The inferred recumbent fold is assumed to have formed during initial incorporation into the accretionary prism and is consistent with northward subduction (see Structure below).

The Ankara Melange is widely exposed northwest of Eldivan (Fig. 5f, 16a), mostly as blocks derived by break-up of volcanic-sedimentary units, together with ophiolitic rocks (e.g., sheared serpentinite, diabase dykes, gabbros). A locally intact volcanic-sedimentary succession, c. 10 km NNW of Eldivan, near Genek (Akçalı) (Fig. 17, log 15), is dominated by pillow lava with abundant intra-pillow pelagic carbonate. Intercalations of pink pelagic carbonate (<4 m thick) were previously dated as Early Jurassic based on ammonites (Fig. 18f), belemnites and benthic foraminifera (e.g., *Involutina liassica*) (Akyürek et al., 1984). An Early Jurassic age is confirmed here based on the benthic foraminifera present (sample AM/118; Supplementary Table 1). The intact volcanic-pelagic succession is overlain by volcaniclastic conglomerate, with blocks of pillow lava and brecciated pelagic carbonate. Interbedded chert lenses (sample AM/119) (Fig. 18g) were dated as late Cenomanian using Radiolaria (Supplementary Table 2).

Another melange outcrop, c. 9 km NW of Eldivan (3 km E of Kamışköy; GPS 36 T 31785/89580), is dominated by red chert, pillow lava and serpentinite, and includes a lens (15 m × 7 m) of pale grey, thinly bedded pelagic limestone. Calpionellids and benthic foraminifera from similar pelagic limestone in this area indicate an Early Cretaceous age. Orbitolinids of Barremian-Cenomanian age are also present (Akyürek et al., 1984, 1997). An $^{40}Ar/^{39}Ar$ whole-rock age of 96.6 ± 1.8 Ma (Cenomanian) was reported from alkaline pillow lava, stratigraphically associated with similar pink pelagic limestones (Sarayköy-

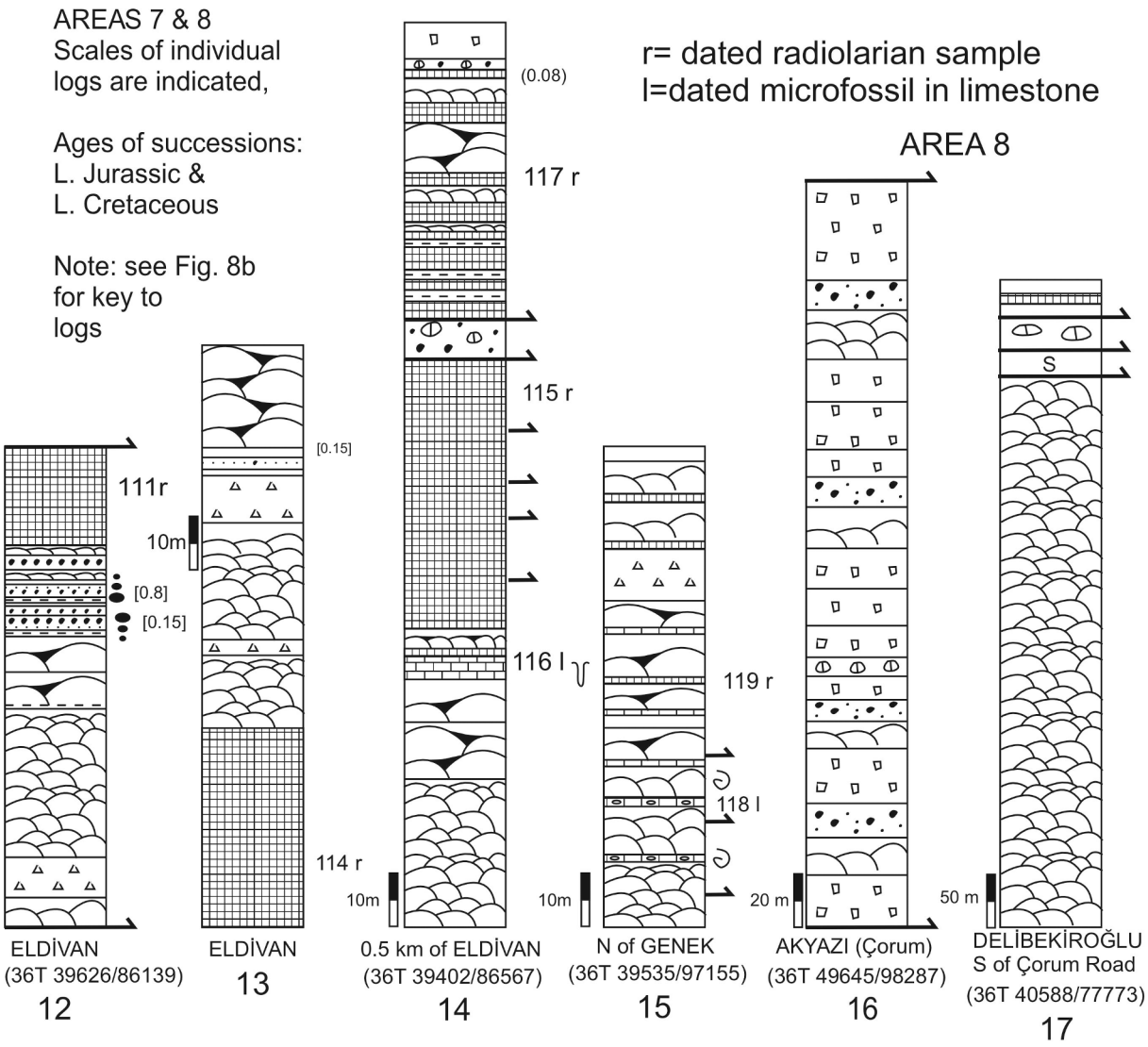

Fig. 17. Measured sedimentary logs of volcanic-sedimentary successions in Area 7, near Eldivan and N of Genek; also for Area 8, near Akyazı (Çorum) and Delibekiroğlu, south of Çorum road; see Fig. 3 for location and Fig. 8b for key to logs).

Şabanözü road) (Sarıfakıoğlu et al., 2011, 2017). The locally dated basalt and also the rarely dated radiolarian chert and pelagic limestone in the Eldivan area point to the presence of Upper Cretaceous seamount-type volcanism and deep-sea pelagic deposition within the Neotethyan Ankara Melange. Upper Cretaceous radiolarites also occur in Area 1, Karacakaya (see above). In addition, Upper Cretaceous basaltic rocks and Upper Cretaceous limestones are reported from probable correlatives of the Neotethyan Ankara Melange along the northern margin of the Çankırı Basin (Area 8) (see below) and to the north of our study area (Tüysüz, l990; Rice et al., 2006; see Robertson et al., 2023).

The Eldivan ophiolite, which structurally overlies the melange (Fig. 5f), encompasses a virtually complete SSZ-type ophiolite, with a highly disrupted metamorphic sole (c. 15 km N of Eldivan) (Üner and Çakır, 2011, 2014). The ophiolite encompasses upper mantle peridotite (serpentinised), layered and isotropic gabbro, small plagiogranite bodies, sheeted dykes (cut by small plagiogranite intrusions) and both massive basalt and pillow basalt. In small local outcrops, the basalts are depositionally overlain by alternations of radiolarian chert, pelagic carbonate and mudstone (still undated). A plagiogranite intrusion west of Eldivan yielded a U-Pb crystallisation age of 179 ± 15 Ma (Toarcian) (Dilek and Thy, 2006).

Amphibolites of the metamorphic sole occur as blocks within serpentinite, and are associated with calcschist, quartzite, micaschist and epidosite (Üner and Çakır, 2011). Although mapped as part of the Eldivan ophiolite (Sarıfakıoğlu et al., 2011, 2017), the outcrop includes 'low-grade metamorphosed radiolarites, cherts, shales, sandstone, tuffs, and volcanic rock association' (Çelik et al., 2011), suggesting an origin as the low-grade-metamorposed sole of the Eldivan ophiolite. The protoliths of the amphibolites range from OIB, to N-MORB, to IAT and were metamorphosed during the late Early to Middle Jurassic (177.08 ± 0.96 Ma and 166.9 ± 1.1 Ma), based on Ar-Ar dating, partly coeval with the over-riding Eldivan ophiolite (Çelik et al., 2011).

The southern part of Area 7 (SW of Eldivan) consists largely of steeply inclined, sheared ophiolitic melange, with embedded blocks of basalt, andesite, dacite and rhyolite. Ophiolitic pillow basalts are locally interbedded with radiolarite. Disrupted units of pelagic sediments in this area (<10 m thick) are lithologically similar to the *in situ* deep-sea sedimentary cover of the more intact Eldivan ophiolite farther north (see above). However, unusually, they are reported to include sparse sandstone turbidites. Detrital zircons from these sandstones yielded U-Pb zircon ages of 164.1 ± 2 Ma (Callovian) and 143.2 ± 2 Ma (Berriasian), suggesting a maximum Early Cretaceous age for the Eldivan ophiolite (Dangerfield et al., 2011). Zircon ages from a sandstone that was collected from near the base of the transgressively overlying Upper

Fig. 18. Field photographs of Area 7, Eldivan. a, Unusually thick and intact radiolarite associated with basalt and pelagic limestone; person for scale; view northwards; b, Normal-graded volcanogenic debris-flow deposits with abundant interstitial pink pelagic limestone; hammer for scale; c, Small pillows in a matrix of pink pelagic carbonate; the result of slope eruption; average size of the small pillows = 9 cm; d, Hyaloclastite composed of spalled volcanic glass (palagonite) with clasts of vesicular basalt; e, Pillow basalt with abundant interstitial pink pelagic carbonate; pen for scale; a-e Volcanic-sedimentary units exposed SW of Eldivan; near GPS: 36 T 39402/86567; f, Lower Jurassic ammonite-rich pelagic limestone; N of Genek, GPS: 36 T 39535/97155; pen for scale (on right); g, Nodular pelagic carbonate (brecciated and stylolitic) with layer of diagenetically formed chalcedonic chert that contains Cenomanian radiolarians; location near f; pen for scale (lower left); h, Jurassic pelagic limestone that unconformably overlies the Triassic Karakaya Complex, NE of Ankara, Hasanoğlan quarry, GPS: 36 T 17383/28075; pen for scale (upper edge); i, Thick-bedded, steeply dipping Upper Cretaceous arc-related volcanic and volcaniclastic sedimentary rocks of the Kavak Formation, the more northerly age equivalent of the Karadağ Formation; field of view c. 400 m; j, Large rounded clast of basaltic andesite within volcaniclastic debris-flow deposit (clasts are reworked); Kavak Formation; k, Angular clasts of basaltic andesite with a calcitic cement (clasts are eruptive); Kavak Formation; i-k near Karalar; near GPS: 36 T 47439/39911; l, Typical terrigenous turbidites and debris-flow deposits of the latest Cretaceous-Paleogene Haymana Formation, structurally beneath the Neotethyan Ankara Melange; near GPS: 36S 36975/15275; average bed thickness = c. 30 cm. (For interpretation of the references to colour in this figure legend, the reader is referred to the web version of this article.)

Cretaceous succession ('Karadağ Formation') points to a pre-Late Cretaceous age of melange accretion in this area (Dangerfield et al., 2011).

MORB, E-MORB, IAT, to boninitic-type compositions are all reported from the ophiolitic extrusive rocks, sheeted dykes and isolated dykes of the Eldivan ophiolite as a whole (Sarıfakıoğlu et al., 2011, 2017; Çelik et al., 2013; Dangerfield et al., 2011). The chemically variable igneous rocks have been interpreted to represent a SSZ-setting, in which subduction influence decreased towards the basin axis, similar to some modern SW Pacific marginal basins (Dangerfield et al., 2011). Assuming generally northward subduction, the consensus view of recent authors, implies that the forearc ophiolite originally passed northwards into a marginal basin. There is no field evidence in the Eldivan area of a related magmatic arc in contrast to modern back-arc basins (e.g., Busby et al., 2017 and references). However, Jurassic arc-type intrusives are associated with SSZ-type ophiolites in the eastern Pontide region, farther east (Robertson et al., 2014).

The main contributions from Area 7 (Eldivan) are: (1) An intact volcanic-sedimentary succession including E-MORB of probable Early Cretaceous age; (2) An intersliced succession of Early Jurassic pillow basalt and radiolarites; (3) Evidence of recumbent folding within the intersliced Early Jurassic and Early Cretaceous lavas and deep-sea sediments; (4) A relatively intact over-riding (in part) uppermost Lower Jurassic (c. 179 Ma) SSZ ophiolite; (5) Similar ophiolite and metamorphic sole ages pointing to near-contemporaneous ophiolite and metamorphic sole formation for the earliest formed part the ophiolite, as

reported for some other SSZ-type ophiolites, including elsewhere in Turkey (e.g., Parlak et al., 2013a, 2019 and references); (6) Termination of ophiolite-related magmatism, probably before the Aptian in this area, mainly based on U-Pb dating of detrital zircons from sandstones just beneath and also just above the base of the transgressively overlying Upper Cretaceous succession Dangerfield et al., 2011), coupled with the palaeontologically determined age of the Karadağ and related Kavak formations (Akyürek et al., 1984, 1997); (7) The presence of Upper Cretaceous (Cenomanian) basalt and radiolarian chert suggest that accretion of the Neotethyan Ankara Melange as a whole persisted into Late Cretaceous time.

4.8. Area 8: Northern and eastern margins of the Çankırı Basin

Melange and ophiolitic rocks are also widely distributed along the northern and eastern margins of the Cenozoic Çankırı Basin, including the Yapraklı, İskilip, Laloğlu, Boğazkale and Çekerek areas and also outcrops further north outside our study area (Figs. 4, 5g, h). The information below is mainly from the literature although several outcrops were visited during this work to aid comparison with Areas 1–7 (see Supplementary Fig. 4).

In the south (Laloğlu, Boğazkale and Çekerek areas) there are many similarities with the Ankara Melange as exposed around the western periphery of the Çankırı Basin. In the Boğazkale area, ophiolitic melange includes serpentinised ultramafic rocks, intruded by dykes, that have been dated by the ^{40}Ar-^{39}Ar method as 176.30 ± 0.52 Ma and 178.82 ± 0.80 Ma (Toarcian, Early Jurassic) (Balcı and Sayıt, 2020).

In the north, in the Yapraklı area, the melange (Kirazbaşı melange) is dominated by two recurring units: basalt-chert-pelagic limestone interpreted as oceanic crust, and alkaline basalt-volcaniclastic sediment-neritic carbonates interpreted as emplaced seamounts (Rice et al., 2006). The siliceous matrix of a MORB breccia contains Radiolaria of late Valanginian-early Barremian age (NE of Yapraklı) (Bortolotti et al., 2013, 2018). Associated pelagic limestone blocks have yielded Albian-Maastrichtian planktic foraminifera (Rice et al., 2006). In places, the ophiolitic blocks are enclosed in sheared serpentinite, together with blocks of pelagic limestone, radiolarite and sandstone. The ophiolitic rocks are dominated by serpentinised harzburgite-dunite, together with isotropic gabbro and diabase (Sarıfakıoğlu et al., 2011, 2017). Throughout the northern exposures (e.g.,Yapraklı, İskilip), there are additional slices of Upper Cretaceous oceanic arc units, namely the Kösdağ, Tafano and Yerkuyu units (see Tüysüz, 1990, 1993; Ustaömer and Robertson. 1997, 1999; Rice et al., 2006; Kaymakçı et al., 2009; Berber et al., 2014, 2021; Aygül et al., 2015; Sayıt et al., 2022) and also inferred oceanic fore-arc units (e.g., Yaylaçayı Formation) (Rice et al., 2006; Kaymakçı et al., 2009). The above arc-related units and associated accretionary melanges are likely to relate to the subduction of a remnant of the İzmir-Ankara-Erzincan ocean (Northern Neotethys) that was located to the north of the Neotethyan Ankara Melange accretionary prism, although formation related to subduction of a separate Intra-Pontide ocean to the north has also been suggested (Marroni et al., 2014, 2020; see Robertson et al., 2023 for discussion).

Farther east, in the İskilip area (e.g., 5 km NW of İskilip) a relatively thin slice of melange (Kirazbaşı melange) includes E-MORB (Rojay et al., 2004). Chert associated with basalt farther southeast, near Çorum, contains Radiolaria of late Norian age, and farther south (W of Alaca) basalts and radiolarites are dated as late Tithonian (Bortolotti et al., 2013, 2018). Farther south again along the eastern margin the Çankırı Basin, near Boğazkale, late Barremian-early Aptian radiolarians are reported. Finally, even farther east (southwest of Çekerek), early-middle Bajocian to late Bathonian-early Callovian and also middle-late Oxfordian to late Kimmeridgian-early Tithonian aged Radiolaria are reported from cherts intercalated with basaltic rocks (Bortolotti et al., 2013, 2018).

The main points from the extensive exposures around the northern and eastern margins of the Çankırı Basin are: (1) Variably dismembered volcanic-sedimentary successions range from late Norian to Albian-Aptian; (2) Available analyses indicate MORB to E-MORB compositions of interbedded lavas; (3) The melange includes Upper Cretaceous basalts and radiolarites in places, as in the Kirazbaşı melange in the north; (4) Overlying outcrops of Campanian-Maastrichtian-aged volcanic and pyroclastic rocks, together with fine-coarse-grained clastic sedimentary rocks and pelagic limestones (Sarıfakıoğlu et al., 2011, 2017) are correlated with the Karadağ and Kavak formations farther west and southwest (see above); (5) Upper Cretaceous arc-related units (Kösdağ, Tafano and Yerkuyu units) and fore-arc units (e.g., Yaylaçayı Formation) that are exposed in the north (outside our present study area) are absent from Areas 1–7. These northerly accretionary units appear to record Late Cretaceous subduction of oceanic lithosphere to the north of the pre-Upper Cretaceous Neotethyan Ankara Melange accretionary prism.

5. Sedimentary lithogenesis of the Ankara Melange

Below, we combine the evidence from the different areas to consider the main sedimentary environments and processes that can be inferred from the relatively intact successions within the Neotethyan Ankara Melange in the eight areas studied.

5.1. Lithofacies of volcanogenic-sedimentary successions

5.1.1. Evidence from the measured successions

Upper Triassic and Lower Jurassic sedimentary rocks associated with basaltic rocks are well represented in Area 4, Beynam-Karaali; in Area 7, Eldivan; and in Area 8, Çorum. Upper Triassic lavas in these areas are interbedded with, or overlain by, pelagic carbonates, suggesting that they erupted above the carbonate compensation depth (CCD) (Fig. 17, log 15). Additionally, in Area 4 the basaltic lavas are associated with blocks of Upper Triassic neritic limestone. Lower Jurassic facies (see Supplementary Table 1; e.g., Fig. 19 M−O) are typically pelagic micrite with calcified Radiolaria and thin-shelled bivalves (e.g., Area 7, near Kamış; Fig. 16). Pelagic micrite in Area 4, Beynam-Karaali contains numerous small pelagic bivalves (*Daonella* sp.), calcified Radiolaria and volcanic debris including palagonite (Supplementary Table 1). Calpionellids and sparse planktic foraminifera are present in this area and also in Area 7 (Supplementary Table 1). In places, pelagic carbonates are interbedded with packstones that contain detrital echinoderms, benthic foraminifera, bivalve fragments and iron oxide-coated grains (Supplementary Table 1). Most radiolarites from the measured volcanic-sedimentary successions (e.g., Fig. 8a, logs 1–5; Fig. 15, logs 6–11; Fig. 17, logs 13, 14, 16, 17; see Fig. 8b for the key to the logs) are dated as Late Jurassic-Early Cretaceous (Supplementary Table 2), indicating relatively deep water accumulation during this time interval. In contrast, dated benthic foraminifera are mainly Early Cretaceous (Fig. 19 P-V), and are associated with shallow-water facies. These include internal platform, reef margin and slope facies, all of which are associated with basaltic volcanic detritus.

Pillowed and massive lavas appear to predominate in the more easterly outcrops (e.g., Fig. 17; logs 16, 17; Çorum area; see also Supplementary Fig. 4) suggesting that seafloor topography was subdued in this area compared to farther west. The pillow lavas are interpreted as eruptions on a relatively gentle seafloor (<30°), whereas the massive lavas record local ponding in seafloor hollows. The fragmental lava material has four main origins: (1) pillow disintegration breccia (Fig. 8a, log 1, Karacakaya; Fig. 15, log 10, Kalecik). This breccia formed on steep slopes causing pillows to fragment and accumulate in a volcaniclastic matrix; (2) hyaloclastite breccia; this formed when lava chilled suddenly in contact with cold seawater, spalling glassy fragments that accumulated together with isolated crystalline basalt fragments (Fig. 18d); (3) rare small pillows ‘floating’ in pelagic carbonate, interpreted as peperites that formed where magma intermixed with pelagic carbonate (Fig. 18b, c). (4) epiclastic breccia formed by downslope reworking of

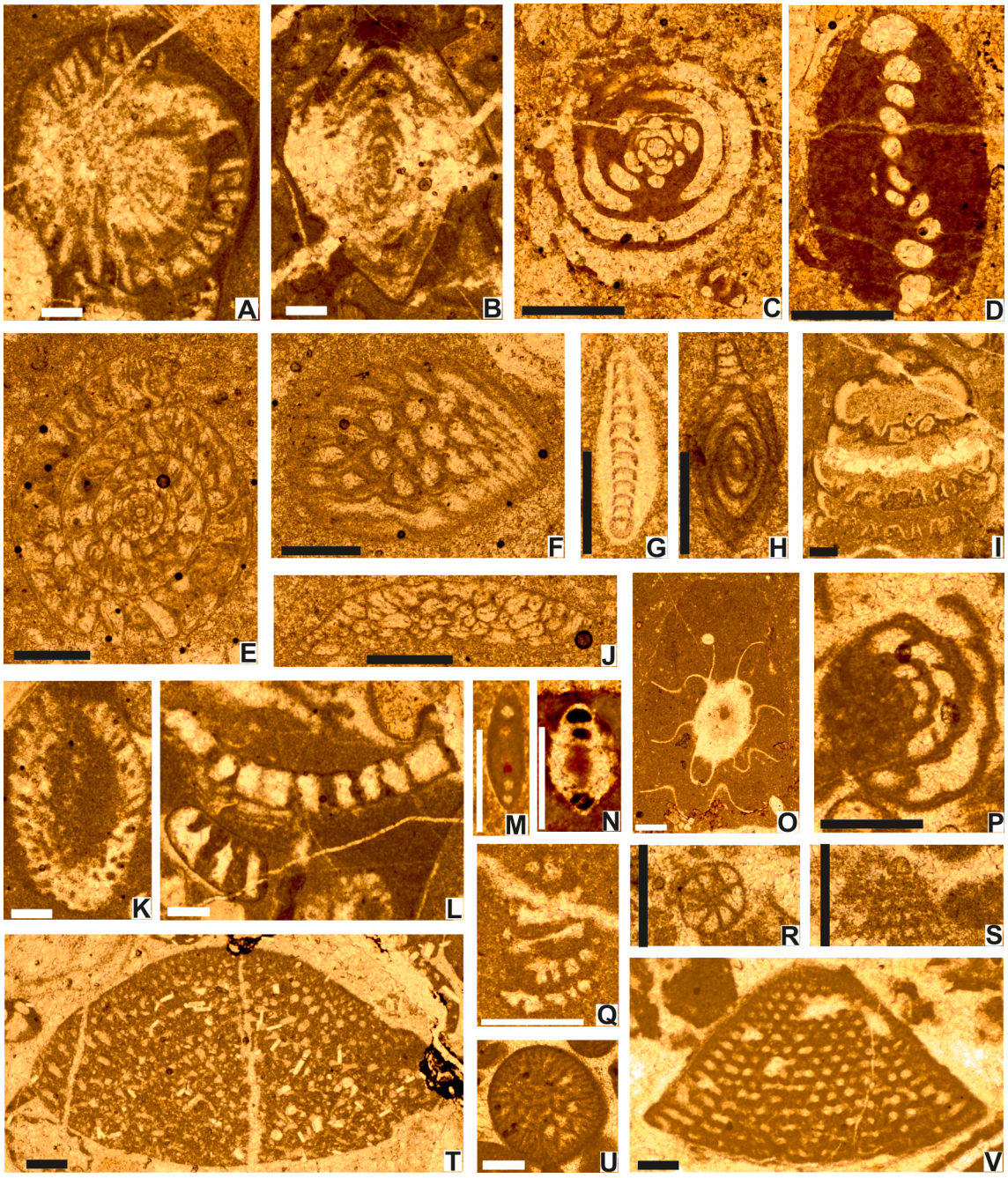

Fig. 19. Photomicrographs of selected, well-preserved calcareous microfossils from the Neotethyan Ankara Melange and the Palaeotethyan Ankara Melange (Karakaya Complex). A-L Late Permian benthic foraminifera and calcareous algae. A, B. *Staffella* sp., AM/98, Area 3, Yeşilyurt; C, D. *Hemigordius* sp., AM/46, Bayındır road, Karakaya Complex; E, F. *Paleofusulina* (*Paradumbarula*) sp., AM/96; G. *Pachyphloia* sp., AM/96; H. *Reichelina* sp., AM/96; I. *Climacammina* sp., AM/96; J. *Paradoxiella* sp., AM/96, Area 3, Yeşilyurt; K. *Gymnocodium* sp., AM/98; L. *Mizzia* sp., AM/98, Area 3, Yeşilyurt; M−O. Benthic foraminifera from the Lower Jurassic, M. *Agerina martana*, AM/81; N. *Involutina liassica*, AM/81, Area 5, Karaali; O. Ammonite, AM/82, Area 5, Karaali; P-V. Benthic foraminifera from the Lower Cretaceous, P. *Charentia cuvillieri*, AM/101, Area 3, Şerefli; Q. *Vercorsella scarsellai*, AM/90, Area 2, Dereköy; R. *Nezzazata* sp., AM/21; S. *Akcaya minuta*, AM/21; Kılıçlar, Area 5; T. *Palorbitolina lenticularis*, AM/69, Area 6 Çandır; U, V. *Montseciella arabica*, AM/101, AM/106, Area 3, Şerefli; Bar scales = 0.25 mm. See Supplementary Table 1 for listing of taxa identified and GPS locations.

previously erupted basalt to form matrix-supported lava breccia. Such lava breccias are commonly associated with clasts of redeposited neritic limestone (Fig. 13a, Kılıçlar). Rarely, volcanic, radiolarite and pelagic limestone are intermixed within individual debris-flow deposits, indicating that some of the pelagic sediment was lithified prior to redeposition (Fig. 8a, log 4, Kılıçlar). As a whole, the debris-flow deposits accumulated at, or near, the base of submarine slopes.

There are also numerous intercalations of volcaniclastic breccia-conglomerate, with clasts typically up to several cm in size, together with normal-graded volcaniclastic sandstones (e.g., Fig. 15, log 6, Kalecik; Fig. 15, log 11, Çandır). The breccia-conglomerate is poorly sorted with angular to sub-rounded clasts/grains and is interpreted as a mass-flow accumulation. The thick bedded normal-graded volcaniclastic sandstones mainly represent high-density turbidites.

The lavas are commonly interbedded with ribbon radiolarites, typically in 10s cm to several metres thick units (e.g., Fig. 15, log 8, Kalecik; Fig. 17, logs 12, 13, 14, Eldivan). Radiolarites between lava flows are exceptionally thick in Area 7 (Eldivan), hinting at spasmodic eruption or

unusually rapid radiolarian sedimentation (Fig. 18a). The radiolarites are homogeneous and lack volcaniclastic layers suggesting that they represent relatively rapid deposition, perhaps in response to fertile oceanic productivity. Pillow lavas commonly include interstratifications of pelagic carbonate, together with abundant intrapillow pelagic carbonate, which is commonly ferruginous, suggesting a hydrothermal influence (e.g., Fig. 9e; Fig. 13c; Fig. 17, log 14, Eldivan). Pelagic limestones that are interbedded with basaltic rocks are mainly calcified radiolarites. In some samples (e.g., in Area 5, Kalecik), radiolarian tests and spines are aligned parallel to bedding, indicating a current influence. The pelagic carbonates are interpreted as hemipelagic ooze that was derived from an adjacent carbonate platform and accumulated above the CCD.

Interbeds rich in redeposited neritic limestone clasts occur in several of the logged sections (e.g., Fig. 8a, logs 4, 5; Kılıçlar). Lithologies range from well-bedded, normal-graded bioclastic calcarenites that are interpreted as calciturbidites, to ungraded matrix-supported or rarely reverse-graded conglomerates that are interpreted as mass-flow and debris-flow deposits (Fig. 8a, log 5; Fig. 13a). Local accumulations of angular to sub-angular neritic limestone clasts are interpreted as slope talus (Fig. 9g). Basaltic lithoclasts and related mineral grains are commonly mixed with limestones that show evidence of reworking as calciturbidites and calcareous debris-flow deposits (calc-debrites), confirming that volcanic rocks existed in the source areas.

5.1.2. Evidence from microfacies

Supporting information from optical microscopy is summarised below, indicative of depositional processes and environments.

The limestones forming isolated blocks (to 100 s m in size) typically have a pelletal texture, with variable abundances of micritic grains and benthic foraminifera (e.g., miliolids), together with fragments of bivalve shells, echinoderms, calcareous algae and locally coral (Fig. 20d-j). A sample from a large limestone block from Area 3, W of Kulu contains unusually well-rounded grains, indicative of relatively high-energy reworking. Some of the blocks are closely associated with basalt in Area 2 (Dereköy), Area 3 (W of Kulu) and Area 4 (Beynam-Karaali), mainly in the southwest.

Two main types of limestone clasts (<1m across) are present within the volcanic-sedimentary successions: (1) micritic carbonate, commonly with evidence of current reworking; (2) redeposited packstone or grainstone. Some samples include small amounts of volcanic glass (palagonite) and altered basalt (e.g., in Area 7, Çandır; see Supplementary Fig. 1j). Terrigenous sediment (e.g., quartz; felspar) is conspicuously absent. Most of the grains in the packstones and grainstones are poorly sorted, subrounded, to subangular, to locally well-rounded. Bioclasts typically exhibit micritic envelopes. Detrital limestone grains (e.g., oolite) are locally present. Exceptionally, limestone clasts are dominated by sub-rounded, variably sorted fragments of thick-shelled rudist bivalves, together with codiacean algae (Area 7, Çandır). The rounded grains indicate reworking in a relatively high-energy environment, prior to gravity redeposition as calciturbidites and debris-flow deposits.

The calciturbidites contain abundant bivalve fragments (e.g., rudists), benthic foraminifera (commonly miliolids), packstone, grainstone, algal micrite, coral, echinoderm plates, ooids and rare pisoids (Fig. 20k, l). Variable amounts of crystalline limestone, radiolarian micrite (calcilutite) and pink radiolarian chert are also present in some lithologies. A sample from Area 6, Kalecik includes grains of plagioclase-rich siltstone (arkosic) and altered basalt. In most limestones, the primary micritic matrix is partially replaced by microspar, whereas reworked or redeposited grains are less affected. Allochems in the Çandır section (Area 7) include small crystals of diagenetic felspar. Additional illustration of the redeposited gravity-flow deposits are given in Supplementary Figs. c-i & k).

The clasts and blocks of carbonate rocks accumulated in three main settings associated with volcanic build-up: (1) interior of shallow-water carbonate platform, affected by extensive current reworking; (2) carbonate margin associated with reef facies; (3) carbonate slope, characterised by mixing of neritic bioclasts, some of which were previously lithified; (3) deep water, where neritic-derived calciturbidites accumulated together with radiolarian-rich sediments and reworked volcanic material.

5.1.3. Volcanic build-ups and associated carbonate facies

The Upper Jurassic-Lower Cretaceous volcanic-sedimentary successions represent the flank facies of a very large volcanic build-up, capped by a carbonate platform (i.e. atoll). The evidence from the Upper Jurassic-Lower Cretaceous successions is consistent with sediment derivation from a single large volcanic build-up, which is mainly preserved in the exposures around the southwestern margin of the Çankırı Basin (Areas 2, 3, 4, 5, 6). However, no evidence is preserved of the core of the volcanic body (i.e. thick massive flows) and there is very little evidence of the intact source carbonate platform. These absences are presumably due to preferential subduction (see Discussion). The size of the inferred capping carbonate build-up is difficult to infer because of break-up and mixing during accretion but is likely to have been up to 10 s km across. A less likely alternative is that the relatively intact thrust slices in Area 3, Kulu represent remnants of a separate carbonate platform perhaps founded on continental crust. Against this hypothesis, the petrography shows that in places basaltic detritus occurs within these shallow-water limestones, consistent with an origin as back-reef facies of a large carbonate platform.

The known record of basaltic volcanism and associated shallow to deep-water deposition points to three main phases of build-up, probably representing different sized atolls in an oceanic setting, free of terrigenous sediment input: 1) Late Triassic-Early Jurassic (e.g., in Area 4, Beynam-Karaali); 2) Late Jurassic-Early Cretaceous (up to c. 60 Ma) in many areas (e.g., areas 3 (Dereköy), 5 (Edige-Kılıçlar) and 6 (Kalecik-Çandır); and 3) Late Cretaceous (Cenomanian) as in areas 1 (Karacakaya) and 8 (north margin of the Çankırı Basin). Of these, the Late Jurassic-Early Cretaceous phase is by far the most represented in the Neotethyan Ankara Melange and could indeed represent several volcanic episodes. The Neotethyan oceanic basin was, therefore, characterised by episodic volcanic build-ups and atoll construction, possibly as a chain of plume-related seamounts that were finally incorporated into the accretionary prism within the İzmir-Ankara Erzincan suture zone.

6. Tectono-magmatic settings of volcanic rocks and metamorphic sole

Within the volcanic-sedimentary units, the extrusive rocks show a wide range in magmatic compositions from N-MORB, to E-MORB to OIB (Tankut, 1990; Çapan and Floyd, 1989; Tankut et al., 1998; Floyd, 1993; Rojay et al., 2004; Sarıfakıoğlu et al., 2014; Okay et al., 2022). In one interpretation, magma was extracted from pockets of enriched, heterogeneous mantle in an ocean ridge setting (Bortolotti et al., 2013, 2018). In this hypothesis, the enrichment was influenced by mantle plume involvement in rifting of the İzmir-Ankara-Erzincan ocean during the Triassic. Alternatively, the enrichment relates to off-axis seamount magmatism and fractionation processes, potentially unrelated to rifting (Rojay et al., 2004). These two alternatives can be partly distinguished based on the associated sedimentary rocks and the time relations of the Ankara Melange.

The variably dismembered ophiolites have SSZ geochemical signatures, ranging from boninitic (fore-arc), to IAT (arc), to BAB (possible back-arc) (Dilek and Thy, 2006; Dangerfield et al., 2011; Sarıfakıoğlu et al., 2014; Okay et al., 2022). Most of the metamorphic sole amphibolites are chemically equivalent to the volcanic rocks of the volcanic-sedimentary units (E-MORB to OIB) (Çelik et al., 2011). In contrast, the melange blocks with SSZ signatures, especially the boninitic extrusive rocks, are likely to have been detached from over-riding fore-arc oceanic lithosphere (future ophiolites), probably during initial accretion

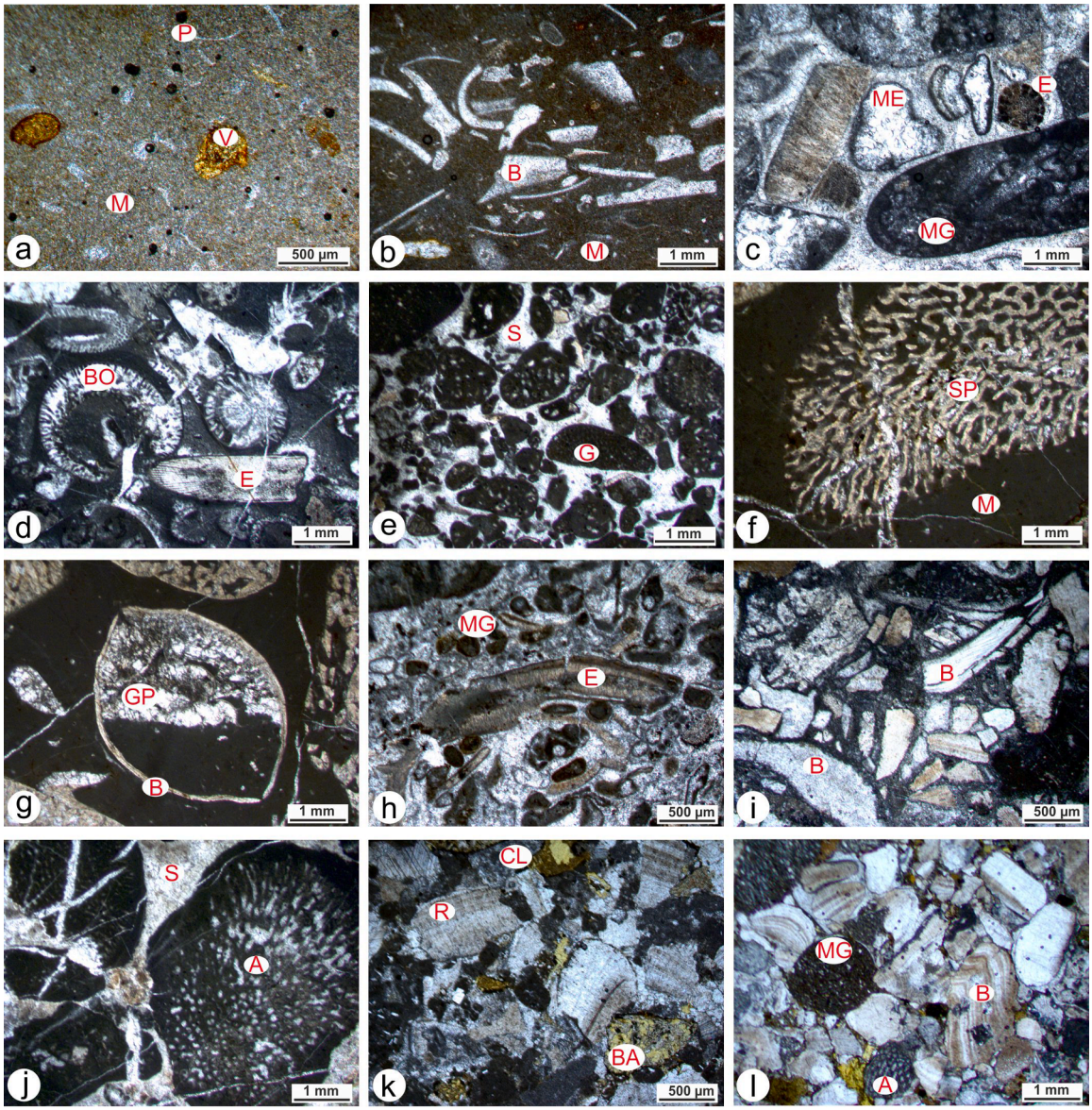

Fig. 20. Photomicrographs of sedimentary facies within the Neotethyan Ankara Melange, viewed under plane-polarised light. a, Lower Jurassic micritic limestone (wackestone) with thin-shelled pelagic bivalves (*Posidonia* sp.) and basic volcanic glass (palagonite); AM/80, Area 4, Karaali, GPS: 36S 94388/89220; b, Lower Jurassic micritic limestone, with scattered, broken reworked bivalve shell fragments, mainly replaced by calcite spar, AM/81, location as a; c, Lower Jurassic bioclastic limestone (packstone) with micritic clasts and echinoderm plates and spines; the grains are variably recrystallised and replaced by calcite spar; the primary micritic matrix is variably replaced by calcite spar; redeposited grains are broken, rounded and coated with prismatic calcite; AM/81, location as a; a-c are from a limestone block within pillow lavas; d, Micritic limestone (wackestone), with scattered, reworked fragments of echinoderms, and bivalve shell fragments, mainly replaced by calcite spar. A bioclastic fragment is bored and oolitically coated, followed by partial dissolution and replacement by calcite spar. Isolated limestone block in melange, AM/96, Area 3, Yeşilyurt, GPS: 36S 73923/21953; e, Rounded micritic grains (pelmicrite) within Lower Cretaceous limestone block. The original micritic matrix is mostly replaced by calcite spar, AM/101, Area 3, Şerefli, GPS: 36S 83446/19120; f, Coral fragment in a micritic matrix; thick-bedded limestone within a very large block; AM/88, near Dereköy, Area 2, GPS: 36S 62894/74545; g, Small bivalve with partial geopetal infill, set in compositionally similar micritic matrix. The pore space in the upper part of the geopetal is infilled with calcite spar; location as h, Lower Cretaceous (Barremian-Aptian) bioclastic packstone, with reworked fragments of bivalves, micritic grains and echinoid debris. The primary micritic matrix is partially replaced by calcite spar; large block of thick-bedded limestone; AM/89, near Dereköy, Area 2, GPS: 36S 61422/75294; i, Early Cretaceous bioclastic limestone clast from an isolated block, with poorly sorted angular bivalve fragments (rudists) in a micritic matrix; AM/72, near Çandır, Area 6, GPS: 36 T 39885/53478 (plane-polarised light); j, Rounded fragments of calcareous algae; pore spaces infilled by calcite spar; micritic matrix is mainly replaced by calcite spar; AM/106; limestone block in a volcaniclastic matrix; near Karacakaya, Area 1; limestone block in a volcaniclastic matrix, GPS: 36 T 74430/33767; k, Packstone dominated by sub-rounded bivalve fragments (rudists), with micritic grains (grapestone) and altered glassy basalt, in a partially recrystallised micritic matrix; the shell fragments have micritic envelopes; AM/20, Area 5, near Kılıçlar, volcaniclastic debris-flow deposit; near GPS: 36S 31534/17307; l. Grainstone (compacted), dominated by well-rounded and well-sorted bioclastic grains, mainly bivalves, together with calcareous algae and micritic grains; some interstitial volcanic glass (yellow-green) is also present; AM/22, Area 5, near Kılıçlar, volcaniclastic sandstone (grain-flow deposit). Key to components: A = Algae (calcareous); B = Bivalve (mainly fragmentary); BA = Basalt; BO = Borings (micrite-filled); C = Coral; CL = Chlorite (altered basic glass); E = Echinoderm (fragments); G = Grapestone (micritic grain); GP = Geopetal (partly infilled void); M = Micritic matrix; ME Micritic envelope; MG = Micritic grain; P = Pelagic bivalve; R = Rudist bivalve; S = Spar cement (calcitic); V = Volcanic glass (altered). (For interpretation of the references to colour in this figure legend, the reader is referred to the web version of this article.)

in a subduction trench setting. Alternatively, the SSZ-type volcanics might represent subduction of an unrelated arc, although independent evidence of this (e.g., tuffs and volcaniclastic units) is lacking. For a more detailed review of the igneous and metamorphic rocks within the Neotethyan Ankara Melange see Robertson et al. (2023).

7. Structure of the Ankara melange

Structural evidence sheds light on the processes of accretion of the Ankara Melange and also on its later development related to late-stage subduction and/or suturing of the İzmir-Ankara-Erzincan ocean.

7.1. Remote-sensing evidence

The main outcrop-scale structural features observed in the melange in the field and on satellite images are as follows:

(1) Volcanic-sedimentary units and ophiolitic units are intersliced throughout the melange (e.g., Figs. 7e; 9j, k). Both the ophiolitic rocks and the volcanic-sedimentary units were dismembered and emplaced by tectonic processes (e.g., Fig. 9j, k; Fig. 13h);
(2) In some areas, volcanic-sedimentary units have a coherent stratigraphy parallel to the local tectonic trend for up to several kilometres but then degenerate into chaotic melange;
(3) Most of the volcanic-sedimentary and ophiolitic outcrops are lenticular (e.g., Fig. 7e) or anastomose on an up to several kilometre scale (Figs. 7f, 9j);
(4) The contacts between the volcanic-sedimentary units and the ophiolitic units are typically shear zones, which in places include tectonically elongated blocks; commonly these include neritic limestones (Fig. 13i-l; Supplementary Fig. 2a, b);
(5) The strike of the strata within slices and blocks of volcanic-sedimentary units is generally sub-parallel to the bounding tectonic contacts (Fig. 9d). Rarely the shear fabric in the adjacent ophiolitic melange transects the bedding in the volcanic-sedimentary units at up to high angles (e.g., Fig. 11d);
(6) The volcanic-sedimentary units and the ophiolitic units (e.g., serpentinite) exhibit a similar range of structural fabrics suggesting that they deformed together;
(7) Many of the blocks, commonly neritic limestone, show evidence of tectonic fragmentation, resulting in complex internal faulting, angular shapes and straight edges (Fig. 7b), as also suggested by regional mapping (e.g., Akyürek et al., 1984);
(8) The strata within some of the blocks were folded or faulted before being emplaced into the melange because the deformation is localised to individual fault blocks (e.g., Fig. 7b);
(9) Some of the volcanic-sedimentary successions are stratigraphically inverted (e.g., Area 7, Eldivan), pointing to the presence of large-scale isoclinal folding, probably associated with late-stage accretion and/or collision (Figs. 14b, c; 16b);
(10) Fine-grained material (e.g., siltstone, shale, marl), where present between blocks, mainly resulted from shearing and disaggregation of previously intact, adjacent volcanic-sedimentary successions, as particularly seen along major tectonic contacts (Fig. 13j, k);
(11) There is evidence of shear zones involving post-accretion strike-slip, for example within and adjacent to the lower unit melange in Area 4, Beynam-Karaali (Akyürek et al., 1984; see also Kaymakçı et al., 2000, 2003, 2009).

7.2. Outcrop evidence

Bedding and fault planes/slickensides were measured routinely, mainly within the logged volcanic-sedimentary successions. Movement directions of fault planes were noted where possible, although kinematic evidence is sparse (e.g., slickensides). The trend and plunge of folds were also measured where rarely observable. The data were plotted as poles using an equal area Schmidt net (lower hemisphere). The more coherent data sets are in Fig. 21, with additional plots in Supplementary Fig. 3.

In Area 1, Karacadağ, the poles to bedding (southern part of Fig. 7a) indicate the presence of a NE-plunging cylindrical open fold (Fig. 21ai-the b on the figure indicates the fold axis). Faults, which dip at moderate to high angles, are mainly inclined to the NW, with a mean strike/dip of 249°/53° (Fig. 21aii).

In Area 2, Dereköy, the poles to bedding suggest the existence of a NW-plunging open fold (poorly constrained) (Fig. 21bi). Faults are generally steeply northward dipping (see Supplementary Fig. 3ai, aii), with a calculated c. N-S maximum compression direction. Slickensides are mainly oblique to strike-slip, without preferred orientation (Fig. 21bii). Insufficient data are available from Area 3 (W of Kulu) for useful interpretation.

In Area 4, Beynam-Karaali, the distribution of poles to bedding is consistent with a NE-plunging cylindrical fold (see Supplementary Fig. 3ai, aii), as in Area 1 (eastern part of the melange in Fig. 7c). Fault planes are scattered, although mainly dipping southwards (especially south-eastwards), subparallel to the tectonic trend in this area.

In Area 5, Edige-Kılıçlar, outcrop data were collected from sections (Fig. 12a-c) to the north and to the south of Kılıçlar, and from highway cuttings between Elmadağ and the Kızılırmak River. The overall bedding data, which are mainly steeply dipping, are relatively scattered but hint at large-scale open folding about a c. NE-SW-trending axis (Fig. 21ci), sub-parallel to the tectonic fabric (but without a statistically defined fold axis). Bedding data were plotted separately for the Hisarköy-Bedesten section (see Supplementary Fig. 3bi, SPA) and for the highway section (see Supplementary Fig. 3bii, SPB). The bedding data from both of the sub-areas plot similarly to the whole data set for Area 5. The Hisarköy-Bedesten section has a regular c. NE-SW trending structural fabric (Fig. 7d). In contrast, the highway section encompasses shear zones, in which bedding is locally deflected around detached limestone blocks (see Supplementary Fig. 2a, b). Fault planes for the whole area predominantly dip northwards, with signs of conjugate faulting (see Supplementary Fig. 3biii). The calculated principal stress direction is c. N-S (Fig. 21cii). Many fault planes have oblique to strike-slip slickensides that are dominantly left-lateral. There are also two NE-SW trending faults, one of which is a left-lateral strike-slip fault. Satellite images of the most structurally coherent volcanic-sedimentary outcrop, SW of Kılıçlar, show that the E-W bedding fabric is transected by spaced shear planes, orientated NE-SW (i.e., c. 40° clockwise to bedding), suggestive of oblique convergence (see Discussion). Apparent drag (i.e., oblique bedding-transection) and rotation of bedding segments within shear zones point to left-lateral displacement. For comparison, the faults in Upper Cretaceous turbidites (Haymana Formation) to the east of the melange (E of bridge over the Kızılırmak River) are dominantly ca. E-W trending and dip northwards at moderate to steep angles (see Supplementary Fig. 3biv).

In Area 6, Kalecik, the stratigraphy is inverted and shows evidence of folding (Fig. 14b, c; Supplementary Fig. 3cii-SPA &B). The bedding, which is generally moderately dipping, appears to define two superimposed fold directions, one E-W (265/32°) and the other NE-SW (20/23°) (Fig. 21di,dii,iii; Supplementary Fig. 3ci-ciii), consistent with the outcrop evidence of refolding. In contrast, a section on the north bank of the river has more NE-SW orientated bedding (Fig. 7f) suggesting that this section forms part of a separate structural block within the melange.

Relatively few faults were measured in Area 6 because the logged successions are relatively undeformed (Fig. 15; logs 7–11). The observed faults in the volcanic-sedimentary successions generally trend NE-SW (Supplementary Fig. 3civ). Insufficient data were available from Area 7 (Eldivan) to allow interpretation.

In addition, the strike/dip and trend/plunge of outcrop-scale folds were plotted together for the wider region (Areas 1–7). Fold axial planes generally dip northwest, with fold hinges displaced generally clockwise, suggesting oblique contraction. Axial planes and fold hinges dip in

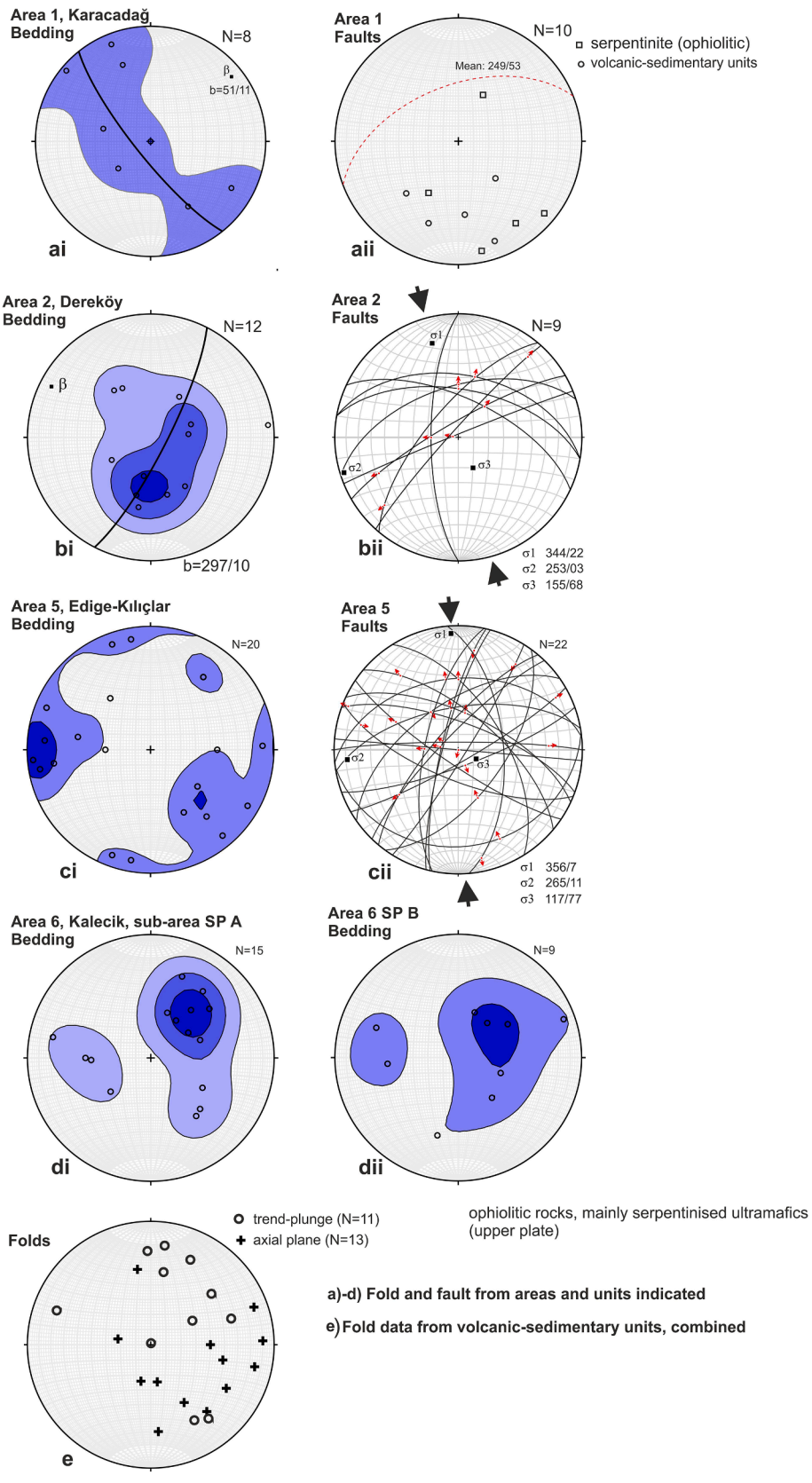

Fig. 21. Equatorial projections of poles to bedding and faults including slickensides, with displacement directions where measurable, and the trend and plunge of rare folds, within the Neotethyan Ankara Melange. Additional stereoplots are given in Supplementary Fig. 3. ai, Area 1, Karacakaya, ai, strike/dip of poles to bedding with average bedding plane shown as great circle and calculated strike/dip of the related open fold plunging to the NE; aii, Area 1, Karacakaya, poles to faults with mean fault plane; bi, Area 2, Dereköy, poles to bedding with average plane shown as great circle and calculated strike/dip of the related open fold plunging to the NW; bii, Area 2, Dereköy, strike and dip of fault planes as great circles with calculated principal stress axes (σ_1, σ_2, σ_3). The arrows in red show angle and sense of movement of slickensides (i.e. the closer to the great circle the greater the strike-slip component); ci, Area 5, Edige-Kılıçlar, poles to bedding; cii, Area 5, Edige-Kılıçlar, strike and dip of fault planes as great circles with calculated principal stress axes (σ_1, σ_2, σ_3). Arrows in red show angle and sense of movement of slickensides; di, Area 6, Kalecik, poles to bedding in sub-area SPA; dii, Area 6, Kalecik, poles to bedding in sub-area SPB (SPA and SPB are both south of the Kızılırmak River); e, Poles to trend and plunge of fold axial planes measured in different lithologies in the study area. Folding was rarely observed. Software use to plot data other than fault planes: 'Stereonet' http://www.geo.cornell.edu/geology/faculty/RWA/programs/stereonet.html; for fault plans with slickenside data with recorded movement direction: FaultKin: http://www.geo.cornell.edu/geology/faculty/RWA/programs/faultkin.html. (For interpretation of the references to colour in this figure legend, the reader is referred to the web version of this article.)

opposing directions, hinting at refolding (Fig. 21e). The generally clockwise relationship between bedding and shear is consistent with left-lateral strike-slip.

The new data can be compared with limited existing data for three of our areas. In Area 1, Karacakaya, the principal axis of compression is to the southwest (Rojay, 2013), consistent with our results (Fig. 21aii). In addition, faults from an isolated NE-SW trending Cenomanian-Turonian bedded sequence near Alcı (Alcı basin), southwest of Ankara (Rojay and

Süzen, 1997) indicate a southeast maximum compression direction (Rojay, 2013). In Area 2, Dereköy, the maximum axis of compression is to the southwest (N = 3) (Rojay, 2013), consistent with broadly dispersed NW-SE folding. The faults in this area are mainly northward-dipping (Fig. 21bii), with a c. N-S maximum axis of compression. Data from Area 6, Kalecik indicate maximum compression towards the southwest (Rojay, 2013), generally consistent with our bedding and fault data (Fig. 21di-dii). In Area 7 (Eldivan) regional-scale stress inversion of fault data indicates an overall NNE-SSW σ-1 and steep σ-3 which has been attributed to pre-Late Palaeocene thrusting (Kaymakçı, 2000, Kaymakçı et al., 2000, 2003b).

The bedding, fault and fold analysis for the area studied as a whole indicate: (1) Bedding and faults in the melange are mainly moderately to steeply dipping; (2) Faults initially dipped predominantly northwards, presumably related to melange accretion; (3) Folding took place after initial/accretion emplacement in some areas; (4) Fault, fold and satellite images point to dominantly oblique left-lateral contraction. This is consistent with right-lateral (oblique) subduction, as inferred along the northwestern margin of the Çankırı Basin (Kaymakçı et al., 2003a); (5) In places (e.g., Area 4, Beynam-Karaali), the melange rotated together with the unconformably overlying latest Cretaceous-Palaeocene succession (Haymana Formation) indicating large-scale, post-accretion (collision-related) folding (Okay et al., 2022).

8. Discussion

Below, we integrate our new and published information to support a model for the formation of the Neotethyan Ankara Melange by dominantly tectonic processes of subduction-accretion, involving the collision of one or more seamounts with fore-arc oceanic lithosphere (future SSZ ophiolites) in an oceanic setting. What we here term the Neotethyan Ankara Melange was initially interpreted as a dismembered regional-scale thrust sheet (Bailey and McCallien, 1950, 1953), or olistostromes (mass-transport units) in a subduction trench setting (Norman, 1973a, 1984). Some authors believed that both tectonic and sedimentary processes contributed to the formation of the accretionary prism (Rojay, 2013; Sarıfakıoğlu et al., 2017; Okay et al., 2022). Alkaline volcanic rocks within the melange were interpreted as accreted oceanic seamounts (Floyd, 1993; Çapan and Floyd, 1985; Tankut, l984; Tankut et al., 1998), some of which were later dated mainly using calcareous and siliceous microfossils (Rojay and Altıner, 1998; Rojay et al., 2001, 2004; Sarıfakıoğlu et al., 2017; Bortolotti et al., 2018; Okay et al., 2022). Exotic blocks of lava and sedimentary rocks of mainly Late Jurassic-Early Cretaceous age in the Ankara region were interpreted as one or more accreted atolls (Rojay et al., 2001, 2004). Some authors inferred the accretion of seamounts of several different ages (Sarıfakıoğlu et al., 2017; Bortolotti et al., 2018; Okay et al., 2022). Ophiolitic rocks in the melange were shown, mainly based on geochemical evidence, to include variably dismembered SSZ ophiolites (Tankut et al., 1998; Dangerfield et al., 2011; Sarıfakıoğlu et al., 2014; Okay et al., 2022); metamorphic sole-type rocks were also recognised (Çelik et al., 2011). Comparable interpretations were made for Neotethyan melanges to the north, west and east of our study area, within other parts of the İzmir-Ankara-Erzincan suture zone (Northern Neotethys) (see Robertson et al., 2023 and references). Our present interpretation links some of the intra-oceanic accretion in the Ankara region to the collision of a large seamount capped by a carbonate platform (atoll-like body), with SSZ oceanic lithosphere that formed in a fore-arc setting (future ophiolites). More widely, seamounts of several different ages and sizes were incorporated into the accretionary prism, the oldest being Late Triassic-Early Jurassic and the youngest Late Cretaceous.

8.1. Accretion of the Ankara melange related to seamount collision

The Ankara Melange in the Ankara region is dominated by two fundamentally different units. (1) Seamounts. The Upper Jurassic-Lower Cretaceous volcanic-sedimentary units are interpreted as mainly the flanks of a large intra-oceanic seamount (potentially up to 10s km across). Fragments of smaller Upper Triassic-Lower Jurassic and Upper Cretaceous seamounts are also present. Radiolarian data from the volcanic-sedimentary units in the eight areas studied here encompass much of late Norian to Cenomanian time (Fig. 22); (2) Uppermost Lower-Upper Jurassic SSZ ophiolites. The ophiolitic fragments in the Neotethyan Ankara Melange are interpreted as remnants of the same regional-scale SSZ oceanic slab. The ophiolitic rocks and metamorphic sole combined are dated as Early-Late Jurassic suggesting that SSZ magmatism could have persisted for >25 Ma, and potentially encompassed fore-arc, arc and back-arc settings. The boninites of the Beynam ophiolite are interpreted as a distal fore-arc ophiolite, whereas the Edige ophiolite with its crosscutting chemically SSZ-type dykes represents a more proximal arc-related setting, and part of the Eldivan ophiolite may represent a back-arc setting based on chemical data (see above).

The timing of melange accretion is constrained by the available radiolarian and carbonate fossil age data. This is supplemented by localised detrital zircon geochronology, especially concerning the age of the oldest transgressive facies ('Karadağ Formation'), where present. Detrital zircons from sandstone in the highest structural level of the melange in Area 8 (Eldivan) (sample no: AD0009) yielded a maximum Berriasian-Valanginian boundary age (139.9 ± 2.1 Ma). The maximum age of unconformably overlying sandstone (Karadağ Formation) in the same area is Albian-Cenomanian (102.2 ± 3.55) (Dangerfield et al., 2011). The accretion of much of the Ankara Melange, at least in this area, is therefore likely to have ended by the late Albian (c. 105 Ma). On the other hand, the local presence of Cenomanian radiolarites that are locally associated with alkaline basaltic lavas (Areas 1, 7) suggests that further accretion took place during the Late Cretaceous.

In some areas (e.g., Areas 5, 6), the Ankara Melange is intersliced with Upper Cretaceous arc-related lithologies (Karadağ and Kavak formations), increasing its structural complexity (see Robertson et al., 2023). Also, in places (e.g., Area 3) the melange includes blocks of Permian marble and Mesozoic shelf limestones (e.g., Fig. 18h) that were probably derived from the Palaeotethyan Ankara Melange and its sedimentary cover within the adjacent Sakarya Zone (Fig. 1). This suggests that latest Cretaceous-Paleogene subduction and/or collisional processes contributed to the complexity of the Ankara Melange, especially close to the Sakarya Zone.

The Upper Triassic-Lower Jurassic inferred small-scale seamount units (e.g., Area 4, Beynam) appear to have initially accreted to the sole of the regional-scale Jurassic SSZ ophiolite. This was followed by the collision of a much larger Upper Jurassic-Lower Cretaceous oceanic seamount capped by a carbonate platform (Fig. 23). When this seamount entered the subduction trench its flank detached and accreted as multiple imbricate slices. These slices then tectonically intermixed, mainly with ultramafic rocks derived from the over-riding SSZ ophiolitic plate.

The shallow-water limestones in the Ankara Melange (Ankara region) are mainly clasts and blocks within debris-flows representing flank facies of the inferred large Upper Jurassic-Lower Cretaceous seamount. Shallow-water detritus was also shed from Upper Triassic-Lower Jurassic and Upper Cretaceous seamounts (atolls). Large blocks and slices of shallow-water limestone in the far south of the area (Area 3, W of Kulu) represent fragments of a sizeable Lower Cretaceous carbonate platform (probable back-reef facies). A likely origin is as the internal part of the large Upper Jurassic-Lower Cretaceous seamount rather than as exotic fragments of a separate, e.g., continental margin platform which lacks supporting evidence.

Some of the shallow-water limestone blocks could have been emplaced gravitationally during melange accretion. This particularly applies to neritic limestone blocks within some of the shear zones that separate intact volcanic-sedimentary and ultramafic ophiolitic units (e.g., Fig. 13k). During subduction, these blocks could have detached from the parent platform and slid into the subduction trench, where they behaved as 'ball-bearings' along accretionary decollements. When the seamount impinged on the ophiolitic fore-arc above the subduction

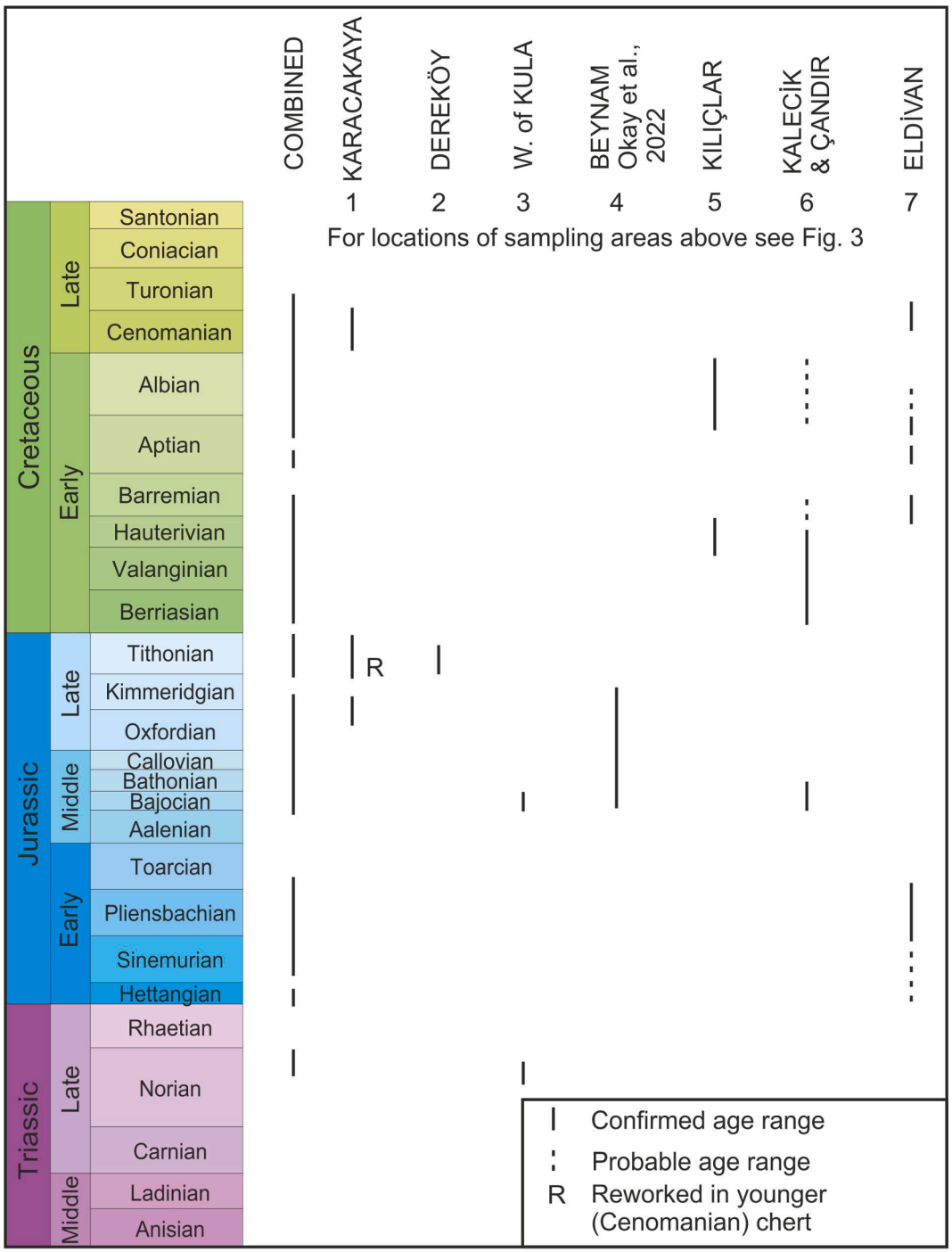

Fig. 22. Summary of new radiolarian age data from the seven areas of the Neotethyan Ankara Melange studied here (see Supplementary Table 2), together with recent data from the Area 4 (Beynam) (Okay et al., 2022), plotted on the time scale of Cohen et al. (2020). The radiolarites are associated with OIB, E-MORB and MORB related to the subducting lower plate. Comparative igneous geochemical data are from Rojay et al. (2004) (Areas 1, 2, 3, 5, 6 and 7) and from Okay et al. (2022) (Area 4). The areas sampled are shown in Fig. 3.

zone, fragments of the over-ridding SSZ ophiolitic plate detached, mainly represented by depleted mantle harzburgite including its metamorphic sole. The margins of accreted ophiolitic slices were sheared to form locally mylonitic fabrics, whereas intact to blocky mantle fabrics commonly remained within the interiors of harzburgitic thrust sheets. In places, accretionary thrusts cut up-section into cumulate ultramafics, layered and isotropic gabbros, sheeted dykes and even extrusives, allowing smaller volumes of these rocks to be incorporated into the melange (e.g., Area 5, Edige-Kılıçlar).

To the east of the region studied, accretionary melange is tectonically overlain by relatively intact SSZ-type ophiolites, notably the Refahiye, and Erzurum ophiolites (Rice et al., 2009; Parlak et al., 2013b; Robertson et al., 2014; Topuz et al., 2013; Uysal et al., 2015). Moving westwards, this tectonostratigraphy persists, but becomes more incomplete and/or dismembered (e.g., Eldivan and Edige ophiolites). Exceptionally, the boninitic Beynam ophiolite (Area 4) is dominated by mafic crustal rocks rather than mantle harzburgite. A possible explanation is that the Beynam ophiolite represents part of the outer feather edge of the SSZ fore-arc oceanic lithosphere that detached and was then re-imbricated with accretionary melange related to out-of-sequence

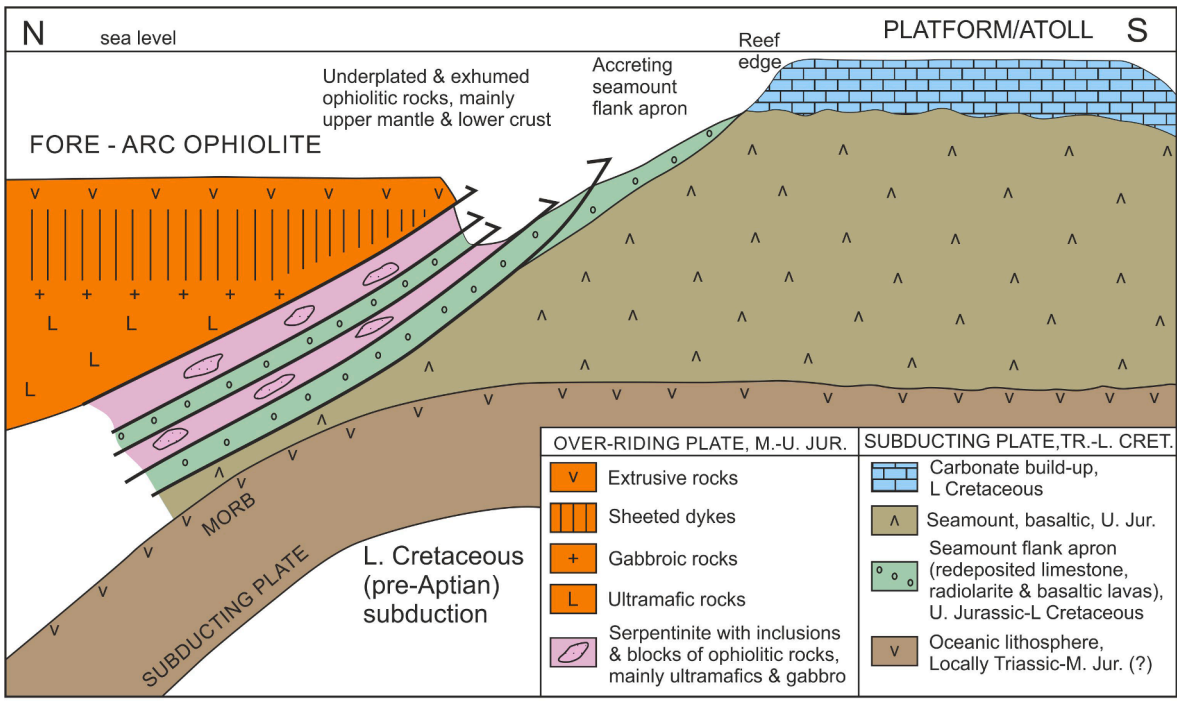

Fig. 23. Formation of part of the Neotethyan Ankara Melange (mainly in Areas 2,3,5 & 6) related to the collision of a large Upper Jurassic-Lower Cretaceous seamount with a latest Middle Jurassic-Upper Jurassic SSZ fore-arc ophiolite (modified from Robertson et al., 2023). The seamount flank was preferentially accreted while the seamount core and its capping carbonate platform mainly subducted. Slices were detached from the overriding fore-arc lithosphere (mainly serpentinised mantle harzburgite). The downgoing plate partly accreted while the over-riding ophiolitic plate underwent subduction erosion. See text for discussion.

thrusting. Out-of-sequence thrusting is well documented in modern subduction zones including the Nankai accretionary prism, SE Japan (e.g., Strasser et al., 2009).

The remarkable repetition of volcanic-sedimentary and ultramafic ophiolitic slices, commonly of sub-equal structural width (i.e., 10 s to 100 s m), as in Area 5, Edige-Kılıçlar (Fig. 7d, e), requires an explanation. Some form of dynamic equilibrium between subduction and accretion seems to have existed at certain times and places. As the seamount entered the trench and attempted to resist subduction, the pressure of the downgoing plate detached an ophiolitic slice from the outer, feather edge of the over-riding SSZ plate. As a result, a volcanic-sedimentary slice was detached from the flank of the incoming seamount and accreted to the over-riding plate. Over time, the net effect was that the seamount flanks preferentially accreted whereas the overriding ophiolitic plate underwent subduction-erosion. Little trench sediment accreted in this dominantly compressional setting. The igneous cores of the seamounts, large or small, mainly subducted. The above processes of seamount collision, accretion, detachment and subduction were repeated numerous times producing the observed systematic repetition of units. However, in many other areas the accreted units are variable, lenticular or anastomosing (e.g., Area 6, Kalecik; Fig. 7f) which could be explained by oblique subduction (e.g., Area 5, Edige-Kılıçlar; see structure, above), re-thrusting or later collision-related deformation.

Blueschists are absent in the Ankara region, although HP/LT metamorphic rocks are widespread within Neotethyan accretionary melanges of the İzmir-Ankara-Erzincan suture zone to the west, the north, and the east of the region studied (Fig. 2) (e.g., Okay and Kelley, 1994; Okay et al., 1998, Göncüoğlu et al., 2000; Çelik et al., 2019; Özkan et al., 2020). The relative absence of HP/LT metamorphic rocks in the Ankara region (Okay et al., 2022) points to high-level accretion without deep exhumation along the subduction channel. This could represent a dominantly compressional subduction-erosion setting associated with large-scale seamount collision that impeded upflow within the subduction channel.

Clues to the likely modes of seamount accretion come from the modern oceans, especially the circum-Pacific. The best documented example is the collision of the Daiichi-Kashima Seamount with the Japan trench adjacent to Honshu, although this is a continental margin rather than oceanic setting. The approaching oceanic seamount is breaking up and subsiding along a major median trench-parallel normal fault, resulting in tilting and partial subduction of the northwest margin of the seamount (Kobayashi et al., 1987; Tani, l989; Konishi, 1989; Dominguez et al., 1998). Material in the opposing fore-arc is pushed upwards and away from the collision zone. During subduction, small volumes of seamount material in the form of debris-flow deposits, blocks and small thrust slices can be transferred to the upper plate of the trench to form melange, as exposed in the adjacent Shimanto belt (e.g., Ogawa, 1985 and references).

Another relevant modern setting is where accretion takes place beneath SSZ fore-arc oceanic lithosphere (potential ophiolites), such in the West Pacific Izu-Bonin-Mariana region (Martinez and Taylor, 2003; Zhang et al., 2016). In the modern oceans, seamounts vary greatly in scale and longevity, from isolated but long-lived edifices, for example the Cape Verde Islands to linear chains, for example the Emperor Seamounts (Xu et al., 2022 and references; Portnyagin et al., 2008) and the Louisville Seamounts (Ballance et al., 1989; Ruellan et al., 2003; Deng et al., 2021). Accretion of modern volcanic seamounts has been reported from modern oceans including New Zealand (Pedley et al., 2010), the Mariana trench (Zhang et al., 2016) and the Middle America trench (Ruh et al., 2016), and has been modelled using analogue and numerical techniques (Dominguez et al., 2000; Ruh et al., 2016). Colliding seamounts can create tectonic embayments (re-entrants) in the accretionary wedge of the over-riding plate. Such collision-related deformation is likely to have affected the Neotethyan Ankara Melange but is difficult to recognise following superimposed collisional deformation.

The formation of the Neotethyan Ankara Melange involving the accretion of seamounts of variable size and age can also be compared with

numerous ancient and modern oceanic accretionary settings (e.g., Yang et al., 2022). Examples of inferred seamount accretion in various orogenic belts, from Precambrian to Recent, include seamounts within the Palaeotethyan accretionary prism of the Karakaya Complex in Turkey (Pickett and Robertson, 2004), and elsewhere in the Tethyan orogen including the Mesozoic of Greece (e.g., Palamakumbura et al., 2013). Accreted seamounts are commonplace around the periphery of the Pacific Ocean, for example in California (MacPherson, 1983; Shervais and Kimbrough, 1987), Japan (Lallemand et al., 1989; Okamura, 1991; Sakai et al., 2021) and the Tonga arc (Ballance et al., 1989). Accreted oceanic seamounts also feature in older oceanic suture zones notably the Late Palaeozoic of New Zealand (Landis and Blake, 1987; Cawood et al., 2002), and the Early Palaeozoic of the Iapetus as in Newfoundland (Zagorevski and McNicoll, 2012). Particularly relevant are examples where accretion took place beneath SSZ ophiolites, as in Oman (Lippard et al., 1986), Greece (Jones and Robertson, 1991) and New Zealand (Landis and Blake, 1987; Robertson, 2019) and Newfoundland (Waldron et al., 1988; Dewey and Casey, 2013).

8.2. Geological development of the Neotethyan Ankara melange

In recent years the overall tectonic development of the Neotethyan Ankara Melange has become increasingly well constrained (Rojay et al., 2004; Sarıfakıoğlu et al., 2017; Dangerfield et al., 2011; Okay et al., 2012, 2019, 2022; Robertson et al., 2022, 2023 and this study). The main stages of development are outlined below (Fig. 24). For brevity, supporting references given above are not repeated.

8.2.1. Upper Triassic ocean with seamounts subducting northwards (Fig. 24a)

Palaeotethys subducted northwards giving rise to the Palaeotethyan Ankara Melange (Karakaya Complex) to the north (Fig. 2). After Permian-Triassic rifting in the south, the Neotethyan İzmir-Ankara-Erzincan ocean (Northern Neotethys) opened by Late Triassic time. One or more small seamounts, locally capped by carbonate build-ups, developed during the Late Triassic (Norian). Radiolarian deposition took place beneath the CCD on the abyssal plain, whereas micritic deposits accumulated above the CCD near marginal platforms and atolls (Robertson et al., 2022).

8.2.2. Mid-Late Jurassic SSZ-spreading (Fig. 24b)

Possibly driven by regional to global plate motion changes, notably the opening of the Central Atlantic (e.g., Smith, 2006), SSZ spreading was initiated across >1000 km of the Neotethyan ocean, at least from the Ankara region eastwards into the Lesser Caucasus region. The locus of subduction initiation is unknown but could have been a transform fault. The setting of SSZ ophiolite genesis was comparable to the mid-Cenozoic of the W Pacific Izu-Bonin-Mariana forearc (e.g., Reagan et al., 2017).

8.2.3. Late Jurassic-Early Cretaceous seamount construction (Fig. 24c)

During the Late Jurassic-Early Cretaceous, a large seamount developed, possibly related to a long-lived intra-oceanic mantle plume. The seamount was capped by a carbonate platform and flanked by shallow to deep-water volcanic, redeposited facies and pelagic sediments including hemipelagic carbonates and radiolarites. Non-calcareous radiolarian deposition continued on the adjacent abyssal plain below the CCD.

8.2.4. Albian accretion of melange related to seamount-forearc collision (Fig. 24d)

Related to northward subduction the Upper Triassic-Lower Jurassic seamounts initially accreted to the over-riding oceanic plate. Probably during the late Albian (c. 105 Ma), the large seamount with its capping carbonate platform/atoll collided with the intra-oceanic trench, leading to successive detachment and accretion of slope-apron lithologies. Material was repeatedly detached from the over-riding SSZ ophiolite and mixed with material derived from the subducting plate. Right-lateral (oblique) subduction is inferred from available structural evidence.

8.2.5. Late Cretaceous-Early Cenozoic development (Fig. 24e-h)

Following accretion in an intra-oceanic setting, the Ankara Melange accretionary prism may have begun to collide with the Sakarya continent to the northwest during the Coniacian (Fig. 24e). This can be inferred from the arrival of mass-transport facies containing melange material on the neighbouring Sakarya carbonate platform during this time (Robertson et al., 2023), although other interpretations exist (Okay et al., 2019). A second phase of SSZ-spreading created Upper Cretaceous oceanic lithosphere within the İzmir-Ankara-Erzincan ocean (Northern Neotethys) that is, however, not preserved associated with the Neotethyan Ankara Melange (Fig. 24e), despite being emplaced over the Kırşehir Massif to the southeast (Fig. 1). As northward subduction continued, the Neotethyan Ankara Melange was covered by Upper Cretaceous arc-related magmatic rocks and associated volcanogenic sedimentary rocks (Kavak Formation) and related fore-arc sedimentary rocks (Karadağ Formation) (Fig. 24f). The melange and arc-related rocks were transgressed by mixed terrigenous-volcaniclastic sediments especially deep-sea turbidites (Fig. 24g) that accumulated in a continental margin fore-arc basin (Haymana Formation and equivalents) during latest Cretaceous-Paleogene time. The melange and cover units were, in places, re-imbricated during late subduction and/or continental collision, culminating in suturing of the İzmir-Ankara-Erzincan ocean during pre-Middle Eocene time (Fig. 24e-h). The collision of the Kırşehir Massif to the southeast is also credited with driving the well-documented c. 45° anticlockwise palaeorotation of the Neotethyan Ankara Melange and the Sakarya Zone farther west (Kaymakçı et al., 2003a, b; Meijers et al., 2010; Çinku et al., 2016a, 2016b).

9. Conclusions

1. The Neotethyan Ankara Melange in the Ankara region partially accreted during the Early Cretaceous (pre-Albian), related to northward subduction of the İzmir-Ankara-Erzincan ocean (=Northern Neotethys) beneath the Sakarya continent to the northwest (in modern co-ordinates). Further subduction-accretion took place during the Late Cretaceous, followed by Maastrichtian-Eocene collision.
2. In many areas, the Ankara Melange exposes two main, contrasting litho-tectonic units: (1) slices of volcanic-sedimentary rocks that are interpreted as slope-apron lithologies of a large intra-oceanic seamount, capped by a shallow-water carbonate platform (atoll); (2) variably dismembered latest Early-Upper Jurassic oceanic lithosphere, mainly composed of ultramafic upper mantle and crustal ophiolitic rocks, locally including boninites that formed in supra-subduction zone settings, potentially ranging from fore arc to back arc.
3. The seamount flank apron developed in response to repeated eruptions of basaltic lavas on the seamount and its slopes, interspersed with radiolarite and pelagic carbonate on its lower slopes. Calciturbidites and calcareous debris-flow deposits between volcanic flows were reworked downslope from the capping carbonate platform. Non-calcareous radiolarian sediments accumulated below the carbonate compensation depth around the seamount and in the adjacent ocean from Late Triassic (Norian) to Late Cretaceous (Cenomanian) in the region studied.
4. New and existing radiolarian data indicate that oceanic seamount construction mainly took place during the Late Jurassic (Tithonian) to early Late Cretaceous (Albian). Benthic foraminiferal data further suggest that the capping carbonate platform mainly formed during the Early Cretaceous (late Barremian-early Aptian). Smaller-scale seamount construction also took place elsewhere during the Late Triassic (Norian)-Early Jurassic and the Late Cretaceous.
5. The Neotethyan Ankara Melange accreted by tectonic processes at shallow structural levels in the forearc of an intra-oceanic subduction

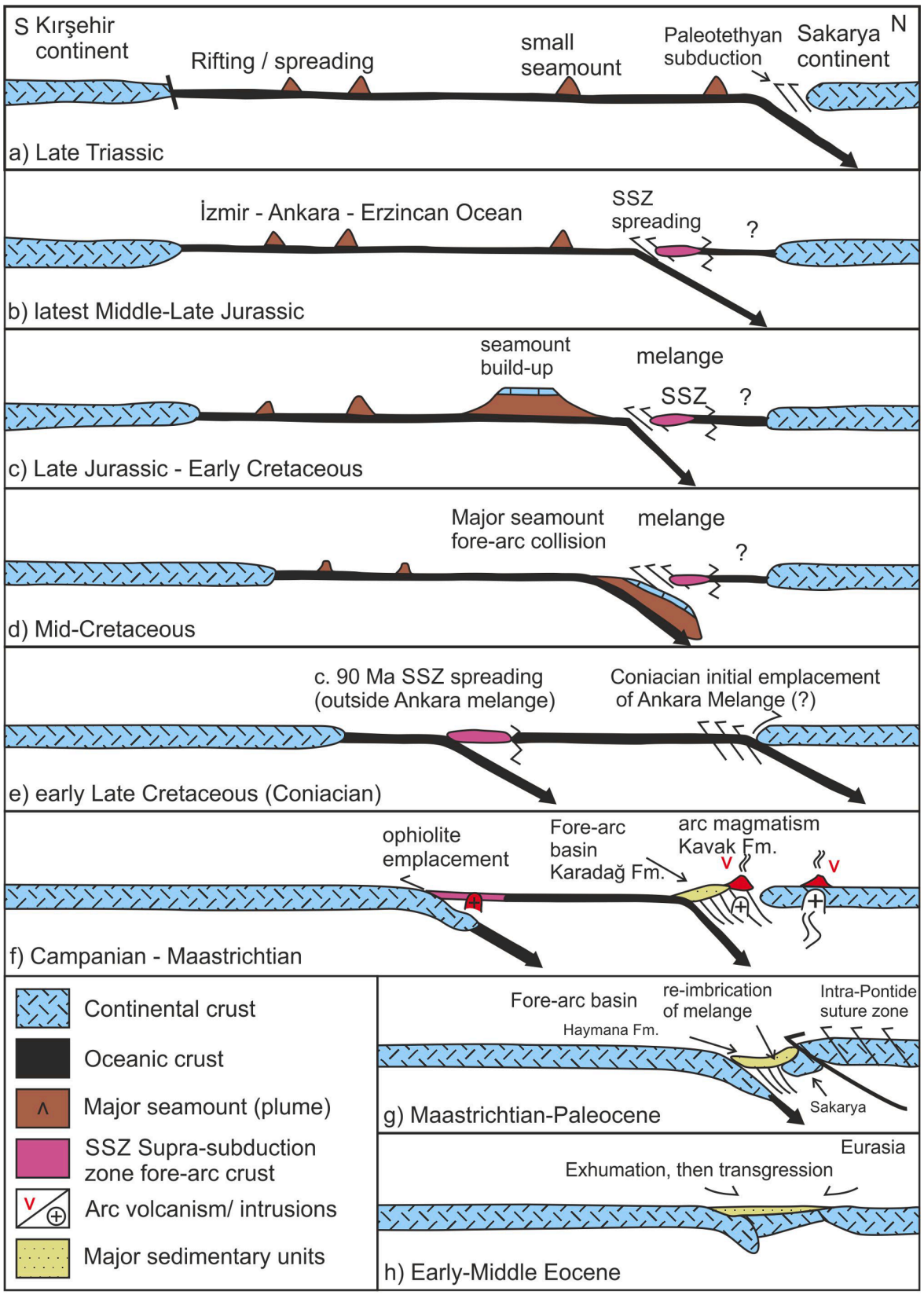

Fig. 24. Proposed N-S tectonic model of the Ankara melange (modified from Robertson et al., 2023). a, Late Triassic. İzmir-Ankara-Erzincan ocean is already open; b, Mid-Late Jurassic SSZ-spreading (e.g., Eldivan ophiolite); c, Late Jurassic-Early Cretaceous major seamount construction, capped by carbonate platform; d, Mid-Cretaceous (Aptian-Albian) accretion of the Ankara Melange related to seamount-forearc (ophiolite) collision; e, Late Cretaceous (Coniacian) potential initial collision of the accretionary wedge with the Sakarya continent; f, Late Cretaceous (Campanian-Maastrichtian) arc magmatism and related fore-arc deposition; g, Maastrichtian-Palaeocene continental collision and fore-arc deposition (Haymana Formation); h, Early-Middle Eocene regional post-collisional transgression of the suture zone. Note: The Intra-Pontide suture zone to the north of the Sakarya continent is not shown (see Fig. 1).

zone. Slices repeatedly detached from the colliding seamount flank and accreted to the overriding plate. The seamount core (basaltic lavas) and its capping carbonate platform subducted, other than for some large blocks and dismembered thrust sheets of neritic limestone in one known area. Slices of the over-riding ophiolitic fore-arc also repeatedly detached and accreted in response to subduction erosion, especially depleted mantle harzburgite and gabbroic rocks. Structural data are consistent with oblique dextral subduction.

6. Trench sediments (e.g., coeval turbidites) are rarely preserved, possibly because the overall compressional setting during subduction inhibited upflow/exhumation of high pressure/low temperature accretionary material (e.g., blueschists) from deep in the accretionary prism. HP/LT melange is, however, present in other areas of the Ankara-İzmir-Erzincan suture zone accretionary melange where tectonic conditions differed.
7. The accretion of the Neotethyan Ankara Melange to supra-subduction zone oceanic lithosphere is similar to seamount accretion, notably beneath the Izu-Bonin-Mariana oceanic forearc in the W Pacific region. The accretion is also similar to some melanges associated with supra-subduction zone ophiolites elsewhere in Tethys (e.g., Oman), the circum-Pacific (e.g., Japan and California) and Iapetus (e.g., Newfoundland).
8. Upper Cretaceous arc magmatism and latest Cretaceous-Eocene late-subduction and/or collision-related processes significantly influenced the tectonostratigraphy of the Neotethyan Ankara Melange.

Declaration of Competing Interest

The authors declare that they have no known competing financial interests or personal relationships that could have appeared to influence the work reported in this paper.

Data availability

Data will be made available on request.

Acknowledgements

We thank Ayhan Zenginoğlu (Çukurova University) for preparation of thin sections and Yağız Demirtay for assistance with drawing the diagrams. The manuscript benefitted from comments by the three anonymous reviewers and the editor, Prof. İbrahim Uysal.

Appendix A. Supplementary data

Supplementary data to this article can be found online at https://doi.org/10.1016/j.jaesx.2023.100151.

References

Akçay, A.E., Dönmez, M., Kara, H., Yergök, A.F., Esentürk, K., 2007. Geological map of the Yozgat I33 Quadrangle: Ankara, Turkey. General Directorate Miner. Res. Explor. (MTA) Publ. 80, 16p.

Akyürek, B., Bilginer, E., Aktaş, B., Hepşen, N., Pehlivan, N., Sunu, O., Soysal, Y., Dağer, Z., Çatal, E., Sözeri, B., Yıldırım, H., Hakymez, H., 1984. The geology of the Ankara-Elmadağ-Kalecik region. Bull. Geol. Eng. Turkey 20, 31–46 [in Turkish with English abstract].

Akyürek, B., Duru, M., Sütçü, Y.F., Papak, I., Şaroğlu, F., Pehlivan, N., Gönenç, Granit, S., Yaşar, T., 1997. 100,000 scale Turkish Geology Map (no: 55), Ankara-İ29 map. General Directorate of Miner. Res. Explor. (MTA), Ankara.

Aygül, M., Okay, A.I., Oberhansli, R., Schmidt, A., Sudo, M., 2015. Late Cretaceous infant intra-oceanic arc volcanism, the Central Pontides, Turkey. Petrogenetic and tectonic implications. J. Asian Earth Sci. 111, 312–327.

Bailey, E.B., McCallien, W.J., 1950. The Ankara mélange and the Anatolian thrust. Miner. Res. Explor. Inst. Turkey 40, 17–21.

Bailey, E.B., McCallien, W.S., 1953. The Ankara Mélange and Anatolia Thrust. Nature 166, 938–941.

Balcı, U., Sayıt, K., 2020. Diabase dykes from Boğazkale (Çorum), Central Anatolia: Geochemical insights into the geodynamical evolution of the northern branch of Neotethys. Geochem. 80, 2. https://doi.org/10.1016/j.chemer.2020.125602.

Ballance, P.F., Scholl, D.W., Vallier, T.L., Stevenson, A.J., Ryan, H., Herzer, R.H., 1989. Subduction of a Late Cretaceous Seamount of the Louisville Ridge at the Tonga Trench: a model of normal and accelerated tectonic erosion. Tectonics 8 (5), 953–962.

Batman, B., 1978. Geological evolution of northern part of Haymana region and study of the mélange in the area-I: stratigraphic units. Bull. Earth Sci. Hacettepe University 4, 95–124 [in Turkish with English abstract].

Batman, B., 1981. Study of the ophiolitic mélange (Dereköy formation) in the northern area of Haymana (SW Ankara). Bull. Earth Sci. Hacettepe University 8, 61–70 [in Turkish with English abstract].

Berber, F., Sayıt, K., Göncüoğlu, M.C., 2021. Geochemistry and U-Pb ages from the Kösdağ Metavolcanics in the southern Central Pontides (Turkey): complementary data for early late Cretaceous island arc development in the Northern Neotethys. Tr. J. Earth Sci. 30, 59–80.

Boccaletti, M., Bortolotti, V., Sagri, M., 1966. Ricerche sulle ofioliti della Catene Alpine; Osservazioni sull'Ankara mélange nella zona di Ankara. Boll. Soc. Geol. Ital. 85, 485–508.

Bortolotti, V., Chiari, M., Göncüoglu, M.C., Marcucci, M., Principi, G., Tekin, U.K., Saccani, E., Tassinari, R., 2013. Age and geochemistry of basalt-chert associations in the ophiolitic complexes of the Izmir-Ankara Mélange East of Ankara, Turkey: preliminary data. Ofioliti 38, 157–173.

Bortolotti, V., Chiari, M., Göncüoğlu, M.C., Principi, G., Saccani, E., Tekin, U.K., Tassinari, R., 2018. The Jurassic-Early Cretaceous basalt–chert association in the ophiolites of the Ankara Mélange, east of Ankara, Turkey: age and geochemistry. Geol. Mag. 155 (2), 451–478.

Bragin, N.Y., Tekin, U.K., 1996. Age of radiolarian-chert blocks from the Senonian Ophiolitic Melange (Ankara, Turkey). Isl. Arc 5, 114–122.

Busby, C.J., Tamura, Y., Blum, P., Guèrin, G., Andrews, G.D.M., Barker, A.K., Berger, J.L. R., Bongiolo, E.M., Bordiga, M., DeBari, S.M., Gill, J.B., Hamelin, C., Jia, J., John, E. H., Jonas, A.S., Jutzeler, M., Kars, M.A.C., Kita, Z.A., Konrad, K., Mahony, S.H., Martini, M., Miyazaki, T., Musgrave, R.J., Nascimento, D.B., Nichols, A.R.L., Ribeiro, J.M., Sato, T., Schindlbeck, J.C., Schmitt, A.K., Straub, S.M., Vautravers, M. J., Yang, Y., 2017. The missing half of the subduction factory: shipboard results from the Izu rear arc. IODP Expedition 350. Int. Geol. Rev. 59, 1677–1708.

Cawood, P.A., Landis, C.A., Nemchin, A.A., Hada, S., 2002. Permian fragmentation, accretion and subsequent translation of a low-latitude Tethyan seamount to the high-latitude east Gondwana margin: evidence from detrital zircon age data. Geol. Mag. 139 (2), 131–144.

Chen, G., Robertson, A.H.F., 2020. User's guide to the interpretation of sandstones using whole-rock chemical data, exemplified by sandstones from Triassic to Miocene passive and active margin settings from the Southern Neotethys in Cyprus. Sediment. Geol. 400, 105616 https://doi.org/10.1016/j.sedgeo.2020.105616.

Cohen, K.M., Harper, D.A.T., Gibbard, P.L., 2020. ICS international chronostratigraphic chart, 2020/01. Int. Comm. Stratigraphy, IUGS, www.stratigraphy.org.

Collins, A.S., Robertson, A.H.F., 1997. Lycian melange, southwestern Turkey: an emplaced Late Cretaceous accretionary complex. Geology 25, 25–258.

Cowan, D.S., 1978. Origin of blueschist-bearing chaotic rocks in the Franciscan Complex, San Simeon, California. Geol. Soc. Am. Bull. 89, 1415–1423.

Çakır, Ü., Üner, T., 2016. The Ankara Mélange: an indicator of Tethyan evolution of Anatolia. Geol. Carpathica 67 (4), 403–414. https://doi.org/10.1515/geoca-2016-0025.

Çapan, U.Z., Buket, E., 1975. Aktepe-Gökdere Bölgesinin Jeolojisi ve Ofiyolitli Melanj. Bull. Geol. Soc. Turkey 18 (1), 11–16.

Çapan, U., Floyd, A., 1985. Geochemical and petrographic features of meta-basalts within units of the Ankara Melange, Turkey. Ofioliti 10, 3–18.

Çelik, Ö.F., Chiaradia, M., Marzoli, A., Billor, Z., Marschik, R., 2013. The Eldivan ophiolite and volcanic rocks in the Izmir–Ankara–Erzincan suture zone, northern Turkey: geochronology, whole-rock geochemical and Nd–Sr–Pb isotope characteristics. Lithos 172–173, 31–46.

Çelik, Ö.F., Marzoli, A., Marschik, R., Chiaradia, M., Neubauer, F., Öz, I., 2011. Early Middle Jurassic intra-oceanic subduction in the Izmir–Ankara–Erzincan Ocean, northern Turkey. Tectonophysics 509, 120–134.

Çelik, Ö.F., Özkan, M., Chelle-Michou, C., Sherlock, S., Marzoli, A., Ulianov, A., Altıntaş, İ.E., Topuz, G., 2019. Blueschist facies overprint of late Triassic Tethyan oceanic crust in a subduction-accretion complex in north-central Anatolia. Turkey. J. Geol. Soc. London 176, 945–957.

Çinku, M.C., Hisarlı, Z.M., Hirt, A., Friedrich, H., Ustaömer, T., Kaya, N., Öksüm, E., Orbay, N., 2016a. Evidence of Late Cretaceous oroclinal bending in north-central Anatolia: palaeomagnetic results from Mesozoic and Cenozoic rocks along the İzmir–Ankara–Erzincan Suture Zone. In: Pueyo, E.L., Cifelli, F., Sussman, A.J., Oliva-Urcia, B., (Eds.), Palaeomagnetism in Fold and Thrust Belts: New Perspectives: Geol. Soc. London, Spec. Publ. 425, pp. 189–212.

Çinku, M.C., Hisarlı, Z.M., Yılmaz, Y., Ülker, B., Kaya, N., Öksüm, E., Orbay, N., Özbey, Z. Ü., 2016b. The tectonic history of the Niğde-Kırşehir Massif and the Taurides since the Late Mesozoic: paleomagnetic evidence for two-phase orogenic curvature in Central Anatolia. Tectonics 35, 772–811. https://doi.org/10.1002/2015TC003956.

Dangerfield, A., Harris, R., Sarıfakıoğlu, E., Dilek, Y., 2011. Tectonic evolution of the Ankara mélange and associated Eldivan ophiolite near Hançili, central Turkey. In: Wakabayashi, J., Dilek, Y. (Eds.), Melange: Processes of formation and Societal Significance, Geol. Soc. Am. Spec. Pap. 198, 153-168.

Dewey, J.F., Casey, J.F., 2013. The sole of an ophiolite: The Ordovician Bay of Islands Complex, Newfoundland. J. Geol. Soc. London 170 (5), 715–722.

Dilek, Y., Ogawa, Y., 2021. Subduction zone processes and crustal growth mechanisms at Pacific Rim convergent margins: modern and ancient analogues. Geol. Mag. 158 (1), 1–12.

Dilek, Y., Thy, P., 2006. Age and petrogenesis of plagiogranite intrusions in the Ankara, mélange, central Turkey. Isl. Arc 15, 44–57.
Deng, J., Zhang, L., Liu, H., Liu, H., Liao, R., Mastoi, A.S., Yang, X., Sun, W., 2021. Geochemistry of subducted metabasites exhumed from the Mariana forearc: implications for Pacific seamount subduction. Geosci. Front. 12 (3), 101117.
Dominguez, S., Lallemand, S.E., Malavieille, J., von Huene, R., 1998. Upper plate deformation associated with seamount subduction. Tectonophysics 293 (3–4), 207–224.
Dominguez, S., Malavieille, J., Lallemand, S.E., 2000. Deformation of accretionary wedges in response to seamount subduction: insights from sandbox experiments. Tectonics 19 (1), 182–196.
Dönmez, M., Akçay, A.E., 2010. 1:100,000-scale Turkish Geological Map, No: 138, Çankırı-H30 Map. Miner. Res. Explor. Inst. Turkey, Ankara.
Dönmez, M., Akçay, A.E., Türkecan, A., Evcimen, Ö., Atakay, E., Görmüş, T., 2009. Ankara ve yakın çevresinin Tersiyer volkanitleri. Miner. Res. Explor. Inst. Turkey, Report No. 11164, 116 pp. Ankara (in Turkish, unpublished).
Duru, M., Aksay, A., 2002. 1:100,000 scale Turkish Geological Map No. 42, Bolu-H29 Map. Miner. Res. Explor. Inst. Turkey, Ankara.
Erdoğan, B., Akay, C., Uğur, M.S., 1996. Geology of the Yozgat region and evolution of the collisional Çankırı basin. Int. Geol. Rev. 38, 788–806.
Festa, A., Dilek, Y., Pini, G.A., Codegone, G., Ogata, K., 2012. Mechanisms and processes of stratal disruption and mixing in the development of mélanges and broken formations: Redefining and classifying mélange. Tectonophysics 568–569, 7–24.
Festa, A., Ogata, K., Pini, G.A., Dilek, Y., Codegone, G., 2015. Late Oligocene–early Miocene olistostromes (sedimentary mélanges) as tectono-stratigraphic constraints to the geodynamic evolution of the exhumed Ligurian accretionary complex (Northern Apennines, NW Italy). Int. Geol. Rev. 57, 540–562.
Festa, A., Pini, G.A., Dilek, Y., Codegone, G., 2010. Mélanges and mélange-forming processes: a historical overview and new concepts. Int. Geol. Rev. 52 (10–12), 1040–1105.
Floyd, P.A., 1993. Geochemical discrimination and petrogenesis of alkali basalt sequences in part of the Ankara mélange, Central Turkey. J. Geol. Soc. London 150, 541–550.
Gansser, A., 1974. The ophiolite mélange: a world-wide problem on Tethyan examples. Eclogae Geol. Helv. 67, 479–507.
Göncüoğlu, M.C., Tekin, U.K., Sayit, K. (Eds.), 2015. Pre-conference excursion: four day field trip to the Karakaya Complex and the İzmir-Ankara Suture belt in central and western Turkey. 14. INTERRAD Guidebook, 1-44.
Göncüoğlu, M.C., Turhan, N., Şentürk, K., Özcan, A., Uysal, S., 2000. A geotraverse across NW Turkey: tectonic units of the Central Sakarya region and their tectonic evolution. In: Bozkurt, E., Winchester, J., Piper, J.A., (Eds.), Tectonics and Magmatism in Turkey and the Surrounding Area. Geol. Soc. London Spec. Publ. 173, 139-161.
Hall, R., 1976. Ophiolite emplacement and the evolution of the Taurus suture zone, southeastern Turkey. Geol. Soc. Am. Bull. 87 (7), 1078–1088.
Hakyemez, Y., Barkurt, M.Y., Bilginer, E., Pehlivan, Ş., Can, B., Dağer, Z., Sözeri, B., 1986. The geology of Yapraklı–Ilgaz– Çankırı–Çandır surroundings. Miner. Res. Explor. Inst. Turkey, Report No. 7966, Ankara (in Turkish, unpublished).
Jones, G., Robertson, A.H.F., 1991. Tectono-stratigraphy and evolution of the Mesozoic Pindos ophiolite and related units, northwestern Greece. J. Geol. Soc. London 148, 267–288.
Kaymakçı, N., 2000. Tectono-stratigraphical evolution of the Çankırı Basin (Central Anatolia, Turkey). PhD Thesis, Geoligica Ultraiecta, Universiteit Utrecht, Netherlands.
Kaymakçı, N., Duermeijer, C.E., Langereis, C., White, S.H., van Dijk, P.M., 2003a. Paleomagnetic evolution of the Çankırı Basin (Central Anatolia, Turkey: Implication for oroclinal bending due to indentation. Geol. Mag. 140, 343–355.
Kaymakçı, N., White, S.H., van Dijk, P.M., 2000. Palaeostress inversion in a multiphase deformed area: kinematic and structural evolution of the Çankırı Basin (Central Turkey), Part 1–Northern Area. In: Bozkurt, E., Winchester, J., Piper, J.A. (Eds.), Tectonics and magmatism in Turkey and the surrounding area. Geol. Soc. London Spec. Publ. 173, 295–323.
Kaymakçı, N., White, S.H., van Dijk, P.M., 2003b. Kinematic and structural development of the Çankiri Basin (Central Anatolia, Turkey): a paleostress inversion study. Tectonophysics 364 (1–2), 85–113.
Kaymakçı, N., Özçelik, Y., White, S.H., and van Dijk, P.M., 2009. Tectono-stratigraphy of the Çankırı Basin: late Cretaceous to early Miocene evolution of the Neotethyan suture zone in Turkey. In: van Hinsbergen, D.J.J., Edwards, M. A., Govers, R. (Eds.), Collision and Collapse at the Africa - Arabia - Eurasia Subduction Zone. Geol. Soc. London Spec. Publ. 311, 67–106.
Kobayashi, K., Cadet, J.P., Aubouin, J., Boulegue, J., Dubois, J., Von Huene, R., Jolivet, L., Kanazawa, T., Kasahara, J., Koizumi, K., Lallemand, S., Nakamura, Y., Pautot, G., Suyehiro, K., Tani, S., Tokuyama, H., Yamazaki, T., 1987. Normal faulting of Daiichi Kashima seamount in the Japan trench revealed by the Kaiko 1 cruise, Leg 3. Earth Planet. Sci. Lett. 83, 257–266.
Koçyiğit, A., 1988. Examples from the forearc basin remnants at the active margin of northern Neo-Tethys; development and emplacement ages of the Anatolian Nappe, Turkey. METU J. Pure Appl. Sci. 21, 183–210.
Koçyiğit, A., 1991. An example of an accretionary fore arc basin from Northern Central Anatolia and its implications for the history of subduction of Neo-Tethys in Turkey. Geol. Soc. Am. Bull. 103, 22–36.
Konishi, K., 1989. Limestone of the Daiichi Kashima Seamount and the fate of a subducting guyot: fact and speculation from the Kaiko “Nautile” dives. Tectonophysics 160 (1–4), 249–265.
Landis, C.A., Blake Jr, M.C., 1987. Tectonostratigraphic terranes of the Croissilles Harbour region, South Island, New Zealand. Terrane Accret. Orog. Belts 19, 179–198.
Lallemand, S., Culotta, R., Huene, R.V., 1989. Subduction of the Daiichi Kashima Seamount in the Japan Trench. Tectonophysics 160 (1–4), 231–247.
Lippard, S.J., Shelton, A.W., Gass, I.G., 1986. The ophiolite of northern Oman. Geol. Soc. London Mem. 11 (1), 167–178.
MacPherson, G.J., 1983. The Snow Mountain volcanic complex: an on-land seamount in the Franciscan terrain, California. J. Geol. 91 (1), 73–92.
Marroni, M., Frassi, C., Göncüoğlu, M.C., Di Vincenzo, G., Pandolfi, L., Rebay, G., Ellero, A., Ottria, G., 2014. Late Jurassic amphibolite-facies metamorphism in the intra-pontide suture zone (Turkey): an eastward extension of the Vardar ocean from the Balkans into Anatolia? J. Geol. Soc. Lond. 171, 605–608.
Marroni, M., Göncüoğlu, M.C., Frassi, C., Sayit, K., Pandolfi, L., Ellero, A., Ottria, G., 2020. The Intra-Pontide ophiolites in Northern Turkey revisited: From birth to death of a Neotethyan oceanic domain. Geosci. Frontiers 11, 129–149.
Martinez, F., and Taylor, B., 2003. Controls on back-arc crustal accretion: insights from the Lau, Manus and Mariana basins. In: Larter, R.D., Leat, P.T. (Eds.), Intra-Oceanic Subduction Systems: Tectonic and Magmatic Processes, Geol. Soc. London Spec. Publ. 219, 19–54.
Meijers, M.J.M., Kaymakcı, N., Van Hinsbergen, D.J.J., Langereis, C.G., Stephenson, R. A., Hippolyte, J.C., 2010. Late Cretaceous to Paleocene oroclinal bending in the central Pontides (Turkey). Tectonics 29. https://doi.org/10.1029/2009TC002620.
Mori, R., Ogawa, Y., Hirano, N., Tsunogae, T., Kurosawa, M., Chiba, T., 2011. Role of plutonic and metamorphic block exhumation in a forearc ophiolite mélange belt: an example from the Mineoka belt, Japan. In: Wakabayashi, J., Dilek, Y. (Eds.), Mélanges: Processes of Formation and Societal Significance, Geol. Soc. Am. Spec. Pap. 480, 95–115, doi: 10.1130/2011.2480(04).
MTA, 2011. Geological map of Turkey 1:250,000. Miner. Res. Explor. Inst. Turkey, Ankara.
Nairn, S., Robertson, A.H.F., Taslı, K., Inan, N., Ünlügenç, U.C., 2012. Tectonostratigraphic evolution of the Upper Cretaceous–Cenozoic Central Anatolian basins: An integrated study of diachronous ocean basin closure and continental collision. In: Robertson, A.H.F., Parlak, O., Ünlügenç, Ü.C. (Eds.), Geological Development of Anatolia and the Easternmost Mediterranean region, Geol. Soc. London Spec. Publ. 372, 383–384.
Norman, T.N., 1972. Stratigraphy of Upper Cretaceous-Lower Tertiary strata of Yahşihan area, east of Ankara. Bull. Geol. Soc. Turkey 15 (2), 180–276 [in Turkish with English abstract].
Norman, T., 1973a. On the structure of the Ankara mélange. In: Proc. Symp. Occasion 50th Anniver. Turkish Republic. Miner. Res. Explor. Inst. Turkey Spec. Publ., pp. 77–94 [in Turkish with English abstract].
Norman, T.N., 1973b. Post Eocene tectonic development of Ankara Yahşihan region. Bull. Geol. Soc. Turkey 16, 67–81 [in Turkish with English abstract].
Norman, T.N., 1984. The role of the Ankara Melange in the development of Anatolia (Turkey). In: Dixon, J.E., Robertson, A.H.F. (Eds.), The Geological Evolution of the Eastern Mediterranean, Geol. Soc. London Spec. Publ. 17, 441–447.
Ogawa, Y., 1985. Variety of subduction and accretion processes in Cretaceous to Recent plate boundaries around southwest and central Japan. Tectonophysics 112 (1–4), 493–518.
Okamura, Y., 1991. Large-scale melange formation due to seamount subduction: an example from the Mesozoic accretionary complex in central Japan. J. Geol. 99 (5), 661–674.
Okay, A.İ., Altıner, D., 2016. Carbonate sedimentation in an extensional active margin: Cretaceous history of the Haymana region, Pontides. Int. J. Earth Sci. 105, 2013–2030.
Okay, A.İ., Altıner, D., Kylander-Clark, A.R.C., 2019. Major Late Cretaceous mass flows in central Turkey recording the disruption of the Mesozoic continental margin. Tectonics 38, 960–989.
Okay, A.İ., Altıner, D., Danelian, T., Topuz, G., Özcan, E., Kylander-Clark, A.R.C., 2022. Subduction-accretion complex with boninitic ophiolite slices and Triassic limestone seamounts: Ankara Mélange, central Anatolia. Geol. Mag. https://doi.org/10.1017/S0016756822000504.
Okay, A.İ., Göncüoğlu, M.C., 2004. The Karakaya Complex: a review of data and concepts. Tr. J. Earth Sci. 13, 75–95.
Okay, A.İ., Harris, N.B., Kelley, S.P., 1998. Exhumation of blueschists along a Tethyan suture in northwest Turkey. Tectonophysics 285, 275–299.
Okay, A.İ., Işıntek, İ., Altıner, D., Özkan-Altıner, S., Okay, N., 2012. An olistostrome–mélange belt formed along a suture: Bornova Flysch zone, western Turkey. Tectonophysics 568, 282–295.
Okay, A.İ., Kelley, S.P., 1994. Tectonic setting, petrology and geochronology of jadeite+ glaucophane and chloritoid+ glaucophane schists from north-west Turkey. J. Metamorphic Geol. 2, 455–466.
Özkan, M., Çelik, Ö.F., Soycan, H., Çörtük, R.M., Marzoli, A., 2020. The Middle Jurassic and Early Cretaceous basalt-radiolarian chert association from the Tekelidağ Mélange, eastern İzmir-Ankara-Erzincan suture zone (northern Turkey). Cretaceous Res. 107, 104280.
Palamakumbura, R.N., Robertson, A.H., Dixon, J.E., 2013. Geochemical, sedimentary and micropaleontological evidence for a Late Maastrichtian oceanic seamount within the Pindos ocean (Arvi Unit, S Crete, Greece). Tectonophysics 595, 250–262.
Parlak, O., Karaoğlan, F., Rızaoğlu, T., Klötzli, U., Koller, F., Billor, M.Z., 2013a. U-Pb and ^{40}Ar–^{39}Ar geochronology of the ophiolites and granitoids from the Tauride belt: implications for the evolution of the Inner Tauride suture. J. Geodyn. 65, 22–37.
Parlak, O., Çolakoğlu, A., Dönmez, C., Sayak, H., Yıldırım, N., Türkel, A., Odabaşı, İ., 2013b. Geochemistry and tectonic significance of ophiolites along the Izmir–Ankara–Erzincan suture zone in Northeastern Anatolia. In: Robertson, A.H.F.,

Parlak, O., Ünlügenç, U.C. (Eds.), Geological Development of Anatolia and the Easternmost Mediterranean Region: Geol. Soc., London, Spec. Publ. 372, 75–105.
Parlak, O., Dunkl, I., Karaoğlan, F., Kusky, T.M., Zhang, C., Wang, L., Koepke, J., Billor, Z., Hames, W.E., Şimşek, E., Şimşek, G., 2019. Rapid cooling history of a Neotethyan ophiolite: Evidence for contemporaneous subduction initiation and metamorphic sole formation. Geol. Soc. Am. Bull. 131 (11–12), 2011–2038.
Pedley, K.L., Barnes, P.M., Pettinga, J.R., Lewis, K.B., 2010. Seafloor structural geomorphic evolution of the accretionary frontal wedge in response to seamount subduction, Poverty Indentation, New Zealand. Mar. Geol. 270 (1–4), 119–138.
Pickett, E.A., Robertson, A.H.F., 1996. Formation of the Late Palaeozoic-Early Mesozoic Karakaya Complex and related ophiolites in NW Turkey by Paleotethyan subduction-accretion. J. Geol. Soc. London 153, 995–1009.
Pickett, E.A., Robertson, A.H., 2004. Significance of the volcanogenic Nilüfer Unit and related components of the Triassic Karakaya Complex for Tethyan subduction/accretion processes in NW Turkey. Tr. J. Earth Sci. 13 (2), 97–143.
Polat, A., Casey, J.F., 1995. A structural record of the emplacement of the Pozantı-Karsantı ophiolite onto the Menderes-Taurus block in the Late Cretaceous, eastern Taurides, Turkey. J. Struct. Geol. 17, 1673–1688.
Portnyagin, M., Savelyev, D., Hoernle, K., Hauff, F., Garbe-Schönberg, D., 2008. Mid-Cretaceous Hawaiian tholeiites preserved in Kamchatka. Geology 36, 903–906.
Raymond, L.A., 1984 (Ed.). Melanges: Their Nature, Origin and Significance. Geol. Soc. Am. Spec. Pap. 198, Boulder, Colorado.
Raymond, L.A., 2018. What is Franciscan?: Revisited. Int. Geol. Rev. 60, 1968–2030.
Reagan, M.K., Pearce, J.A., Petronotis, K., Almeev, R.R., Avery, A.J., Carvallo, C., Chapman, T., Christeson, G.L., Ferre, E.C., Godard, M., Heaton, D.E., Kirchenbaur, M., Kurz, W., Kutterolf, S., Li, H., Li, Y., Michibayashi, K., Morgan, S., Nelson, W.R., Prytulak, J., Python, M., Robertson, A.H.F., Ryan, J.G., Sager, W.W., Sakuyama, T., Shervais, J.W., Shimizu, K., Whattam, S.A., 2017. Subduction initiation and ophiolite crust: New insights from IODP drilling. Int. Geol. Rev. 59, 1–12.
Rice, S.P., Robertson, A.H.F., Ustaömer, T., 2006. Late Cretaceous-Early Cenozoic tectonic evolution of the Eurasian active margin in the Central and Eastern Pontides, northern Turkey. In: Robertson, A.H.F., Mountrakis, D. (Eds.), Tectonic Development of the Eastern Mediterranean Region, Geol. Soc. London Spec. Publ. 260, 413–445.
Rice, S.P., Robertson, A.H.F., Ustaömer, T., 2009. Late Cretaceous-Early Cenozoic tectonic evolution of the Eurasian active margin in the central and eastern Pontides, northern Turkey. Geol. Mag. 146, 567–590.
Robertson, A.H., 2019. Patuki and Croisilles melanges in South Island, New Zealand: genesis related to Permian subduction–accretion processes. Paleozoic-Mesozoic Geology of South Island, New Zealand: Subduction-related processes adjacent to SE Gondwana. Geol. Soc. London Mem. 49, 119–156.
Robertson, A.H.F., Parlak, O., Dumitrica, P., 2022. Role of Late Cretaceous volcanic-sedimentary melanges, specifically the Aladağ melange, E Turkey, in the rift-drift-subduction-accretion-emplacement history of the Tethyan Inner Tauride ocean. Int. Geol. Rev. 64 (8), 1139–1190.
Robertson, A.H.F., Parlak, O., Ustaömer, T., 2009. Melange genesis and ophiolite emplacement related to subduction of the northern margin of the Tauride-Anatolide continent, central and western Turkey. In: Van Hinsbergen, D.J.J., Edwards, M.A., Govers, R. (Eds.), Collision and collapse at the Africa–Arabia–Eurasia subduction zone, Geol. Soc. London Spec. Publ. 311, 9–66.
Robertson, A.H.F., Parlak, O., Ustaömer, T., 2023. Neotethyan Ankara Melange, in its Triassic-Eocene regional tectonic setting including accretionary melanges, magmatic arcs and continental units. Int. Geol. Rev. https://doi.org/10.1080/00206814.2023.2178034.
Robertson, A.H.F., Parlak, O., Ustaömer, T., Taslı, K., İnan, N., Dumitrica, P., Karaoğlan, F., 2014. Subduction, ophiolite genesis and collision history of Tethys adjacent to the Eurasian continental margin: New evidence from the Eastern Pontides, Turkey. Geodin. Acta 263 (4), 230–293.
Rojay, B., 2013. Tectonic evolution of the Cretaceous Ankara Ophiolitic Mélange during the Late Cretaceous to pre-Miocene interval in Central Anatolia, Turkey. J. Geodyn. 65, 66–81.
Rojay, B., Altıner, D., 1998. Middle Jurassic-Lower Cretaceous biostratigraphy in the Central Pontides (Turkey): remarks on the paleogeography and tectonic evolution. Riv. Ital. Paleontol. S. 104, 167–180.
Rojay, B., Altıner, D., Altıner Özkan, S., Önen, A.P., James, S., Thirlwall, M.F., 2004. Geodynamic significance of the Cretaceous pillow basalts from North Anatolian Ophiolitic Mélange (Central Anatolia, Turkey): geochemical and paleontological constraints. Geodin. Acta 17 (5), 349–361.
Rojay, B., Altıner, D., Altıner, Ö., Önen, P., Hall, R., 2000. İzmir-Ankara-Erzincan kenet kuşağında yeralan Mesozoik yaşlı yastık lavlarının jeokimyası ve yaşı: yastık lavların okyanusal kabukla olan ilişkisi ve Neo-Tetis'in jeodinamik evrimindeki önemi. Türkiye Bilimsel ve Teknik Araştırma Kurumu, Project no. YDABÇAG-292 (196YO84).
Rojay, B., Süzen, L., 1997. Tectonostratigraphic evolution of an arc-trench basin on accretionary ophiolitic mélange prism, Central Anatolia, Turkey. Bull. Turkish Assoc. Petrol. Geol. 9, 1–12.
Rojay, B., Yalınız, K., Altıner, D., 2001. Age and origin of some pillow basalts from Ankara mélange and their tectonic implications to the evolution of northern branch of Neotethys, Central Anatolia. Tr. J. Earth Sci. 10 (3), 93–102.
Ruellan, E., Delteil, J., Wright, I., Matsumoto, T., 2003. From rifting to active spreading in the Lau Basin-Havre Trough back-arc system (NW Pacific): Locking/unlocking induced by seamount chain subduction. Geochem. Geophy. Geosy. 4, 8909. https://doi.org/10.1029/2001GC000261.
Ruh, J.B., Sallarès, V., Ranero, C.R., Gerya, T., 2016. Crustal deformation dynamics and stress evolution during seamount subduction: High-resolution 3-D numerical modelling. J. Geophy. Res. Solid Earth 121 (9), 6880–6902.
Sakai, S., Hirano, N., Dilek, Y., Machida, S., Yasukawa, K., Kato, Y., 2021. Tokoro Belt (NE Hokkaido): an exhumed, Jurassic-Early Cretaceous seamount in the Late Cretaceous accretionary prism of northern Japan. Geol. Mag. 158 (1), 72–83.
Sarıfakıoğlu, E., Sevin, M., Esirtgen, E., Bilgiç, T., Duran, S., Parlak, O., Karabalık, N., Alemdar, S., Dilek, Y., Uysal, İ., 2011. The geology of ophiolitic rocks around Çankırı–Çorum Basen: petrogenesis, tectonics and ore deposits. Miner. Res. Explor. Inst. Turkey (MTA), Report No: 11449, 196 pp, (in Turkish, unpublished).
Sarıfakıoğlu, E., Dilek, Y., Sevin, M., 2014. Jurassic-Paleogene intraoceanic magmatic evolution of the Ankara Mélange, north-central Anatolia, Turkey. Solid Earth 5, 77–108.
Sarıfakıoğlu, E., Dilek, Y., Sevin, M., 2017. New synthesis of the İzmir-Ankara–Erzincan suture zone and the Ankara mélange in northern Anatolia based on new geochemical and geochronological constraints. In: Sorkhabi, R. (Ed.), Tectonic Evolution, Collision, and Seismicity of Southwest Asia: In Honor of Manuel Berberian's Forty-five Years of Research Contributions. Geol. Soc. Am. Spec. Pap. 525, 613–675.
Sayıt, K., Göncüoğlu, M.C., Ellero, A., Ottria, G., Frassi, C., Marroni, M., Pandolfi, L., 2022. Late Cretaceous arc magmatism in the southern Central Pontides: constraints for the closure of the northern Neotethyan branches. Ofioliti 47, 19–35.
Şengör, A.M.C., 2003. The repeated rediscovery of mélanges and its implications for the possibility and the role of objective evidence in the scientific enterprise. In: Dilek, Y., Newcomb, S. (Eds.), Ophiolite concept and the evolution of geological thought, Geol. Soc. Am. Spec. Pap. 373, 385–445.
Şengör, A.M.C., Yılmaz, Y., 1981. Tethyan evolution of Turkey: a plate tectonic approach. Tectonophysics 75, 181–241.
Shervais, J.W., Kimbrough, D.L., 1987. Alkaline and transitional subalkaline metabasalts in the Franciscan Complex melange, California. In South-Central Section meeting on alkalic rocks and kimberlites. Geol. Soc. Am. Spec. Pap. 215, 165–182.
Smith, A.G., 2006. Tethyan ophiolite emplacement, Africa to Europe motions, and Atlantic spreading. In: Robertson, A.H.F., Mountrakis, D. (Eds.), Geol. Soc. London Spec. Publ. 260, 11-34.
Strasser, M., Moore, G.F., Kimura, G., Kitamura, Y., Kopf, A.J., Lallemant, S., Park, J.O., Screaton, E.J., Su, X., Underwood, M.B., Zhao, X., 2009. Origin and evolution of a splay fault in the Nankai accretionary wedge. Nature Geosci. 2 (9), 648–652.
Tani, S., 1989. Detailed topographic study of the Daiichi-Kashima Seamount. Palaeogeogr. Palaeocl. 71 (1–2), 31–47.
Tankut, A., 1984. Basic and ultrabasic rocks from the Ankara Mélange, Turkey. In: Dixon J.E., Robertson, A.H.F. (Eds.), The Geological Evolution of Eastern Mediterranean. Geol. Soc. London Spec. Publ. 17, 441–447.
Tankut, A., 1990. Geochemical implications for tectonic setting of the ophiolitic rock from the ophiolite mélange belt of the Ankara Mélange. Bull. Miner. Res. Explor. Inst. Turkey 110, 17–28.
Tankut, A., Dilek, Y., Önen, P., 1998. Petrology and geochemistry of the Neo-Tethyan volcanism as revealed in the Ankara mélange. Turkey. J. Volcanol. Geoth. Res. 85, 265–284.
Tekin, U.K., Göncüoğlu, M.C., Turhan, N., 2002. First evidence of late Carnian radiolarians from the Izmir-Ankara Suture Complex, central Sakarya, Turkey: Implications for the opening age of the Izmir-Ankara Branch of Neo-Tethys. Geobios 35, 127–135.
Topuz, G., Çelik, Ö. F., Şengör, A.M.C., Altıntaş, İ.E., Zack, T., Rolland, Y., Barth, M., 2013, Jurassic ophiolite formation and emplacement as back-stop to a subduction-accretion complex in northeast Turkey, the Refahiye ophiolite, and relation to the Balkans ophiolites. Am. J. Sci. 313, 1054–1087.
Tüysüz, O., 1990. Tectonic evolution of a part of the Tethyside orogenic collage: The Kargı Massif, northern Turkey. Tectonics 9, 141–160.
Tüysüz, O., 1993. A geotraverse from the Black Sea to the Central Anatolia: tectonic evolution of the northern Neo-Tethys. Bull. Turkish Assoc. Petrol. Geol. 5, 1–33.
Uğuz, M.F., Turhan, N., Bilgin A.Z., Umut, M., Şen, A.M., Acarlar, M., 1999. Kulu (Konya) Haymana (Ankara) ve Kırıkkale Dolayının Jeolojisi. Miner. Res. Explor. Inst. Report No: 10399 (unpublished).
Ünalan, G., 1981. Ankara Güneyindeki Ankara Melanjının stratigrafisi. In: Proc. Symp. Geol. Central Anatolia. Geol. Soc. Turkey 35th Annual Meeting, 46-52 [in Turkish with English abstract].
Ünalan, G., Yüksel, V., Tekeli, T., Gönenç, O., Seyirt, Z., Hüseyin, S., 1976. Haymana-Polatlı yöresinin (SW Ankara) Üst Kretase-Alt Tersiyer stratigrafisi ve paleocoğrafik evrimi. Bull. Geol. Soc. Turkey 19 (2), 156–176.
Üner, T., Çakır, Ü., 2011. Mineralogical, petrographical and geochemical characteristics of Eldivan Ophiolite (Çankırı) Harzburgitic Tectonites. Bull. Miner. Res. Explor. Inst. Turkey 143, 75–94 [in Turkish with English abstract].
Üner, T., Çakır Ü., Özdemir, Y., Arat, I., 2014. Geochemistry and origin of plagiogranites from the Eldivan Ophiolite, Çankırı (Central Anatolia, Turkey). Geol. Carpathica 65 (3), 195–205.
Uysal, İ., Ersoy, E.Y., Dilek, Y., Escayola, M., Sarıfakıoğlu, E., Saka, S., Hirata, T., 2015. Depletion and refertilization of the Tethyan oceanic upper mantle as revealed by the early Jurassic Refahiye ophiolite, NE Anatolia-Turkey. Gondwana Res. 27, 594–611.
Ustaömer, T., Robertson, A.H.F., 1997, Tectonic-sedimentary evolution of the North-Tethyan margin in the Central Pontides of northern Turkey. In: Robinson, A.G. (Ed.), Regional and Petroleum Geology of the Black Sea and Surrounding Region. Amer. Assoc. Petrol. Geol. Mem. 68, 255–290.
Ustaömer, T., Robertson, A.H.F., 1999. Geochemical evidence used to test alternative plate tectonic models for pre-Upper Jurassic (Palaeotethyan) units in the Central Pontides. N. Turkey Geol. J. 34, 25–53.
Ustaömer, T., Ustaömer, P.A., Robertson, A.H., Gerdes, A., 2016. Implications of U-Pb and Lu–Hf isotopic analysis of detrital zircons for the depositional age, provenance and tectonic setting of the Permian-Triassic Palaeotethyan Karakaya Complex, NW Turkey. Int. J. Earth Sci. 105 (1), 7–38.

Wakabayashi, J., 2012. Subducted sedimentary serpentinite mélanges: Record of multiple burial-exhumation cycles and subduction erosion. Tectonophysics 568–569, 230–247.
Waldron, J.W.F., Turner, D., Stevens, K.M., 1988. Stratal disruption and development of mélange, western Newfoundland: effect of high fluid pressure in an accretionary terrain during ophiolite emplacement. J. Struct. Geol. 10 (8), 861–873.
Xu, C., Dunn, R.A., Watts, A.B., Shillington, D.J., Grevemeyer, I., Gomez de la Pena, L., Boston, B.B., 2022. A seismic tomography, gravity, and flexure study of the crust and upper mantle structure of the Emperor Seamounts at Jimmu Guyot. J. Geophy. Res. Solid Earth 127, 6.
Yang, G., Si, G., Tong, L., Li, H., Lindagato, P., Zeng, R., 2022. The effect of seamount chain subduction and accretion. Geol. J. 57 (7), 2712–2734.
Yılmazer, İ., 1994. Ankara'nın doğusunda yer alan Yayla olistostromunun jeolojisi. Bull. Geol. Soc. Turkey 37 (1), 47–52.
Zagorevski, A., McNicoll, V., 2012. Evidence for seamount accretion to a peri-Laurentian arc during closure of Iapetus. Can. J. Earth Sci. 49 (1), 147–165.
Zhang, B., Li, G., Li, S., Dada, O.A., 2016. Docking and subduction of the West Pacific seamounts along the Mariana Trench and their effects. Geol. J. 51, 579–592.